



National Library
of Canada

Bibliothèque nationale
du Canada

Canadian Theses Service

Services des thèses canadiennes

Ottawa, Canada
K1A 0N4

CANADIAN THESES

THÈSES CANADIENNES

NOTICE

The quality of this microfiche is heavily dependent upon the quality of the original thesis submitted for microfilming. Every effort has been made to ensure the highest quality of reproduction possible.

If pages are missing, contact the university which granted the degree.

Some pages may have indistinct print especially if the original pages were typed with a poor typewriter ribbon or if the university sent us an inferior photocopy.

Previously copyrighted materials (journal articles, published tests, etc.) are not filmed.

Reproduction in full or in part of this film is governed by the Canadian Copyright Act, R.S.C. 1970, c. C-30.

**THIS DISSERTATION
HAS BEEN MICROFILMED
EXACTLY AS RECEIVED**

AVIS

La qualité de cette microfiche dépend grandement de la qualité de la thèse soumise au microfilmage. Nous avons tout fait pour assurer une qualité supérieure de reproduction.

S'il manque des pages, veuillez communiquer avec l'université qui a conféré le grade.

La qualité d'impression de certaines pages peut laisser à désirer, surtout si les pages originales ont été dactylographiées à l'aide d'un ruban usé ou si l'université nous a fait parvenir une photocopie de qualité inférieure.

Les documents qui font déjà l'objet d'un droit d'auteur (articles de revue, examens publiés, etc.) ne sont pas microfilmés.

La reproduction, même partielle, de ce microfilm est soumise à la Loi canadienne sur le droit d'auteur, SRC 1970, c. C-30.

**LA THÈSE A ÉTÉ
MICROFILMÉE TELLE QUE
NOUS L'AVONS REÇUE**

THE UNIVERSITY OF ALBERTA

STUDIES OF DEEP LEVELS IN SEMI-INSULATING GALLIUM ARSENIDE

by

TIN CHIN CHE

A THESIS

SUBMITTED TO THE FACULTY OF GRADUATE STUDIES AND RESEARCH

IN PARTIAL FULFILMENT OF THE REQUIREMENTS FOR THE DEGREE

OF DOCTOR OF PHILOSOPHY

IN

SOLID STATE PHYSICS

DEPARTMENT OF PHYSICS

EDMONTON, ALBERTA

SPRING 1987

Permission has been granted to the National Library of Canada to microfilm this thesis and to lend or sell copies of the film.

The author (copyright owner) has reserved other publication rights, and neither the thesis nor extensive extracts from it may be printed or otherwise reproduced without his/her written permission.

L'autorisation a été accordée à la Bibliothèque nationale du Canada de microfilmer cette thèse et de prêter ou de vendre des exemplaires du film.

L'auteur (titulaire du droit d'auteur) se réserve les autres droits de publication; ni la thèse ni de longs extraits de celle-ci ne doivent être imprimés ou autrement reproduits sans son autorisation écrite.

ISBN 0-315-37665-1

Letter of Permission

The undersigned hereby grant permission to TIN CHIN CHE to include any relevant material from the papers that he has coauthored with us in his thesis entitled STUDIES OF DEEP LEVELS IN SEMI-INSULATING GALLIUM ARSENIDE.

Frank L. Weichman

Dr. F.L. Weichman

C.K. Teh

C.K. Teh

Date: March 11, 1987

THE UNIVERSITY OF ALBERTA

RELEASE FORM

NAME OF AUTHOR TIN CHIN CHE
TITLE OF THESIS STUDIES OF DEEP LEVELS IN
 SEMI-INSULATING GALLIUM ARSENIDE
DEGREE FOR WHICH THESIS WAS PRESENTED: DOCTOR OF PHILOSOPHY
YEAR THIS DEGREE GRANTED: SPRING 1987

Permission is hereby granted to THE UNIVERSITY OF ALBERTA LIBRARY to reproduce single copies of this thesis and to lend or sell such copies for private, scholarly or scientific research purposes only.

The author reserves other publication rights, and neither the thesis nor extensive extracts from it may be printed or otherwise reproduced without the author's written permission.

(SIGNED) *Tin Chin Che*

PERMANENT ADDRESS:
 .SUNGAI RAYA ESTATE

 .BATU PAHAT, JOHORE

 .MALAYSIA

DATED MARCH 11 1987

THE UNIVERSITY OF ALBERTA
FACULTY OF GRADUATE STUDIES AND RESEARCH

The undersigned certify that they have read, and recommend to the Faculty of Graduate Studies and Research for acceptance, a thesis entitled STUDIES OF DEEP LEVELS IN SEMI-INSULATING GALLIUM ARSENIDE submitted by TIN CHIN CHE in partial fulfilment of the requirements for the degree of DOCTOR OF PHILOSOPHY in SOLID STATE PHYSICS.

Frank H. Weirhman
.....

Supervisor

E. J. ...
.....

P. ...
.....

D. G. ...
.....

S. ...
.....

Albert N. ...
.....

External Examiner

Date: March 11, 1987

*Dedicated
to the
loving memory
of my parents*

Abstract

A microcomputer-controlled photo-induced transient spectroscopy (PITS) system was constructed to provide an effective analytical system to study the deep defect levels in liquid-encapsulated Czochralski-grown semi-insulating gallium arsenide (SI GaAs).

Various aspects of PITS are discussed to show how such a system can be used to characterize high-resistivity semiconductors where the conventional deep level transient spectroscopy (DLTS) technique fails.

Specifically, the PITS system was then used to study how deep levels in SI GaAs are affected by the presence of carbon and different growth conditions and to determine the various levels created by copper impurity. The overall objective was to determine the nature of the previously unassigned deep levels in SI GaAs.

From the PITS measurements on a series of samples with different carbon concentrations, we found that the intensity of the EL2 family of levels increases with the moisture content of the boric oxide encapsulant that was used during the growth process. We have also found that the intensity of the signal due to EL5 is inversely dependent on the carbon content of the samples. From this observation, we propose that the origin of EL5 is related to free arsenic vacancies, V_{As} , which indirectly indicates that the defects EL6 and EL3 are also related to arsenic vacancies.

A series of PITS and photoluminescence experiments was carried out to study the presence of copper in SI GaAs in an effort to reconcile many conflicting published results. We observed three different copper-related levels at about 0.5, 0.4 and 0.19 eV from the valence band. We found that the concentration of the defect, with a level at about $E_v + 0.5$ eV and a hole capture cross-section of about 10^{-17} cm², correlates with the concentration profile of V_{As} . We postulate that this level is a copper-related complex, most probably of the form $Cu_{Ga}V_{As}$. The studies of the copper-related levels have provided a model which explains many of the conflicting results reported in the literature.

Acknowledgements

The author wishes to express his appreciation to the following:

Dr. F.L. Weichman, my thesis supervisor, for his guidance, patience and tolerance,

Teh Chin Khuan, my wife, for her help in some of the experiments, her encouragement and her patience and tolerance with my temperament during the ups and downs of my graduate study,

my brothers and sisters, for their encouragement, moral and financial support that enabled me to begin my graduate study and who provide an inspiration for me to finish my graduate program,

Dr. Roelof Bult, of Cominco Ltd., Electronic Materials Division, Trail, British Columbia, for providing the gallium arsenide samples,

Department of Physics, University of Alberta, for financial support in the form of a graduate teaching assistantship,

Natural Sciences and Engineering Research Council of Canada, for supporting the research work,

George Christie and Ken Marsh for some technical assistance,

the technicians in the Electronics Shop for helpful discussions, and

all those whom I have met and befriended and who made my stay in Canada more pleasant.

Table of Contents

Chapter	Page
1. Introduction	1
1.1 Importance of GaAs devices	1
1.2 LEC semi-insulating GaAs	2
1.3 Concept of defects and deep levels and their significances	4
1.4 Experimental Methods	8
1.4.1 Photoluminescence	9
1.4.2 Deep-Level Transient Spectroscopy (DLTS) ..	10
1.4.3 Photo-Induced Transient Spectroscopy (PITS)	12
1.5 Deep Levels in GaAs	13
Bibliography	18
2. Photo-Induced Transient Spectroscopy (PITS)	21
2.1 Introduction	21
2.2 Theory of PITS	22
2.2.1 Emission rate, ν	22
2.2.2 Transient current	25
2.3 PITS signal	26
2.4 Different Relaxation Times	32
2.5 Presence of Non-Exponential Transients	36
2.6 Contact Configurations	37
2.7 PITS system	38
2.7.1 Input-output board	41
2.7.2 Temperature-controller	41
2.7.3 Programmable power supply	42
2.7.4 Analogue-to-digital converter	43
2.7.5 Electro-mechanical shutter system	44

2.7.6	Amplifier	44
2.7.7	Software	44
Bibliography	46
3.	PITS studies of deep levels in LEC SI GaAs with different carbon concentrations	47
3.1	Introduction	47
3.2	Experimental details	50
3.3	Results	51
3.4	Discussion	51
3.5	Conclusion	60
Bibliography	62
4.	PITS and Photoluminescence Studies of Copper-contaminated LEC SI GaAs	64
4.1	Introduction	64
4.2	Experimental details	67
4.3	Results	71
4.4	Discussion	79
4.5	Conclusion	87
Bibliography	89
5.	PITS and Photoluminescence Studies of Copper-diffused LEC SI GaAs - Annealing at 550°C	91
5.1	Introduction	91
5.2	Experimental details	92
5.3	Results	93
5.4	Discussion	98
5.5	Conclusion	101
Bibliography	102
6.	General Discussion and Conclusions	103
6.1	General Discussion	103

6.2 Conclusions	109
Bibliography	111
Appendix A	113
Appendix B	117
VITA	130

List of Tables

Table	Page
2.1 Emission rate	29
3.1 Samples used in PITS measurements.	52
3.2 Trapping parameters for the peaks in figures 3.1 and 3.2.	53
4.1 Trapping parameters from PITS curves.	76

List of Figures

Figure	Page
2.1 A single trap model	23
2.2 Sampling of the photocurrent signal	27
2.3 Analysis of PITS curve	31
2.4 Equivalent RC network	33
2.5 PITS system	39
3.1 PITS curves for samples with different grades of B_2O_3 , but same mass of charge.	54
3.2 PITS curves for samples with the same grade of B_2O_3 , but different mass of charge.	55
4.1 PITS curves for both unannealed and control samples	72
4.2 PITS curves for copper-contaminated sample	73
4.3 Photoluminescence spectra at 4.2 K for both unannealed and control samples	77
4.4 Photoluminescence spectra at 4.2 K for copper-contaminated sample	78
4.5 Intensities of A and B peaks from PITS curves	82
5.1 PITS curves for both original and copper-diffused samples	94
5.2 Sample for PITS measurements.	95
5.3 Photoluminescence spectra at different depths from the surface	96
5.4 Sample for photoluminescence measurements.	97

B1 I/O board124
B2 Shutter driver124
B3 Programmable power supply125
B4 12 bit A to D converter126
B5 Temperature controller127
B6 Amplifier128
B7 Mechanical part of PITS system129

1. Introduction

1.1 Importance of GaAs devices

Gallium arsenide (GaAs) devices have higher electron mobility and saturated drift velocity than silicon devices which allows GaAs devices to operate in the high-frequency regimes where silicon devices would fail. The higher resistance of GaAs devices to radiation damage has permitted the use of such devices in space.

The increasing use of GaAs devices in such varied applications as satellite communications, high-speed computers, radar, solar cells, optical telecommunication, etc., has created a demand for GaAs devices. The high market potential of GaAs devices has spurred increasing research and development efforts to produce new devices and to improve industrial processes that would not only make GaAs devices more economical to use but also of higher reliability and better performance.

An advantage of using GaAs is the fact that it is possible to produce high resistive semi-insulating GaAs which can be used as substrates on which devices can be fabricated. The increasing demand for high quality devices has therefore created a demand for high quality semi-insulating GaAs material.

Currently, semi-insulating GaAs material is mainly produced using the liquid-encapsulated Czochralski growth technique and research efforts are still being directed into

the characterizations of this material in an effort to improve the quality.

1.2 LEC semi-insulating GaAs

Liquid-encapsulated Czochralski (LEC) growth technique was first adopted for the growth of semi-insulating (SI) GaAs by Mullin et al. (1968). The use of high pressure LEC technique (AuCoin et al., 1979) is now the most widely implemented growth technique in many laboratories and in industry. In this technique for producing semi-insulating GaAs, the melt is contained in a high-purity pyrolytic boron nitride crucible. The melt is encapsulated by an inert liquid such as boric oxide (B_2O_3) to reduce the loss of the more volatile element, As. To further reduce the loss of As, high argon overpressures are applied. Compounding of high-purity Ga and As occurs exothermically at about $800^\circ C$. After compounding, the temperature of the melt is raised to $1238^\circ C$. Growth of the crystal begins when a low dislocation density seed is inserted, through the liquid B_2O_3 encapsulant, into the melt and gradually withdrawn at a rate of a few millimeters per hour. Further details of this process have been described by Kirkpatrick et al. (1984, 1985), Thomas et al. (1984) and Mullin (1975, 1985).

Other methods of growing semi-insulating GaAs are the horizontal Bridgman and the gradient-freeze techniques (Mullin, 1975, 1985). In the horizontal Bridgman technique, the boat containing the melt is moved relative to the

furnace so that the freezing front moves along the length of the boat. In the gradient-freeze technique, the freezing interface is moved away from the seed by changing the temperature profile of the boat. The disadvantage of these techniques is that the crystal ingot has the D shape of the boat and significant material has to be removed to produce a cylindrical ingot from which circular wafers can be obtained.

The large-size circular wafers of GaAs that can be sliced from cylindrical ingots obtained using the LEC technique are preferred, mainly because processing of large-size wafers can utilize the existing technology that is being used in the fabrication of silicon devices. The ability to capitalize on the technological "spin-off" from the silicon IC manufacturing industry without the need for expensive process development costs is very important for the budding GaAs IC industry because only by doing so can the GaAs devices be manufactured at a reasonable cost which would then lead to widespread acceptance by potential users.

The use of LEC SI GaAs as substrates for IC fabrication has significantly increased the quality and reliability of GaAs devices. Prior to the development of the LEC techniques, SI GaAs grown from the Bridgman or gradient-freeze techniques provided poor quality substrates which posed great difficulties in the development of new devices.

The semi-insulating property of GaAs substrates is important for device isolation and reduction of parasitic capacitance which would then allow full integration of devices on a chip. The active regions for devices such as field-effect transistors (FETs), diodes and resistors are produced by either epitaxial growth or ion implantation or both. It is most economical to do the implantation process directly onto the semi-insulating substrates without the need for an epitaxial buffer layer. This puts a very stringent requirement on the quality of the substrate material because the characteristics of the devices will then be sensitive to the properties of the substrate. Essential features of GaAs substrates for device fabrication are high purity, thermal stability, electrical uniformity and reproducibility of the material characteristics. Hence, there is a great need to understand the roles and natures of various defects in semi-insulating GaAs and to examine the cause-and-effect relationships between the growth process, occurrence of defects and the electrical characteristics of the material. The solutions to these problems result in the improvement of device performance.

1.3 Concept of defects and deep levels and their significances

In a real crystal, the periodic symmetry of the lattice can be broken by defects. Lattice defects produce localized energy states which may have energy levels occurring within

the band gap. A carrier (electron or hole) bound to such a defect in a lattice has a decaying wavefunction as opposed to a carrier in the allowed energy bands (conduction or valence bands) which is free to move.

Crystal imperfections known as point defects can be vacancies or impurities which are introduced deliberately or as a result of the growth process. Some defects are unavoidable and they play a key role in determining the properties of a semiconductor. Chemical impurities that form point defects may exist interstitially or substitutionally and can cause vacancies or a combination of them. An interstitial atom may be of the same species as the atoms in the lattice (intrinsic defects) or of a different species (extrinsic defects).

Besides point defects, there are also one dimensional defects such as dislocations, two-dimensional defects such as surfaces and grain boundaries, and three-dimensional defects such as cavities.

Defects occur in accordance with the laws of thermodynamics and the laws of mass action. Hence, the removal or suppression of one type of defect will enhance the effects of another type. For instance, the removal of defects such as grain boundaries and dislocations increases the significance of point defects.

The presence of defects in semiconductors can be either beneficial or detrimental depending on the nature of the defects and the actual use of the material in devices.

Gold impurity in silicon junctions is used to provide fast recombination resulting in faster switching time. Impurities such as gold, zinc, mercury, etc., in silicon and germanium produce high quantum efficiency photodetectors. The emission wavelength of light-emitting diodes (LEDs) is determined by the presence of deep levels. In undoped semi-insulating GaAs, a deep donor level, commonly known as EL2, together with a carbon impurity are mainly responsible for the semi-insulating property. Chromium is also used to dope GaAs to produce semi-insulating GaAs:Cr although this is no longer in widespread use.

On the other hand, device performance and reliability are greatly affected by the presence of defects. The success of the new generation of telecommunication systems employing optical fibres depend critically on the lifetime of the laser diodes and LEDs. The degradation of laser diodes and LEDs has been widely attributed to formation of local regions where non-radiative recombinations occur. There is general agreement that these regions are due to the motion of dislocations that interact with defect centers to promote non-radiative recombinations. It has been proposed that the energy released from non-radiative recombination processes may be responsible for diffusion of defects and dislocation climbs (O'Hara et al., 1977; Lang and Kimmerling, 1974). The exact mechanism for non-radiative recombination-enhanced diffusion of defects is still unknown and there is a need to understand this process in light of the technological

importance of lasers and LEDs. A dislocation array can also propagate from a substrate into the active layers resulting in device failure. This is a reason why semi-insulating GaAs of low dislocation density is required.

Device fabrication processes usually involve ion-implantation, annealing, contact formation, mechanical scribing and cleaving, all of which introduce dislocations in one way or another. Dislocations in devices may be of little significance by themselves. The problems only arise when these dislocations induce the formation of metal precipitates giving rise to "decorated" dislocations. Impurities tend to gather around dislocations and diffusion of impurities is also enhanced at dislocations. It is difficult to differentiate between the effects of point defects and dislocations, owing to the fact that production of dislocations also generates point defects such as interstitial atoms and vacancies.

The topic of reliability and degradation of devices is wide-ranging and the above examples only serve to show the significance of the studies of defects in devices. Comprehensive discussions of such topics have been published by Howes and Morgan (1981) and Mahajan and Corbett (1983).

The localised states within the band gap can range from a few millielectron-volts to a few tenths of an electron-volt from either the conduction or valence bands. The determination of whether a level can be considered deep or shallow is rather arbitrary. A depth ≥ 0.1 eV is usually

termed *deep level*. It must also be noted that in any experiment which involves the measurement of the thermal emission of carriers from the trapping levels, either electrically or photoelectronically, the accuracy in the determination of any level below 0.1 eV is always questionable.

A defect center can either be a recombination or a trapping center depending on the probabilities in which each of the two processes will occur. If a carrier bound to a defect center recombines with another carrier of opposite polarity, before it can be thermally released to the nearest band, then that center is a recombination center. However, if the carrier can escape to the nearest band by thermal energy, before recombination can occur, then that center is a trapping center. The probability of escape is therefore higher if a level is nearer to either band which means that a donor or acceptor level near a band is more likely to be a trapping center.

1.4 Experimental Methods

There is an extensive range of methods that can be employed to study deep levels in semiconductors. The sections below deal only with those methods relevant to the studies to be discussed in the following chapters.

1.4.1 Photoluminescence

Photoluminescence spectroscopy is a method in which electrons are optically excited into the conduction band or to a defect level within the bandgap. These electrons subsequently recombine at a recombination center and, in the process of doing so, emit photons of a frequency corresponding to the energy difference between the excited state and the recombination level. The emission wavelengths are characteristic of the types of defects in the material.

This method can be used to study both shallow and deep levels and it provides a non-ambiguous and simultaneous determination of defect species without destruction of the samples. It is, however, only applicable when there is radiative recombination, which essentially limits this method to low temperatures. Low temperature is also necessary for better resolution and a decrease in line widths. At increasing temperatures, a competing non-radiative process becomes more probable resulting in a reduced photoluminescent output. Besides that, certain deep levels are non-radiative centers which require other means to probe their characteristics. However, the presence of shallow non-radiative centers can be studied by the effects of phonon coupling on the photoluminescence signals. Photoluminescence is not limited only to the emission wavelength parameter to study recombination processes. It can also utilize other parameters such as temperature and pressure variations which would allow quenching and

enhancement processes to be studied. The strengths of photoluminescence spectroscopy reside in the speed, efficiency and the spectroscopic nature of the technique.

In spite of the problem with non-radiative recombination processes involving deep levels, photoluminescence spectroscopy will remain as one of the most efficient and powerful methods in the study of semiconductors.

1.4.2 Deep-Level Transient Spectroscopy (DLTS)

DLTS was first introduced by Lang (1974) based on the theoretical groundwork of Sah et al. (1970) and Milnes (1973). The basis of this method is the dependence of the capacitance of a space-charge region on the occupancy of the traps.

A p-n junction or a Schottky barrier is first formed on the sample. This junction is initially reverse-biased to empty the traps. When the bias is reduced, part of the space-charge region will be neutralised causing the traps to be occupied by majority carriers. When the bias is restored, the space-charge region will be restored as before, with the only difference that there are trapped carriers now residing in the space-charge region. These carriers will then be thermally re-emitted to the relevant energy band. The change of the occupancy of these trapping centers is reflected in the capacitance of the junction producing a capacitance transient. Minority carrier injection can also occur when

the junction is forward biased during the pulse. In essence, both majority and ~~minority~~ carriers are involved which makes this method all the more effective because emission of each type of carrier can be detected by monitoring the capacitance transients. The trap depth and the capture cross-section can be determined from the temperature dependence of the emission rate. The trap concentration can be determined from the intensity of the capacitance peak and the polarity of the carriers can be found from the sign of the capacitance change.

The efficiency of DLTS lies in the way in which the trapping parameters are obtained experimentally. In the experiment, the capacitance transients are sampled at two different instants of time t_1 and t_2 from the end of the bias pulse. The time interval $(t_2 - t_1)$ can be considered as a time window. As the temperature changes, the emission rate of the carriers varies to a temperature at which the emission rate matches the rate window set by t_2 and t_1 . At this temperature a peak will be produced in the capacitance versus temperature curve. The emission rate is related to the time window by: $e_n = \ln(t_2/t_1)/(t_2 - t_1)$.

Since the first introduction of DLTS, many variations of the experiments have been introduced. Examples of such variations are electron-beam scanning DLTS (Petroff et al., 1977), photo-excited DLTS (Mitonneau et al., 1977a; Brunwin et al., 1980; Takikawa et al., 1980) and current or conductance DLTS (Wessels, 1976; Borsuk et al., 1980).

These methods are not effective for high resistivity materials due to the problems involved in obtaining suitable junctions on such materials. This leads to the introduction of photo-induced transient spectroscopy (PITS) which will be discussed next.

1.4.3 Photo-Induced Transient Spectroscopy (PITS)

PITS, also known as optical transient current spectroscopy (OTCS), is similar in concept to DLTS. The application of PITS was first introduced by Hurtes et al. (1978). Variations of this were subsequently introduced by Fairman et al. (1979) and Yoshie and Kamihara (1983a,b). It must be noted, however, that the study of photocurrent decay in semiconductors has been going on since the early 1950's. The aspect that sets PITS aside from the classical photocurrent studies is the measurement and analytical techniques which are similar to DLTS in certain respects.

In PITS measurements, only ohmic contacts are required which give both advantages and disadvantages. One of the advantages is that the sample is essentially neutral and if the contact configuration is planar, then the effects due to high electric field such as field-assisted detrapping can be neglected. The disadvantage is that electron and hole conduction cannot be distinguished since the contacts are ohmic. Furthermore, the concentrations of the trapping centers cannot be determined directly, although attempts have been made (Bobylev and Kravchenko, 1983; Omel'yanovskii

et al., 1986) but only after making several questionable assumptions.

The basic technique of PITS involves measuring the photocurrent at times t_1 and t_2 after the extinction of the excitation pulse, in contrast to the measurement of capacitances in the case of DLTS. The plot of the difference in photocurrent $\Delta I = I(t_1) - I(t_2)$ against temperature will give a peak whenever the emission rate of the carriers matches the rate window set by t_1 and t_2 . The emission rate is related to t_1 and t_2 but is not the same as the relationship used for DLTS. However, many researchers assume these relationships to be similar for the sake of simplicity which may affect the results to a certain extent. From the temperature dependence of e_n , both the trap depth and the capture cross-section can be obtained.

Details of this method will be given in the next chapter and it suffices to say at this point that this method has been found to be efficient and useful in spite of several shortcomings.

1.5 Deep Levels in GaAs

Deep levels in GaAs have been studied extensively for the past two decades. Although much progress has been achieved, there is still a lack of firm evidence that would lead to the identities of the many levels that have been observed both electrically (DLTS, Hall-effects, etc.) and photoelectronically (thermally-stimulated conductivity,

PITS, etc.). Conflicting conclusions in published papers have further contributed to the controversy surrounding the search for the identities of many deep levels.

The energy levels due to the various defects have been compiled by Milnes (1973), Martin et al. (1977), Mitonneau et al. (1977), Neumark and Kosai (1983) and Look (1983). The designations given by Martin et al. (1977) and Mitonneau et al. (1977) to the defect levels have been quoted most frequently and we will adopt the same designations in all the following discussions.

The most often seen deep levels in LEC semi-insulating GaAs are electron trapping levels EL2, EL3, EL5 and EL6. These traps corresponds to energy levels around 0.82, 0.58, 0.42 and 0.35 eV respectively from the conduction band. Except for the EL2 level, the origins of the other levels are still dubious. There have been many conflicting assignments.

Theoretical calculations can play an important role in unravelling the mess surrounding the identification of the above-mentioned levels. Unfortunately, there are also conflicting results from theoretical calculations (Blakemore and Rahimi, 1984) which make it all the more difficult if one tries to correlate experimental and theoretical results.

The deep electron trap, EL2, has been widely studied and to date there are several dozen papers discussing this level in view of the significant role that it plays in the semi-insulating property of SI GaAs. A discussion on the

electrical properties of GaAs would not be complete without the mention of EL2. Hence, we will review some of the properties of this level which have attracted so much attention.

The origin of EL2 was formerly thought to be due to an oxygen-related defect, O_{As} (Milnes, 1973). It was later found that there is no correlation between the concentration of this defect and the oxygen content in the crystal (Huber et al., 1979; Martin et al., 1982). The donor nature of EL2 was confirmed by Mircea et al., (1976). A peculiar property of EL2 is the quenching of the transient photocapacitance response by infrared light of 0.9 - 1.5 eV (Bois and Vincent, 1977) at 77 K. This has been attributed to the existence of a metastable state which is different from the normal state and having an Auger-like transition between the two states (Bois and Vincent, 1977). Levinson (1983) proposed that the transition to the metastable state is due to strong Coulombic repulsion and the return to equilibrium is due to Coulombic attraction between two charged states of EL2.

In photoluminescence studies, EL2 has been proposed to be responsible for the emission band at 0.64 eV (Shanabrook et al., 1981). Others have also attributed the emission band at 0.68 eV to EL2 (Yu, 1984) and Martin et al. (1984) reported that both bands are due to EL2.

The concentration of EL2 has been observed to depend on the As/Ga ratio in the melt during the growth process, with

increasing As content favouring higher concentration of EL2 (Holmes et al., 1982). Lagowski et al. (1982) found that there is also a dependence of the concentration of EL2 on the arsenic partial pressure during the growth of GaAs by the Bridgman process.

The identification of the nature of EL2 with an As_{Ga} antisite defect was proposed by Holmes et al. (1982) and Lagowski et al. (1982) after the observation of As_{Ga}^{4+} EPR signal by Wagner et al. (1980). Since then, EL2 has been widely accepted as being related to As_{Ga} . However, there are still differences in opinions as to the exact nature of EL2. Lagowski et al. (1983) believe that EL2 is a defect complex involving arsenic vacancy, $As_{Ga}V_{As}$. Fizielski et al. (1985) proposed that it is $(As_{Ga})_2$ but von Bardeleben et al. (1985) suggested that it is $As_{Ga}As_i$. Zou et al. (1982) proposed that it could be either As_{Ga} or $As_{Ga}V_{Ga}V_{As}$.

There have been recent reports that there is another mid-gap level close to, but shallower than, the position of EL2 (Taniguchi and Ikoma, 1982, 1983; Lagowski et al., 1984). This level has been attributed to oxygen (Taniguchi and Ikoma, 1982; Lagowski et al., 1984).

It can be seen from the brief review of the properties of EL2 that there is still a lot to be done before one can conclusively determine the exact nature of EL2. The dependence of this defect on the other growth parameters is also another important subject but this will be dealt with in later chapters.

Besides the electron trapping levels mentioned above, there are also hole trapping levels which are equally important in determining the properties of LEC SI GaAs. The impurity in GaAs that has also been widely studied is copper, which is a very common but pernicious impurity. Copper has a detrimental effect on devices but the complete understanding of copper in GaAs is also lacking and there are conflicting data on the roles of copper in GaAs. Attempts will be made in this thesis to contribute to a better understanding of the roles of copper in GaAs and to provide a consistent picture in which one can correlate all the available experimental data from DLTS, thermally stimulated conductivity and other capacitance studies.

Bibliography

- AuCoin, T.R., Ross, R.L., Wade, M.J., and Savage, R.O.,
Solid State Technol. 22, 59 (1979)
- Blakemore, J.S., and Rahimi, S., Semiconductors and
semimetals, Vol. 20, p. 233 (1984)
- Bobylev, B.A., and Kravchenko, A.F., Sov. Phys. Semicond.
17, 1256 (1983)
- Bois, D., and Vincent, G., J. Phys. Lett. (Paris) 38, L351
(1977)
- Borsuk, J.A., and Swanson, R.M., IEEE Trans. Electron
Devices ED-27, 2217 (1980)
- Brunwin, R., Hamilton, B., Jordan, P., and Peaker, A.R.,
Electron. Lett. 15, 349 (1979)
- Fairman, R.D., Morin, F.J., and Oliver, J.R., Inst. Phys.
Conf. Ser. No. 45, p. 134 (1979)
- Figielski, T., Kaczmarek, E., and Wosinski, T., Appl. Phys.
A 38, 253 (1985)
- Hurtes, Ch., Boulou, M., Mitonneau, A., and Bois, D., Appl.
Phys. Lett. 32, 821 (1978)
- Holmes, D.E., Chen, R.T., Elliott, K.R., and Kirkpatrick,
C.G., Appl. Phys. Lett. 40, 46 (1982)
- Howes, M.J., and Morgan, D.V., eds., *Reliability and
Degradation* (J. Wiley & Sons, 1981)
- Huber, A.M., Linh, N.T., Valladon, M., Debrun, J.L., Martin,
G.M., Mitonneau, A., and Mircea, A., J. Appl. Phys. 50,
4022 (1979)
- Kirkpatrick, C.G., Chen, R.T., Holmes, D.E., Asbeck, P.M.,
Elliott, K.R., Fairman, R.D., and Oliver, J.R.,
Semiconductors and semimetals, Vol. 20, p. 159 (1984)
- Kirkpatrick, C.G., Chen, R.T., Holmes, D.E., and Elliott,
K.R., In *Gallium Arsenide Materials, Devices, and
Circuits* (M.J. Howes and D.V. Morgan, eds.), p. 39 (J.
Wiley & Sons Ltd., 1985)
- Lagowski, J., Gatos, H.C., Parsey, J.M., Wada, K., Kaminska,
M., and Walukiewicz, W., Appl. Phys. Lett. 40, 342
(1982)

- Lagowski, J., Kaminska, M., Parsey, J., Gatos, H.C., and Walukiewicz, W., *Inst. Phys. Conf. Ser. No. 65*, p. 41 (1983)
- Lagowski, J., Lin, D.G., Aoyama, T., and Gatos, H.C., *Appl. Phys. Lett.* **44**, 336 (1984)
- Lang, D.V., *J. Appl. Phys.* **45**, 3023 (1974)
- Lang, D.V., and Kimmerling, L.C., *Phys. Rev. Lett.* **33**, 489 (1974)
- Levinson, M., *Phys. Rev.* **B28**, 3660 (1983)
- Look, D.C., *Semiconductors and semimetals*, Vol. 19, p. 75 (1983)
- Mahajan, S., and Corbett, J.W., eds., *Defects in Semiconductors II* (North-Holland, 1983)
- Martin, G.M., Mitonneau, A., and Mircea, A., *Electron. Lett.* **13**, 191 (1977)
- Martin, G.M., Jacob, G., Hallais, J.P., Grainger, F., Roberts, J.A., Clegg, J.B., Blood, P., and Poiblaud, G., *J. Phys. C* **15**, 1841 (1982)
- Martin, G.M., and Makram-Ebeid, S., In *Deep Levels in Semiconductors* (S. Pantelides, ed., Gordon and Breach, 1984)
- Milnes, A.G., *Deep Impurities in Semiconductors* (Wiley, New York, 1973)
- Mircea, A., Mitonneau, A., Hollan, L., and Briere, A., *Appl. Phys.* **11**, 153 (1976)
- Mitonneau, A., Martin, G.M., and Mircea, A., *Inst. Phys. Conf. Ser. No. 33a*, p. 73 (1977a)
- Mitonneau, A., Martin, G.M., and Mircea, A., *Electron. Lett.* **13**, 666 (1977b)
- Mullin, J.B., Heritage, R.J., Holiday, C.H., and Straughan, B.W., *J. Cryst. Growth* **34**, 281 (1968)
- Mullin, J.B., In *Crystal Growth and Characterization* (R. Ueda and J.B. Mullin, eds.), p. 61 (North-Holland, 1975)
- Mullin, J.B., In *Crystal Growth of Electronic Materials* (E. Kaldis, ed.), p. 269 (North-Holland, 1985)
- Neumark, G.F., and Kosai, K., *Semiconductors and semimetals*, Vol. 19, -1 (1983)

- O'Hara, S., Hutchinson, P.W., and Dobson, P.S., Appl. Phys. Lett. 30, 368 (1977)
- Omel'yanovskii, E.M., Polyakov, A.Ya., Rytova, N.S., and Raikhshtein, V.I., Sov. Phys. Semicond. 20, 897 (1986)
- Petroff, P.M., and Lang, D.V., Appl. Phys. Lett. 31, 60 (1977)
- Sah, C.T., Forbes, L., Rosier, L.L., and Tasch, Jr., A.F., Solid-State Electron. 13, 759 (1970)
- Shanabrook, B.V., Klein, P.B., Swiggard, E.M., and Bishop, S.G., J. Appl. Phys. 54, 336 (1984)
- Takikawa, M., and Ikoma, T., Jpn. J. Appl. Phys. 19, L436 (1980)
- Taniguchi, M., and Ikoma, T., Inst. Phys. Conf. Ser. No. 65, p. 65 (1982)
- Taniguchi, M., and Ikoma, T., J. Appl. Phys. 54, 6448 (1983)
- Thomas, R.N., Hobgood, H.M., Eldridge, G.W., Barrett, D.L., Braggins, T.T., Ta, L.B., and Wang, S.K., Semiconductors and semimetals, Vol. 20, p. 1 (1984)
- von Bardeleben, H.J., Stievenard, D., Bourgoïn, J.C., and Huber, A., Appl. Phys. Lett. 47, 970 (1985)
- Wagner, J.R., Krebs, J.J., Stauss, G.H., and White, A.M., Solid State Commun. 36, 15 (1980)
- Wessels, B.W., J. Appl. Phys. 47, 1131 (1976)
- Yoshie, O., and Kamihara, M., Jpn. J. Appl. Phys. 22, 621 (1983a)
- Yoshie, O., and Kamihara, M., Jpn. J. Appl. Phys. 22, 629 (1983b)
- Yu, P.W., Appl. Phys. Lett. 44, 330 (1984)
- Zou, Y.X., Zhou, J.C., Mo, P.G., Lu, F.Z., Li, L.S., Shao, J., Huang, L., Sun, H.H., Sheng, C., and Sun, Q., Inst. Phys. Conf. Ser. No. 65, p. 49 (1983)

2. Photo-Induced Transient Spectroscopy (PITS)

2.1 Introduction

Various methods have been applied to study the thermal emission of trapped carriers in semiconductors, the most notable of which is deep-level transient spectroscopy (DLTS) (Lang, 1974). This method uses a *time-window* or *rate-window* technique to study the temperature dependence of the emission rate of trapped carriers in a space-charge region. The parameter of interest is the capacitance across a p-n junction or a Schottky barrier.

The shortcoming of DLTS is the need to create a suitable junction or Schottky barrier. This junction can be easily created in low resistivity semiconductors but is difficult to achieve for high resistivity semiconductors. The principal reason is that once a barrier or junction is formed in a low carrier concentration material, the whole sample becomes a space-charge region (Bois, 1980) making the electrical generation of carriers ineffective.

In the past, the technique of thermally-stimulated conductivity has been the only photoelectronic method suitable for deep-level studies in high-resistivity or semi-insulating materials. However, this method suffers from the fact that the dark current tends to obscure the results especially at temperatures above 300 K.

A more efficient method is therefore needed for deep-level studies in high-resistivity material such as LEC.

SI GaAs. To solve this problem, a method known either as optical transient current spectroscopy (OTCS) or photo-induced transient spectroscopy (PITS) has been introduced (Hurtes et al., 1978; Fairman et al., 1979; Martin and Bois, 1978; Yoshie and Kamihara, 1983a,b). This method is similar in concept to that of DLTS with the main difference being that PITS uses optical excitation and involves the measurement of current, whereas DLTS uses electrical excitation and measures the capacitance transient.

In this chapter, we will discuss the theoretical basis of PITS and the design of a microcomputer-controlled PITS system.

2.2 Theory of PITS

2.2.1 Emission rate, ν

For simplicity, we will consider a simple model where there is only one electron trapping level in the band gap as shown in figure 2.1.

The processes shown in figure 2.1 are the emission of an electron from the trap with emission rate, ν , and the capture of an electron having a thermal velocity, v , from the conduction band by an unoccupied center which has a capture cross-section, σ .

It can be shown that at thermal equilibrium, the emission rate, ν , is given by:

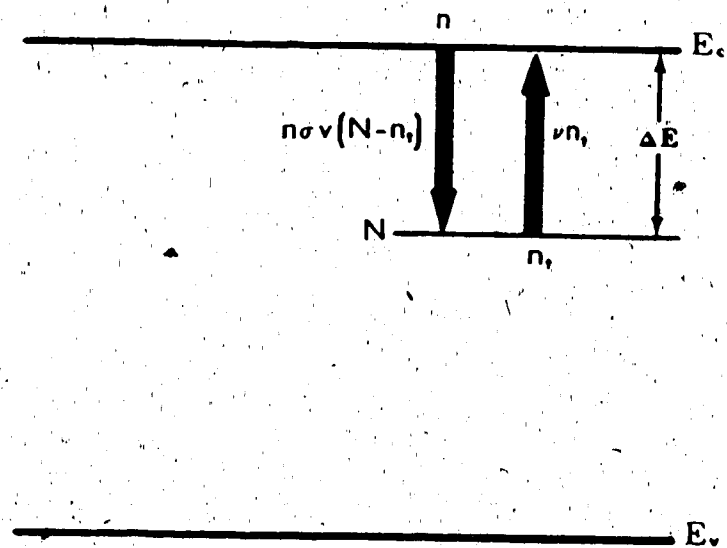


Figure 2.1 A single trap model

$$\nu = \frac{N_0 \sigma v}{g} \exp\left(-\frac{\Delta E}{kT}\right) \quad (2.1)$$

where N_0 = density of states in the conduction band

k = Boltzmann constant

ΔE = activation energy

T = temperature

g = degeneracy factor

v = thermal velocity

$$= (8kT/\pi m^*)^{1/2}$$

m^* = effective mass

$$\therefore \nu = \frac{16\pi m^* k^2 \sigma T^2}{gh^3} \exp\left(-\frac{\Delta E}{kT}\right) \quad (2.2)$$

where h = Planck's constant.

From a plot of $\ln(T^2/\nu)$ against $1/T$, the trap depth, ΔE , and the capture cross-section, σ , can be determined. The value of ΔE calculated from this equation is only an apparent value since the capture cross-section, σ , can be temperature dependent of the form $\sigma = \sigma(\infty) \exp(-E_b/kT)$, where E_b is the activation energy of the capture cross-section (Henry and Lang, 1977). Furthermore, the activation energy, ΔE , has also been found to be linearly dependent on temperature according to: $\Delta E = \Delta E_0 - \eta T$, where η is a constant (Mircea et al., 1977). However, the trapping parameters, ΔE and σ , calculated according to equation (2.2) are the values quoted in the literature and are used as the *signature* of a trapping center. Hence, we will dispense with the correction terms and proceed to use equation (2.2) even

though the trapping parameters may not have a direct physical meaning.

2.2.2 Transient current

By modifying the equations of Look (1983), the equation for the transient current can be written as:

$$i(t) = \frac{Cq\mu\nu}{\tau^{-1}-\nu} \frac{N}{1+(\nu/\beta)} [\exp(-\nu t) - \exp(-t/\tau)] + i_0 \exp(-t/\tau) \quad (2.3)$$

where $i(t)$ is the current, C is a constant containing the sample dimensions and applied voltage, μ is the electron mobility, q is the electronic charge, ν is the emission rate of the trapped carriers, N is the concentration of the trapping centers, t is the time from the end of the excitation pulse, τ is the free carrier lifetime, β is the filling rate of the traps, and i_0 is the maximum steady state photocurrent. A complete derivation of equation (2.3) is given in Appendix A.

It can be seen from equation (2.3) that the photocurrent decay consists of two components: a fast component due to free carrier recombination and a slow component due to detrapping from the defect centers. The volume free carrier lifetime, τ , in SI GaAs is $\sim 10^{-8}$ to 10^{-9} s (Look, 1983; Girard et al., 1984). Therefore, a few milliseconds after the end of the excitation pulse, or $t \gg \tau$, the terms involving $\exp(-t/\tau)$ will have become negligibly small. Thus, for $t \gg \tau$, and assuming that $\tau^{-1} \gg \nu$ and $\beta \gg$

equation (2.3) can be simplified to:

$$i(t) = Cq\mu\tau N\nu \exp(-\nu t) \quad (2.4)$$

This equation is similar to equation (9) of Yoshie and Kamihara (1983a). This equation assumes only electron conduction. A similar equation also applies for hole conduction.

2.3 PITS signal

The PITS signal is obtained by sampling the photocurrent signal at two different instants of time, t_1 and t_2 , after the extinction of the excitation source (figure 2.2). Since the mobility, μ , and the free carrier lifetime, τ , are also temperature dependent, it is more convenient to normalise the PITS signal to eliminate the effects of the temperature dependence of these two terms.

The normalised PITS signal, $\Delta I(T)$, is then given by:

$$\Delta I(T) = \frac{1}{i_0} [i(t_1) - i(t_2)] \quad (2.5)$$

where $i_0 = Cq\mu I_0\alpha\tau$
 $=$ maximum photocurrent
 $I_0 =$ excitation intensity
 $\alpha =$ absorption constant

$$\therefore \Delta I(T) = \frac{N\nu}{I_0\alpha} [\exp(-\nu t_1) - \exp(-\nu t_2)] \quad (2.6)$$

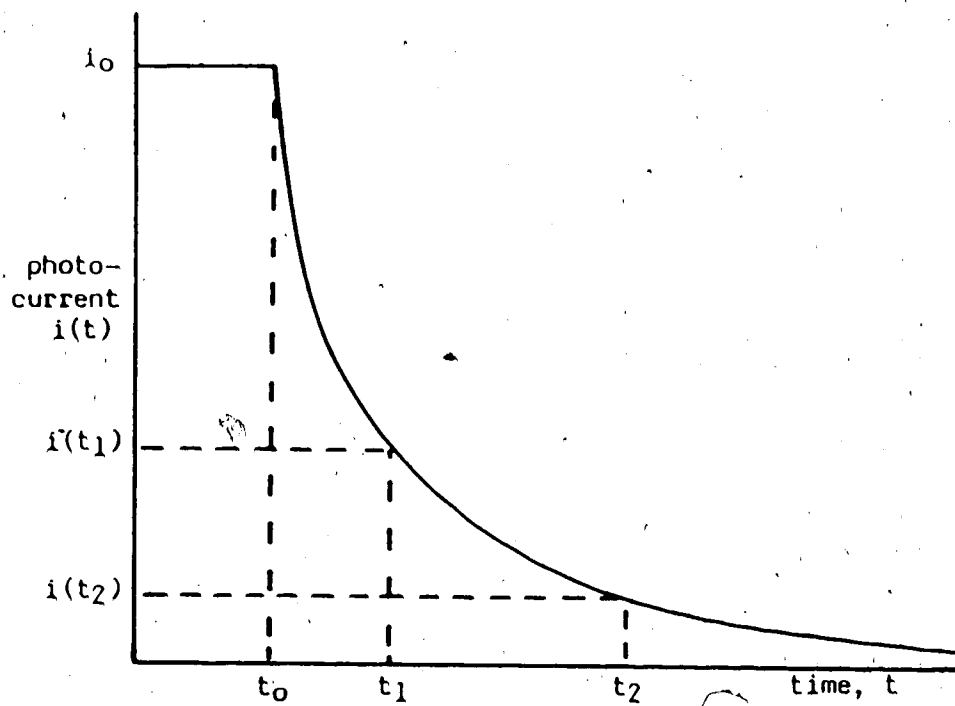


Figure 2.2 Sampling of the photocurrent signal

The thermal emission rate, ν , can be determined by differentiating equation (2.6) with respect to ν and equating it to zero:

$$\frac{d\Delta I(T)}{d\nu} = (1-\nu t_1)\exp(-\nu t_1) - (1-\nu t_2)\exp(-\nu t_2) \quad (2.7)$$

$$= 0$$

$$\therefore \exp[-\nu(t_2-t_1)] = \frac{1-\nu t_1}{1-\nu t_2} \quad (2.8)$$

For particular values of t_1 and t_2 , ν can be calculated from equation (2.8) using an iterative procedure. Table 2.1 lists the corresponding value of ν for a given value of t_1 and a fixed ratio $(t_2/t_1) = 5$, calculated from equation (2.8). Table 2.1 can be used to find the value of ν corresponding to a particular value of t_1 without having to recalculate the value of ν whenever ν is required.

A PITS curve is a plot of PITS signal against temperature for given values of t_1 and t_2 . The values of t_1 and t_2 actually determine the rate window according to equation (2.8). At different temperatures, the emission rate of the trapped carriers will be different and a peak will appear at a temperature in the PITS curve, when the emission rate at that temperature is equal to the rate window set by t_1 and t_2 . It is advisable to keep t_2/t_1 a constant and vary t_1 and t_2 to set the different rate windows. PITS signals for a series of t_1 and t_2 (series of different rate windows) have to be plotted in order to obtain a series of peaks corresponding to emission from a trapping center. Each of these peaks will occur at a different temperature, T_n , for a

Table 2.1: Emission rate, ν (s⁻¹),
for different delay, t_1 (s), with $t_2/t_1 = 5$.

DELAY, t_1	EMISSION RATE, ν
0.005	211.47
0.006	176.06
0.007	151.48
0.008	132.30
0.009	117.71
0.010	105.24
0.011	95.58
0.012	87.53
0.013	80.95
0.014	75.74
0.015	69.82
0.016	66.15
0.017	61.67
0.018	58.35
0.019	55.18
0.020	52.12
0.021	50.16
0.022	47.29
0.023	45.49
0.024	43.77
0.025	42.09

given rate window. From a series of t_1 and t_2 values, a corresponding series of ν values and the corresponding temperatures, T_m , can be obtained. A plot of $\ln(T_m^2/\nu)$ against $1/T_m$ will allow the trapping parameters to be obtained according to equation (2.2). The above procedure is illustrated in figure 2.3.

In the above derivation of the PITS equations, we have assumed that ohmic contacts are used. There are several reports in the literature (Hurtes et al., 1978; Martin and Bois, 1978) which treat the contacts as Schottky barriers. The corresponding equation for the photocurrent is given by:

$$i(t) = \frac{qWA}{2} \mu N \nu \exp(-\nu t) \quad (2.9)$$

where W = depth of the space-charge region

A = contact area.

The analysis of the PITS curves using equation (2.9) is similar to the treatment given above.

In the case of DLTS, the emission rate, ν , is given by:

$$\nu = \frac{\ln(t_2/t_1)}{t_2 - t_1} \quad (2.10)$$

From equation (2.10) a set of t_1 and t_2 values will give ν exactly. This is one of the significant differences between DLTS and PITS. However, there are reports which use equation (2.10) in the analysis of PITS data for the sake of simplicity. This practice is not advisable because the PITS peak occurs at higher temperature than that of DLTS for given values of t_1 and t_2 .

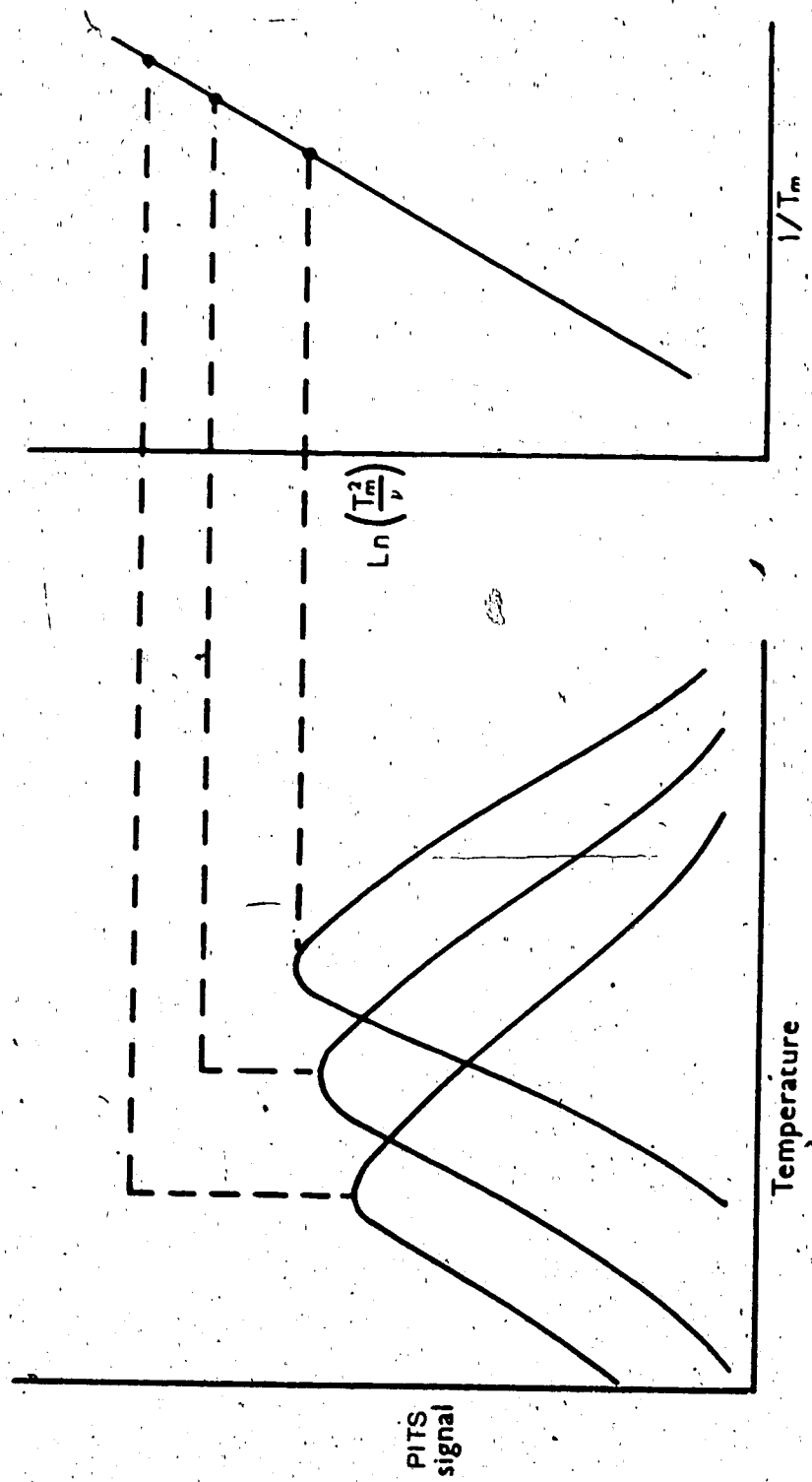


Figure 2.3 Analysis of PITS curves

2.4 Different Relaxation Times

It is important at this stage to consider the different time domains at which electronic processes occur within a semiconductor in which excess carriers have been generated.

Decay of space charge

When excess carriers are generated, whether by electrical injection or photoexcitation, a space charge $\rho(t)$ will be created. According to Spence (1958), the rate of change of this space charge is given by:

$$\frac{\partial \rho}{\partial t} = -\frac{4\pi\sigma_0}{\epsilon}\rho \quad (2.11)$$

where σ_0 = conductivity

ϵ = dielectric constant

The solution of equation (2.11) is:

$$\rho(t) = \rho_0 \exp(-t/\tau_{sp}) \quad (2.12)$$

$$\text{where } \tau_{sp} = \frac{\epsilon}{4\pi\sigma_0} \quad (2.13)$$

This expression for τ_{sp} can also be considered as the RC time constant of the sample and an identical expression can be obtained by considering the resistance and capacitance of the sample.

The sample and the two contacts can be considered as a network of capacitors and resistors as shown in figure 2.4. The RC product of the network can be found as follows:

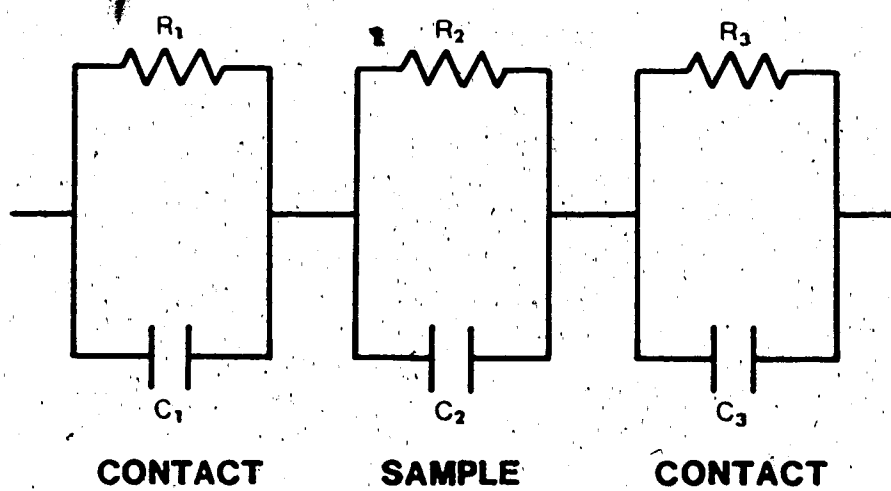


Figure 2.4 Equivalent RC network

$$\text{Total } R = R_1 + R_2 + R_3 \quad (2.14)$$

$$\text{Total } C = \frac{C_1 C_2 C_3}{C_1 C_2 + C_1 C_3 + C_2 C_3} \quad (2.15)$$

$$\begin{aligned} \tau_0 &= RC \\ &= (R_1 + R_2 + R_3) C_2 \end{aligned} \quad (2.16)$$

if $C_2 \ll C_1$ and $C_2 \ll C_3$.

For ohmic contacts, $R_1 \ll R_2$ and $R_3 \ll R_2$,

$$\therefore \tau_0 = R_2 C_2 \quad (2.17)$$

The resistance of the sample can be written as:

$$R = \frac{l}{\sigma_0 S} \quad (2.18)$$

where l = distance between the contacts

S = cross-sectional area of sample

σ_0 = conductivity.

The capacitance of the sample is:

$$C = \frac{\epsilon S}{4\pi l} \quad (2.19)$$

$$\therefore RC = \frac{\epsilon}{4\pi\sigma_0} \quad (2.20)$$

which is identical with equation (2.13).

For SI GaAs, $\epsilon = 12.85$; $\sigma_0 \approx 10^{-8} \Omega^{-1} \text{cm}^{-1}$

$$\therefore \tau_{sp} \approx 0.11 \text{ ms}$$

Mean free time

The mean free time of an electron, or the time between collisions, can be estimated from the equation:

$$\tau' = \frac{\mu m^*}{q} \quad (2.21)$$

For SI GaAs, $\mu \approx 4000 \text{ cm}^2/\text{Vs}$ at 300 K

$$m^* = 0.067 m_0$$

$$\therefore \tau' \approx 1.5 \times 10^{-13} \text{ s}$$

Free carrier lifetime of an electron

If a clean, polished surface is assumed with negligible surface recombination, then the effective lifetime, $\tau_{\text{eff}} \approx \tau \approx 10^{-8} - 10^{-9} \text{ s}$ in SI GaAs (Look, 1983; Girard et al., 1983).

It can be seen from the above discussion of the relaxation times of different physical mechanisms, that the limiting quantity is the dielectric relaxation time of the sample. It is important to realize that such a mechanism exists and precautions must be taken in the analysis of the PITS data. The photocurrent decay in a PITS experiment is usually sampled at a frequency of a few kilohertz. This means that the determination of the cut-off point of the excitation source has an error of the order of $10^{-4} - 10^{-3} \text{ s}$. Hence, the determination of t_1 and t_2 may be off by the same order. The calculated emission rate, ν , will also be affected. Although this may not seriously affect the slope of the graph of $\ln(T_m^2/\nu)$ versus $1/T_m$, it will affect the y-intercept. This means that the value of ΔE may not be affected much, but the value of the capture cross-section, σ , may be off by as much as a factor of 5. To avoid such a large error, it is advisable, therefore, to digitise or sample the photocurrent decay at the highest rate possible. However, the values of t_1 chosen for analysis should be a

few milliseconds after the extinction of the excitation source to take into account the large dielectric relaxation time.

2.5 Presence of Non-Exponential Transients

The theoretical basis of the PITS equations assumes that the decay of the photocurrent follows an exponential law, indicating that only the contribution from a single trapping level is predominant. In certain cases, however, the transient can be non-exponential due to contributions from two or more trapping levels. This means that there could be two or three components in the decay curve. In most cases where non-exponential transients occur, the decay consists of two exponential components.

Various techniques have been reported for dealing with non-exponential transients (Kirchner et al., 1981; Thurber et al., 1982; Yoshie and Kamihara, 1983b; Zdansky and Hien, 1984). Basically, there are two techniques for PITS and DLTS curves.

The first technique uses numerical curve-fitting of the raw data to give the emission rate, ν , directly. Suitable algorithms exist for numerical curve-fitting, the most popular of which is non-linear least-squares curve-fitting (Bevington, 1969). When a numerical curve-fitting technique is preferred, it is not necessary to use the rate window technique. Although the curve-fitting technique is immune to problems with non-exponential transients, it is an

inconvenient method for rapid and automatic characterisations of samples, besides requiring large computer memory.

The second technique involves choosing appropriate values of t_1 and t_2 which will allow the peaks to separate. This has been discussed, in the case of PITS, by Yoshie and Kamihara, (1982). A peak consisting of multiple components can be separated into two or more separate peaks by using small ratio of t_2/t_1 and widely changing the value of t_1 .

2.6 Contact Configurations

There are two different configurations for the contacts.

The first is the sandwich structure in which a semi-transparent thin film of metal is deposited on the front surface followed by a thicker layer on the back. The electric field applied across these two contacts is longitudinal to the direction of the excitation source. In this configuration, the electric field across the sample is usually higher than for the other configuration for a given thickness of the sample and the same voltage. The disadvantages of this configuration are: i) photovoltaic effect, ii) field-assisted detrapping and iii) non-uniformity of the contacts' characteristics from sample to sample.

The photovoltaic effect may cause the decay to be non-exponential. Field-assisted detrapping phenomenon such

as the Poole-Frenkel effect increases the emission rate of the carriers from the traps by lowering the potential barriers. This will also cause a change in the capture cross-section according to the relationship: $\sigma \propto E^{-3/2}$ (Dussel and Bube, 1966). The uniformity of the contacts from sample to sample is important if comparisons between the results are to be made. Uniformity of contacts is also important for different experiments on the same sample, such as depth profiling and annealing studies.

The second contact configuration is the coplanar structure. In this configuration, the two contacts are fabricated on the same surface. The distance between the contacts must be larger than the size of the illuminated spot. This enables the contacts to be shielded from illumination thus preventing photovoltaic effects. The metal deposited as contacts can also be of any thickness and the characteristics of the contacts are highly uniform from sample to sample. Owing to the fact that the distance between the contacts is usually about 2-3 mm, the applied electric field is usually less than 300 V/cm for $V = 50$ volts. This is a low field regime where field-assisted detrapping will be negligible.

2.7 PITS system

The schematic diagram of the PITS system is shown in figure 2.5.

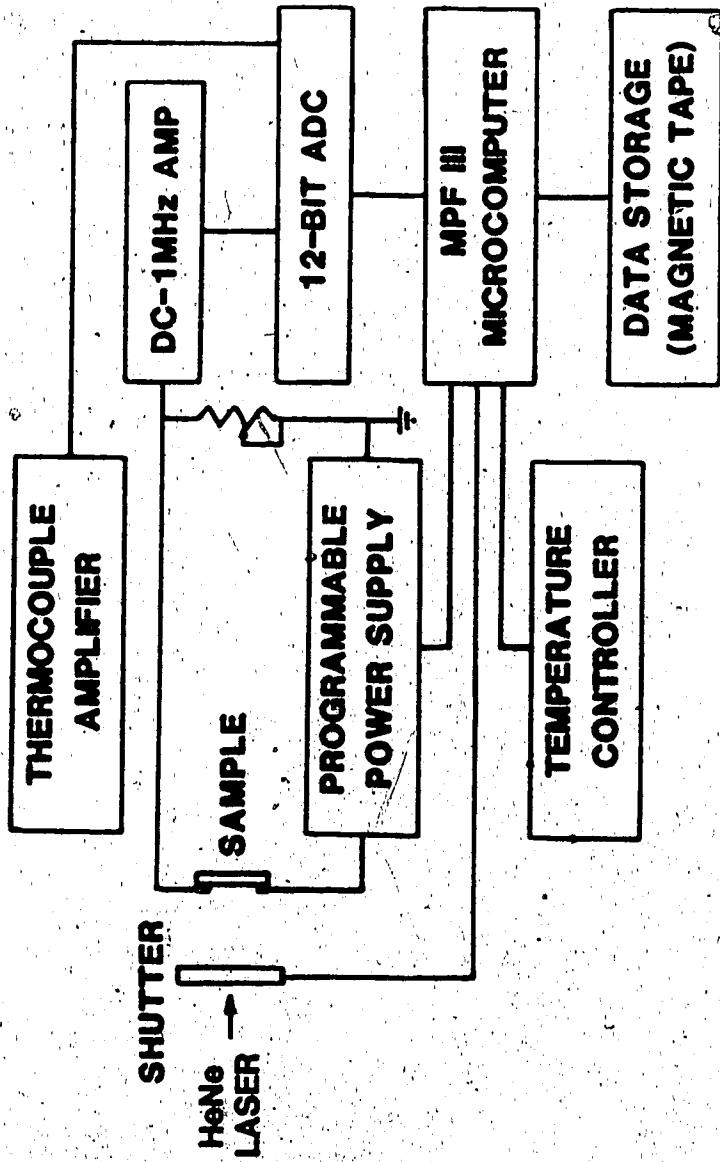


FIGURE 2.5 PITS SYSTEM

The heart of the system is a 64 K microcomputer (Multitech MPFIII) which controls a 12-bit, 8-channel analogue-to-digital (A-D) converter, a temperature-controller, a programmable power supply and the driver for an electro-mechanical shutter.

Basically, the microcomputer samples the temperature of the sample and activates the shutter driver when the temperature is within a given range of the temperature set-point. The shutter driver will then open the electro-mechanical shutter for 200 ms. The excitation source is a 1 mW He-Ne laser. The voltage created across a suitable load resistor by the photocurrent is first amplified by a fast amplifier before being fed into the 12-bit A-D converter. This signal is monitored using a Tektronix 7623A storage oscilloscope. A few milliseconds before the closure of the shutter, the microcomputer begins to digitize the amplified photovoltage signal using the 12-bit A-D converter. The subroutine to control the A-D converter is written in 6502 microprocessor machine language so that data transfer between the A-D converter and the microcomputer is done more rapidly. The PITS signal is then calculated immediately and the results stored in an array. A new temperature set-point is then sent to the temperature-controller and the sequence of events will repeat again until a final temperature is reached. The interval between temperature set-points can be varied through the software. At the end of the experiment, the PITS

data are automatically transferred to a floppy diskette. The data from this diskette will then be transferred, at a later time, to the University of Alberta's Amdahl 5870 computer for compiling and storage on 9-track magnetic tape.

We will discuss briefly the function of each component in the system. Detailed circuit diagrams are given in Appendix B.

2.7.1 Input-output board

The function of the input-output (I/O) board is to act as an intermediary between the microcomputer and the external devices such as the temperature-controller, programmable power supply and the electro-mechanical shutter driver. The I/O board has 16 control lines which means, theoretically, that it can control 16 different devices. However, in practice, certain devices require more than 1 control line.

2.7.2 Temperature-controller

The temperature set-point for the temperature-controller is provided by the microcomputer. The function of this controller is to provide regulation of the temperature of the sample while the microcomputer is busy performing other tasks such as analysing the PITS data. Another function of this controller is to provide a gradual increase in temperature of the sample to ensure thermal equilibrium and avoid thermal *backlash*. The temperature sensor is a

copper-constantan thermocouple and the range of temperature regulation is from 80 to 395 K.

Usually, this controller is not critically needed if the power to the heater is kept low such that the increase in temperature is about $1^\circ/\text{minute}$.

For experimental measurements below room temperature, the important factor for good temperature regulation is the ability to control and maintain the flow rate of liquid nitrogen to cool the sample.

2.7.3 Programmable power supply

A programmable power supply is needed in cases where a constant bias may lead to Joule heating of the sample. This can occur in low resistivity materials. When a continuous bias is not required the microcomputer will switch on the bias only when measurements are about to be made. However, when the resistance of the sample is low, an on-off bias will give a voltage spike.

A load resistor is connected in series with the sample so that the voltage drop due to the photocurrent can be obtained. The bias voltage appearing across the load resistor depends on the ratio of $R_{\text{load}}/(R_{\text{sample}}+R_{\text{load}})$. If the resistance of the sample is much larger than that of the load, or $R_{\text{sample}} \gg R_{\text{load}}$, then the bias appearing across the load will be $(R_{\text{load}}V_{\text{bias}}/R_{\text{sample}})$ and will be small. At high temperatures, the resistance of the sample will decrease and R_{sample} will no longer be very much larger than R_{load} , hence a

large proportion of the bias will be detected across the load resistor. To avoid this problem, a large capacitor, C_{load} , is connected at the output to filter out the DC voltage. An on-off bias in this mode will produce a voltage spike of the magnitude: $\delta V = \delta Q / C_{load}$, where δQ is the change of the charge across the capacitor. This voltage spike can be very large depending on the voltage being switched on or off and the switching time. If this problem is not remedied when it occurs, the fast amplifier will deteriorate due to constant overloading, which is also detrimental to the A-D converter, not mentioning the fact that no accurate measurement can be made, if measurements can be made at all.

In view of the above problem, we chose to use a constant bias because the resistivities of the SI GaAs samples are high and the current that flows through the sample is negligible.

2.7.4 Analogue-to-digital converter

The analogue-to-digital (A-D) converter is a 12-bit converter (Analogue Devices DAS1128) with a 20 μs conversion time. The 16 inputs are connected as 8 differential inputs. The full scale range is set at ± 5.12 V giving a resolution of 2.5 mV/bit. The microcomputer uses this A-D converter to keep track of the temperature and to digitize the signal. The interface for this A-D converter is designed for the Apple II+/e data bus and so can be used for all Apple II+/e microcomputers and compatibles, as long as it is located on

slot #4 of the microcomputer.

2.7.5 Electro-mechanical shutter system

The electro-mechanical shutter system (A.W. Vincent Associates, Inc.) consists of a driver (SD10) and a shutter (26L). The shutter driver is triggered by the microcomputer and the exposure time can be set on the front panel of the shutter driver. The present exposure time is set at 200 ms to ensure equilibrium of the trapping kinetics in the sample.

2.7.6 Amplifier

The amplifier* has a bandwidth of DC to 0.8 MHz. The gain of the amplifier can be set at either 87.7, 152.6 or 219.3. Noise from the microcomputer is reduced by an RC filter in the amplifier. Proper shielding and grounding of the components in the system have also contributed significantly in reducing the noise from the microcomputer. The signal from the amplifier is clean enough that signal averaging is not required. To overcome the effect of the dark current from the sample, a bias compensation circuit was added at the input of the amplifier.

2.7.7 Software

The complete listing of the software used is given in Appendix B. The program consists of a machine language

* This fast amplifier was designed and constructed by W. Siewert of the Electronics Shop.

subroutine to control the A-D converter and a main program written in Applesoft Basic.

The machine language subroutine can be modified to digitize any number of points. The delay between data points can also be set by changing the length of the delay loop in the subroutine.

The program is flexible and can be altered to suit any change in experimental procedure.

Bibliography

- Bevington, P.R., *Data Reduction and Error Analysis for the Physical Sciences* (McGraw-Hill, New York, 1969)
- Bois, D., In *Electronic Structure of Crystal Defects and of Disordered Systems*, p. 345 (Les Editions de Physique, France, 1980)
- Dussel, G.A., and Bube, R.H., *J. Appl. Phys.* 37, 2797 (1966)
- Fairman, R.D., Morin, F.J., and Oliver, J.R., *Inst. Phys. Conf. Ser. No. 45*, p. 134 (1979)
- Girard, P., Sicart, J., and Pistoulet, B., *Solid-State Electron.* 27, 195 (1984)
- Henry, C.H., and Lang, D.V., *Phys. Rev.* B15, 989 (1977)
- Hurtes, Ch., Boulou, M., Mitonneau, A., and Bois, D., *Appl. Phys. Lett.* 32, 821 (1978)
- Kirchner, P.D., Schaff, W.J., Maracas, G.N., and Eastman, L.F., Chappel, T.I., and Ransom, C.M., *J. Appl. Phys.* 52, 6462 (1981)
- Lang, D.V., *J. Appl. Phys.* 45, 3023 (1974)
- Look, D.C., *Semiconductors and semimetals*, Vol. 19, p. 75 (1983)
- Martin, G.M., and Bois, D., *Proc. Electrochem. Soc.* 78, 32 (1978)
- Mircea, A., and Mitonneau, A., *J. Phys. (Orsay, Fr)* 38, L41 (1977)
- Spence, E., *Electronic Semiconductors*, p. 116 (McGraw-Hill, 1958)
- Thurber, W.R., Forman, R.A., and Phillips, W.E., *J. Appl. Phys.* 53, 7397 (1982)
- Yoshie, O., and Kamihara, M., *Jpn. J. Appl. Phys.* 22, 621 (1983a)
- Yoshie, O., and Kamihara, M., *Jpn. J. Appl. Phys.* 22, 629 (1983b)
- Zdansky, K., and Hien, N.T.T., *phys. stat. sol. (a)* 81, 353 (1984)

3. PITS studies of deep levels in LEC SI GaAs with different carbon concentrations

3.1 Introduction

The technologically important semi-insulating behaviour of semi-insulating (SI) GaAs grown by the liquid-encapsulated Czochralski (LEC) process has been known to depend on the concentration of the deep donor, EL2 (Martin et al., 1980a,b; Thomas et al., 1981; Holmes et al., 1982). The semi-insulating characteristic is actually due to a compensation process between the EL2 level and a shallow acceptor level at about $E_v + 0.025$ eV which is due to carbon impurity (Sze and Irvin, 1966; Ashen et al., 1975). In order to produce the semi-insulating property, the concentration of EL2 must be greater or equal to the concentration of carbon. The preceding statement is true only for samples grown from an arsenic-rich melt. In samples grown from a gallium-rich melt, there is another level at $E_v + 0.073$ eV which also plays an important role in the compensation process. This deeper acceptor level at $E_v + 0.073$ eV has yet to be identified conclusively. There have been suggestions that this acceptor level at $E_v + 0.073$ eV could be due to either excess Ga (Ta et al., 1982), Ga_{As} (Elliott et al., 1982), V_{As} -B, Ga_1 -B or Ga_{As} -B (Thomas et al., 1984).

A version of this chapter has been accepted for publication in the May, 1987 issue of the Canadian Journal of Physics.

The critical As composition in the GaAs melt needed to produce semi-insulating n-type GaAs crystals is about 0.475 As atomic fraction. Crystals grown from melts having an As composition below this critical value are p-type. The p-type behaviour is due to the fact that the EL2 concentration is insufficient to compensate the carbon and the acceptor level at $E_v + 0.073$ eV. The effects of the stoichiometry of the melt on the EL2 concentration has been well-documented (Holmes et al., 1982; Thomas et al., 1984).

Presently, LEC SI GaAs crystals are grown from an As-rich melt in order to achieve a high-resistivity n-type material. Thus, the amount of carbon plays a critical role.

A high concentration of carbon in LEC SI GaAs crystals is detrimental to the thermal stability of the crystals (Obokata, 1986). The presence of a high concentration of carbon also affects the operating characteristics of field-effect transistors.

Carbon contamination of the crystals during the growth process is unavoidable and a complete removal of carbon is not only impossible but also inadvisable bearing in mind that it is involved in a compensation process with the deep donor level, EL2. A critical balance has thus to be achieved. Efforts to control the amount of carbon by varying the growth conditions, such as the water content of the boric oxide encapsulant (Hunter et al., 1984), the use of As-rich melt (Kikuta et al., 1986) and the size of the charge, have been made in industry in an attempt to arrive

at the optimum growth conditions to give crystals with highly reproducible and uniform characteristics.

Inada et al. (1987) have recently reported that the contamination by carbon is due to a reaction between the GaAs melt and gaseous oxides of carbon and not carbon particles. The source of carbon could be the graphite components in the hot zone of the crystal puller and the use of pyrolytic boron nitride-coated graphite components has resulted in low carbon concentration in the GaAs crystals (Inada, 1987).

The amount of water content in the B_2O_3 encapsulant has been found to affect the amount of impurity incorporation in the GaAs crystals (Kirkpatrick et al., 1984; Thomas et al., 1984). It has been found, for instance, that the concentrations of Si and B in GaAs crystals are dependent on the water content of the B_2O_3 encapsulant. GaAs crystals grown using *wet* B_2O_3 have lower concentrations of Si and B whereas *dry* B_2O_3 gives higher concentrations of Si and B.

There is a critical value of the water content in the B_2O_3 , above which the GaAs crystals produced will be semi-insulating. However, an increase in the amount of water in B_2O_3 also increases the occurrences of twinning.

Since studies of the effects of the water content in the B_2O_3 encapsulant, the mass of the charge and the concentration of carbon on the various defect levels using PITS have not been reported, we have undertaken to do such a study.

From our PITS measurements, we will show that the presence of the deep donor, EL2, is affected by the water content of the B_2O_3 encapsulant. The mass of the charge also affects the EL2 concentration. The carbon content of the sample was found to affect the intensity of the peak at around 240 K ($t_2 - t_1 = 20\text{ms}$; $t_1 = 5\text{ms}$) which corresponds to an energy level at about $E_c - 0.4\text{ eV}$, commonly referred to as EL5. This in turn gives us a clue as to the origin of this previously unassigned peak.

3.2 Experimental details

A range of samples with different growth conditions, together with details of the growth conditions, were supplied to us by Cominco Ltd., Trail, B.C. The concentrations of the carbon impurity were determined from the measurement of the far-infrared absorption at 582.5 cm^{-1} at 80 K using a Fourier Transform Infra-red (FTIR) spectrometer†.

The samples were then prepared for PITS measurements by etching with $5H_2SO_4:1H_2O_2:1H_2O$ solution for about 2 minutes. Ohmic contacts were then made by melting 99.9999 % indium directly onto the samples, followed by annealing at about 300-350 C for approximately 30 seconds in a HCl/N_2 atmosphere.

†Measurements done by C.K. Teh, using a Bruker FTIR spectrometer, courtesy of Dr. J.E. Bertie, Chemistry Department.

Temperature scans were made between 80 and 400 K with readings taken after every 2 degrees increase in temperatures as described in chapter 2. Analysis of the PITS signals was done as discussed in chapter 2.

3.3 Results

The PITS curves for the different samples grown with different grades of B_2O_3 but from the same size of charge are shown in figure 3.1. The PITS curves were obtained with time window $(t_2 - t_1) = 20ms$ and time $t_1 = 5ms$. Figure 3.2 shows the PITS curves for samples grown with the same grade of B_2O_3 but different masses of charge. The grades of B_2O_3 and the charges used in the growth of the samples, together with the carbon content from FTIR measurements, are tabulated in table 3.1. The trapping parameters for the prominent peaks obtained from the analysis of the PITS data are given in table 3.2.

3.4 Discussion

It has been reported that there are several trapping levels with activation energies in the vicinity of the well-known deep donor level, EL2 (Lagowski et al., 1984; Taniguchi and Ikoma, 1983; Yahata et al., 1986) This group of mid-gap levels including EL2 has been referred to as the EL2 family of levels or peaks. This family of levels appear as peaks between 330 and 355 K in the PITS curves reported here.

Table 3.1: Samples used in PITS measurements.

B : 1800-2200 p.p.m. water,

C : 1000-1500 p.p.m. water,

D : 500-800 p.p.m. water.

SAMPLE	CHARGE (kg)	B ₂ O ₃ type	CARBON CONC. x 10 ³ (cm ⁻³)
996S(P2)	8	B	82.03
996T(P2)	8	B	60.27
856S(P2)	8	C	17.91
856T(P2)	8	C	55.23
821S(P2)	8	D	17.27
821T(P2)	8	D	10.31
849S(P1)	4.5	C	0.55
849T(P1)	4.5	C	1.51

Table 3.2: Trapping parameters for the peaks
in figures 3.1 and 3.2.

PEAKS	ΔE (eV)	CROSS-SECTION, σ (cm ²)
A	1.00 ± 0.01	3.9×10^{-12}
B	0.82 ± 0.04	6.9×10^{-12}
C	0.76 ± 0.01	5.1×10^{-12}
D	0.75 ± 0.02	5.8×10^{-12}
E	0.76 ± 0.01	3.8×10^{-12}
F	0.59 ± 0.02	1.0×10^{-12}
G	0.42 ± 0.02	1.1×10^{-12}
H	0.41 ± 0.01	2.0×10^{-12}
I	0.16 ± 0.01	1.4×10^{-12}
J	0.10 ± 0.01	2.7×10^{-12}
K	0.14 ± 0.01	2.1×10^{-12}

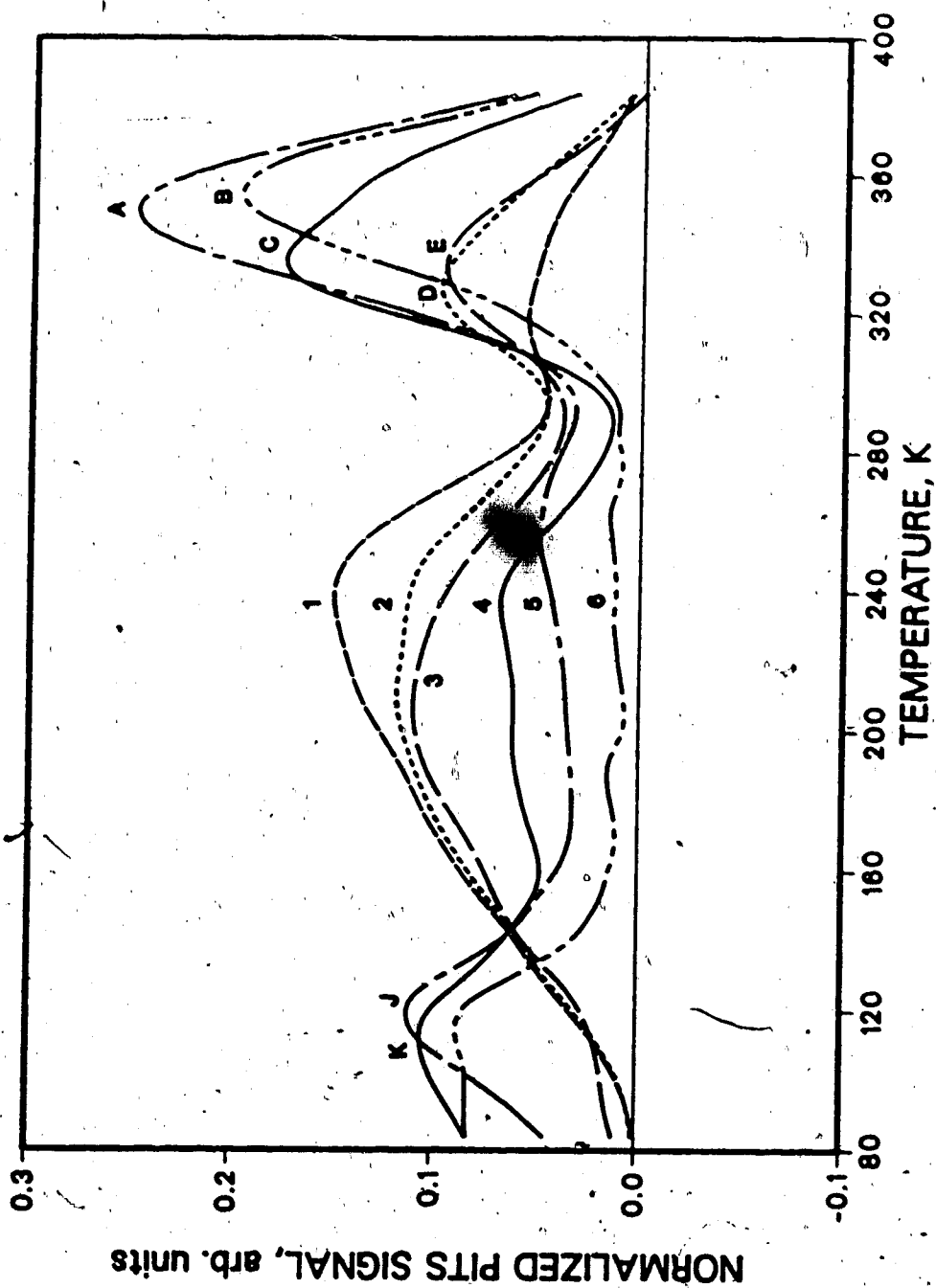


Figure 3.1 PITS curves for samples with different grades of B_2O_3 , but same mass of charge.
 1) 821T(P2); 2) 821S(P2); 3) 856S(P2);
 4) 856T(P2); 5) 996T(P2); 6) 996S(P2)

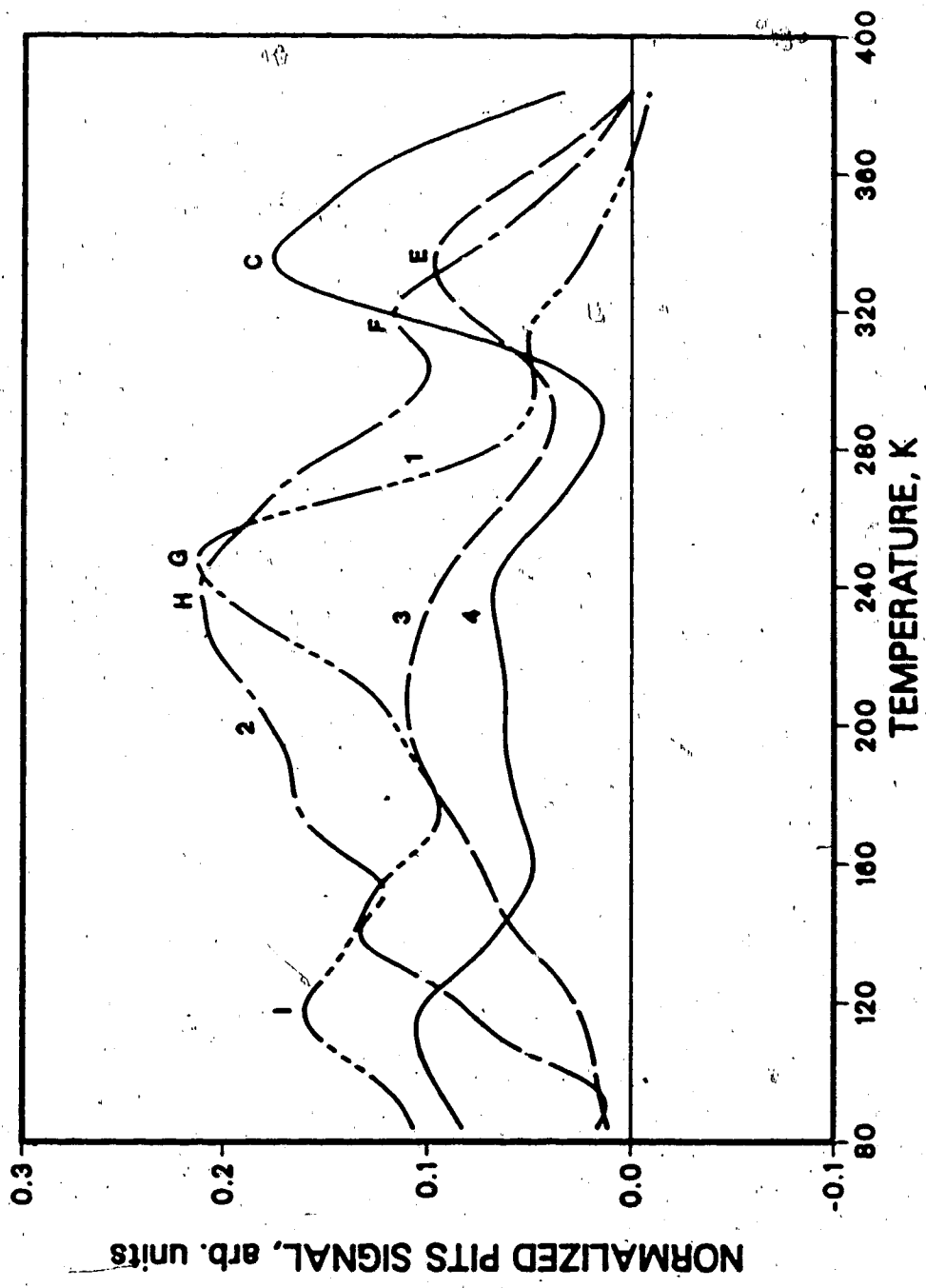


Figure 3.2 PITS curves for samples with the same grade of B₂O₃, but different mass of charge, 1) 849T(P1); 2) 849S(P1); 3) 856S(P2); 4) 856T(P2)

The presence of the EL2 family of levels can be seen in figure 3.1. There are three dominant peaks within the family. A comparison between the intensities of the EL2 family of peaks and the water content of the B_2O_3 encapsulant, for a fixed mass of charge, shows that there is a direct correspondence between the two quantities. At first glance, the intensities of the EL2 family of peaks seems to correspond directly to the carbon concentrations as well. A careful examination shows that this is not always true, which is not surprising in view of the origin of the EL2 defects which have been widely accepted as being due to defects involving As_{Ga} (Wagner et al., 1980; Lagowski et al., 1982a,b).

We will now discuss the possible mechanisms responsible for the observed dependence of the intensities of the EL2 family of peaks on the water content of the B_2O_3 encapsulant. Rumsby and Ware (1981) reported that gallium tends to be preferentially excluded from the melt when the water content of the B_2O_3 encapsulant is high. This exclusion process gives rise to a situation where the crystal is grown from an arsenic-rich melt. The presence of excess As coupled with the presence of V_{Ga} , due to the removal of gallium in the exclusion process, will then result in the formation of EL2.

Another explanation can be found from the relationship between dislocations and EL2. It has been found from etch-pit density (EPD) (which is a measure of dislocation

density) studies, that there is a correlation between the concentration of EL2 and EPD. Martin (1981) proposed that the relationship between EL2 and dislocation density could be due to thermally-induced stresses, although the exact mechanism is still unknown. The various models (Kirkpatrick et al., 1985) that have been suggested to account for the correlation between EL2, stress and dislocation density are dislocation climb, stress-enhanced creation of EL2 during cooling of the crystal after the growth process and gettering of EL2 at dislocations. The correlation between EL2 and dislocation density is not surprising in view of the fact that the phenomenon of migration of point defects to dislocations has been observed for a long time. The migration of defects in the vicinity of dislocations is due not only to a diffusion process resulting from a concentration gradient but also to an interaction potential between the two. A review on the kinetics of the migration of defects to dislocations has been given by Bulloch and Newman (1970). Whether there is any dependence of dislocation density on the moisture content of B_2O_3 has yet to be reported, although it has been known that increasing the water content of B_2O_3 increases the incidence of twinning (AuCoin et al., 1979; Kirkpatrick et al., 1985). Cockayne et al., (1981) found that in the growth of LEC InP crystals, there is a relationship between the water content of B_2O_3 and the formation of defect clusters. It is not preposterous, therefore, to suggest that the water content

of B_2O_3 may contribute to the formation of dislocations by increasing the thermal gradient across the melt/ B_2O_3 interface. This formation of dislocation would then induce the clustering of defects such as EL2.

Referring to figure 3.2, it can be seen that for a given grade of B_2O_3 , the intensities of the EL2 emission peaks are proportional to the size of the charge. This is probably due to the greater number of dislocations that tend to occur in large-size crystals as a result of higher thermally induced stresses. It has been shown that dislocation can be avoided for small-diameter ($< 15\text{mm}$) GaAs crystals (Steinemann and Zimmerli, 1963) but attempts to grow large dislocation-free GaAs have thus far been unsuccessful.

Another peak of interest in figure 3.2 is the peak at about 320 K. This emission peak is usually referred to as EL3. It has been suggested in the literature (Martin and Makram-Ebeid, 1983; Frank, 1986) that this level could be related to the anti-site defect As_{Ga} . If this is true, then the intensity of this peak should increase with the intensity of the EL2 family of peaks. In these studies, however, it can be seen that the intensity of the EL3 peak is inversely related to that of the EL2 peak. In certain cases where there are EL3 peaks, the EL2 peaks are absent. This observation does not support the proposals that EL3 is related to EL2.

The broad emission peaks between 220 and 260 K, as shown in figure 3.1, are believed to be due to a

superposition of EL6 (at 200 K), EL5 (at 240 K) and probably EL3 (at about 300 - 320 K). The intensity of this broad peak is inversely dependent on the amount of carbon. These peaks also seem to depend on the water content of B_2O_3 , but this dependence is not consistent. The activation energy of the broad peak around 240 K is about 0.4 eV. The inverse dependence of the peak at 240 K on the carbon content shows that it is due to V_{As} . This conclusion is arrived at by assuming that the formation of $V_{As}-C_{As}$ complexes depends directly on the carbon concentration and will cause a decrease in the concentration of free V_{As} . Hence, a decrease in the concentration of carbon leads to a decrease in $V_{As}-C_{As}$ and an increase in V_{As} and vice versa.

This proposal is supported by the theoretical calculation of Bachelet et al. (1981) which shows that an ideal V_{As} in GaAs will occupy a level at $E_c - 0.46$ eV.

In electron-irradiated GaAs, a defect level known as E3 is often seen (Lang, 1977). This defect has the same energy level as EL5. It has been found that E3 is formed by displacement in the As sublattice (Lang, 1977; Loualiche et al., 1982). Since the material in which E3 is observed is As-rich, Kirkpatrick et al. (1985) proposed that this defect is an As interstitial. If EL5 is indeed the same as E3, then EL5 could be related to As. The inverse dependence on carbon as mentioned above could then be due to the formation of $C_{As}-As_i$ at the expense of isolated or free As_i . However, As_i is an acceptor whereas EL5 is a donor level. Thus, the

suggestion of EL5 being due to As_i must be erroneous.

The dependence of this broad peak on the carbon content also indicates that the origins of EL6 and EL3 are defects involving V_{As} . This proposal is slightly different from that of Frank (1986) who proposed that EL6 could be due to isolated V_{As} .

The origin of the emission peaks at 120 K is not known. The intensity of this peak does not seem to be related to any of the growth parameters.

3.5 Conclusion

From PITS measurements of different samples of LEC SI GaAs grown with different growth parameters and containing different amount of carbon, we have found that the main electron trapping center, EL2, is dependent on the water content of the B_2O_3 encapsulant. We have proposed that thermally induced stresses and the stoichiometry of the melt are the two possible mechanisms that would explain the relationship between the concentration of EL2 and the water content of B_2O_3 . The high concentrations of EL2 and carbon in those samples grown using B_2O_3 with higher water content explain the reason why GaAs crystals grown using *wet* B_2O_3 encapsulant has a higher resistivity than those grown with *dry* B_2O_3 . On the other hand, a *wet* B_2O_3 encapsulant causes twinning to occur. A compromise, therefore, has to be found so that the crystals can be both highly resistive and monocrystalline.

We have also found that the larger the charge used, the higher will be the EL2 concentration due probably to a higher thermally-induced stress.

The inverse dependence of the intensity of the EL5 peak on the carbon concentration shows that the origin of the EL5 level could be isolated V_{AB} . The results also allow us to conclude that both EL6 and EL3 are related to V_{AB} .

Bibliography

- Ashen, D.J., Dean, P.J., Hurle, D.T.J., Mullin, J.B., White, A.M., and Green, P.D., *J. Phys. Chem. Solids* 36, 1041 (1975)
- AuCoin, T.R., Ross, R.L., Wade, M.J., and Savage, R.O., *Solid State Technol.* 22, 59 (1979)
- Bachelet, G.B., Baraff, G.A., and Schluter, M., *Phys. Rev. B* 24, 15 (1981)
- Bullogh, R., and Newman, R.C., *Rep. Prog. Phys.* 33, 101 (1970)
- Chen, R.T., Holmes, D.E., and Asbeck, P.M., *Appl. Phys. Lett.* 45, 459 (1984)
- Cockayne, B., Brown, G.T., and MacEwan, W.R., *J. Cryst. Growth* 51, 461 (1981)
- Elliott, K.R., Holmes, D.E., Chen, R.T., and Kirkpatrick, C.G., *Appl. Phys. Lett.* 40, 898 (1982)
- Frank, W., *Inst. Phys. Conf. Ser. No. 79*, p. 217 (1986)
- Holmes, D.E., Chen, R.T., Elliott, K.R., and Kirkpatrick, C.G., *Appl. Phys. Lett.* 40, 46 (1982)
- Hunter, A.T., Kimura, H., Baukus, J.P., Winston, H.V., and Marsh, O.J., *Appl. Phys. Lett.* 44, 74 (1984)
- Inada, T., Fujii, T., Kikuta, T., and Fukuda, T., *Appl. Phys. Lett.* 50, 143 (1987)
- Kikuta, T., Emori, H., Fukuda, T., and Ishida, K., *J. Cryst. Growth* 76, 517 (1986)
- Kirkpatrick, C.G., Chen, R.T., Holmes, D.E., Asbeck, P.M., Elliott, K.R., Fairman, R.D., and Oliver, J.R., *Semiconductors and semimetals*, Vol. 20, p. 159 (1984)
- Kirkpatrick, C.G., Chen, R.T., Holmes, D.E., and Elliott, K.R., In *Gallium Arsenide Materials, Devices and Circuits* (M.J. Howes and D.V. Morgan, eds.), p. 39 (J. Wiley & Sons Ltd., 1985)
- Lagowski, J., Gatos, H.C., Parsey, J.M., Wada, K., Kaminska, M., and Walukiewicz, W., *Appl. Phys. Lett.* 40, 342 (1982a)

- Lagowski, J., Parsey, J.M., Kaminska, M., Wada, K., and Gatos, H.C., In *Semi-Insulating III-V Materials* (S. Makram-Ebeid and B. Tuck, eds.), Vol. 2, p. 154 (Shiva, Nantwich, England, 1982b)
- Lagowski, J., Lin, D.G., Aoyama, T., and Gatos, H.C., *Appl. Phys. Lett.* 44, 336 (1984)
- Lang, D.V., *Inst. Phys. Conf. Ser. No. 31*, p. 70 (1977)
- Loualiche, S., Giullot, G., Nouhailhat, A., and Bourgoïn, J., *Phys. Rev. B* 26, 7090 (1982)
- Martin, G.M., Jacob, G., and Poiblaud, G., *Acta Electron.* 23, 37 (1980a)
- Martin, G.M., Farges, J.P., Jacob, G., Hallais, J.P., and Poiblaud, G., *J. Appl. Phys.* 51, 2840 (1980b)
- Martin, G.M., Jacob, G., Poiblaud, G., Goltzene, A., and Schwab, C., *Inst. Phys. Conf. Ser. No. 59*, p. 281 (1981)
- Martin, G.M., and Makram-Ebeid, S., *Physica* 116B, 371 (1983)
- Obokata, T., Okada, H., Katsumata, T., and Fukuda, T., *Jpn. J. Appl. Phys.* 25, L179 (1986)
- Steinemann, A., and Zimmerli, U., *Solid-State Electron.* 6, 597 (1963)
- Sze, S.M., and Irvin, J.C., *Solid-State Electron.* 9, 143 (1966)
- Ta, L.B., Hobgood, H.M., and Thomas, R.N., *Appl. Phys. Lett.* 41, 1091 (1982)
- Taniguchi, M., and Ikoma, T., *J. Appl. Phys.* 54, 6448 (1983)
- Thomas, R.N., Hobgood, H.M., Eldridge, G.W., Barrett, D.L., and Braggins, T.T., *Solid-State Electron.* 24, 337 (1981)
- Thomas, R.N., Hobgood, H.M., Eldridge, G.W., Barrett, D.L., Braggins, T.T., Ta, L.B., and Wang, S.K., *Semiconductors and semimetals*, Vol. 20, p. 1 (1984)
- Wagner, J.R., Krebs, J.J., Stauss, G.H., and White, A.M., *Solid State Commun.* 36, 15 (1980)
- Yahata, A., Kikuta, T., and Ishida, K., *Jpn. J. Appl. Phys.* 25, L133 (1986)

4. PITS and Photoluminescence Studies of Copper-contaminated LEC SI GaAs

4.1 Introduction

Liquid-encapsulated Czochralski (LEC)-grown semi-insulating GaAs is presently used as substrate material in the fabrication of GaAs devices such as laser diodes, light-emitting diodes (LED), field-effect transistors (FET) etc. The maintenance and durability of the semi-insulating property of the substrates is critical to the efficiency and reliability of such devices. The presence of copper in the device substrate can easily cause a rapid deterioration of the device by forming non-radiative recombination centers and also by compromising the high-resistive nature of the substrate. The presence of copper has been shown to play a detrimental role in devices such as GaAs tunnel diodes (Bahraman and Oldham, 1972) and LEDs (Bergh and Dean, 1972). The presence of non-radiative recombination centers, that can be created by copper in GaAs through complex formation with native defects, can facilitate the diffusion of defects and induce dislocations climb.

Copper is an ubiquitous impurity with a high diffusion coefficient and high solubility (Hall and Racette, 1964) in GaAs. Its ability to form electrically active complexes in GaAs after annealing at high temperatures is a pressing problem because annealing at 850°C for 15 minutes in an

A version of this chapter has been submitted for publication in the Journal of Applied Physics.

argon atmosphere is a standard procedure after ion implantation in the device fabrication process (Stolte, 1984).

The presence of copper impurities in GaAs has been studied extensively using luminescence (eg. Fabre, 1972; Vorobkalo et al., 1973; Glinchuk et al., 1982; Wang et al., 1985), photoconductivity (Bube and MacDonald, 1962), Hall effect (Quisser and Fuller, 1966; Rosi et al., 1960), thermally-stimulated conductivity (Blanc et al., 1964) and deep-level transient spectroscopy (DLTS) (Mitonneau et al., 1977; Lang and Logan, 1975; Kumar and Ledebro, 1981; Kullendorff et al., 1983). A survey of the results shows that copper is responsible for a wide variation of energy levels ranging from $E_v + 0.2$ to $E_v + 0.6$ eV. The observed range of energy levels could, for example, be due to any of the following: 1) the formation of copper complexes (Guisland et al., 1978; Vorobkalo et al., 1973; Mil'vidskii et al., 1971); 2) the concentration dependence of the activation energy of the trapping centers (Harvey, 1961) and 3) the multiple charge state of copper (Hall and Racette, 1964; Milnes, 1973). Each of these proposals is equally plausible in explaining the wide variation of the activation energies of copper-related defects in GaAs as observed by various investigators. The problem that still remains is to determine which is the most likely mechanism. The ability of copper to form complexes with the native defects in GaAs has been most widely accepted. However, the variety of complexes

that can be formed is stupendous and to date, copper-related complexes such as $V_{As}Cu_{Ga}V_{As}$ (Guislain et al., 1978), $Cu_{Ga}V_{As}$ (Guislain et al., 1978; Vorobkalo et al., 1973; Mil'vidskii et al., 1971) and $Cu_{Ga}V_{As}Cu_{Ga}$ (Mil'vidskii et al., 1971) have been proposed. In spite of widespread interest for the past two decades, there is still a lack of consensus as to the most probable mechanism of formation and the nature of the complexes. Furthermore, there is very little correlation between results from optical and electrical measurements, which contributes further to the controversy surrounding the nature of copper complexes in GaAs.

In this chapter, the results to be presented are based on photo-induced transient spectroscopy (PITS) and photoluminescence studies of copper-contaminated LEC SI GaAs. The application of PITS in these studies allows depth profiling measurements to be made by chemical etching, giving details of defects levels much deeper into the sample. This is one advantage over DLTS besides the fact that it is unnecessary to make junctions or Schottky barriers, which is a very difficult, if not impossible, process for semi-insulating materials.

The defect levels between $E_v + 0.50$ and $E_c - 0.59$ eV will be the main subject of this chapter in view of the fact that the competition between the two emission processes as a result of copper impurities has not been observed by photoelectronic measurements. These two trapping levels are due to different defect centers as can be seen from the fact

that the capture cross-sections differ by about three orders of magnitude.

Supporting evidence from photoluminescence spectra, measured at different depths from the surface of the samples, will also be presented to show the presence of copper.

4.2 Experimental details

In this study, an annealing step at 850°C was carried out to simulate the annealing process during device fabrication. However, the length of annealing time in these studies was much longer than 15 minutes in order to increase the effect. The major problem is to introduce a limited amount of copper into the samples such that the resistivity of each sample is still high enough for accurate PITS measurements to be made. Deliberate introduction of copper by vacuum evaporation of a copper film or electroplating in copper sulphate solution, followed by annealing at 850°C, always produce samples with low resistivities due to the very rapid diffusion and high solubility of copper in GaAs at elevated temperatures.

In one exploratory experiment, we tried copper diffusion by placing a piece of 99.9999 % copper near to a SI GaAs sample, followed by annealing in an evacuated quartz ampoule at 850°C for 24 hours with an arsenic pressure of about 1 Torr, resulted in a low-resistivity wedged shaped GaAs sample. We believe that this baffling result is due to

an enhanced rate of removal of Ga and As from the sample. Arsenic is then deposited on the copper, forming a liquid compound at 850°C, which is probably Cu_3As (m.p. 830°C). We further postulate that the partial pressure of As_4 within the ampoule is considerably reduced when the As_4 molecules react with the nearby copper to form Cu_3As . To maintain the partial pressure, more GaAs material has to dissociate to give free As_4 until an equilibrium is reached, which resulted in a wedge-shaped sample. In the process, copper also diffuses into the GaAs sample resulting in a low-resistivity material. Annealing in the absence of copper did not produce such a wedge-shaped sample which supports the above proposal.

An indirect method of copper introduction was finally adopted. Since standard quality quartz tubing is known to be copper contaminated, annealing in a quartz ampoule at 850°C for about 24 hours was used to introduce sufficient copper into the samples.

Samples of SI GaAs were annealed, in the presence of excess arsenic at 850°C for 24 hours in a quartz ampoule which was then evacuated to about 2×10^{-5} Torr and then sealed. The arsenic partial pressure in the ampoule was maintained at about 1 Torr by heating the excess amount of arsenic in a low temperature zone of the furnace. The quartz ampoule had first been cleaned with aqua regia ($2\text{HCl}:\text{HNO}_3$), followed by dilute HF solution and then finally rinsed with deionised water. Neutron activation analysis has shown that

in spite of the cleaning process mentioned above, the amount of copper in the quartz tubing was about 1.4 ppm (Hulicius et al., 1986). This amount of copper is high enough to contaminate the samples after prolonged exposure at elevated temperatures. The amount of copper in the annealed samples was such that the resistivity at 25°C was about $2.5 \times 10^5 \Omega \text{ cm}$. This value of the resistivity shows that the amount of copper in the samples has not reached the solubility limit of copper in GaAs ($\approx 5 \times 10^{17} \text{ cm}^{-3}$ at 850°C). A longer annealing time would allow the amount of copper in the samples to reach its solubility limit. This would increase the conductivity of the samples to a level where PITS measurements would be impractical.

Before annealing, the samples were etched in $5\text{H}_2\text{SO}_4:1\text{H}_2\text{O}_2:1\text{H}_2\text{O}$ solution for about 1 minute. After annealing, the samples were first chemo-mechanically polished with 2% bromine solution on lint-free tissue paper (LABX 170), followed by etching in $5\text{H}_2\text{SO}_4:1\text{H}_2\text{O}_2:1\text{H}_2\text{O}$ solution for about 30 seconds to remove surface damage. Ohmic contacts for PITS measurements were made by melting 99.9999% indium directly onto the sample, followed by annealing at about 300-350°C for about 30 seconds in a HCl/N_2 atmosphere.

The description of the computerised PITS system has been given in chapter 2. Most of the PITS results reported here were obtained between 273 and 400 K because the peaks of interest for this study occur between 300 and 390 K. PITS data were analysed in the standard way, by finding the

temperature, T_m corresponding to a peak of the PITS curves for various values of the time gate ($t_2 - t_1$). The time ratio (t_2/t_1) is fixed at 5. The emission rate, ν , is obtained by iteratively solving the equation:

$$\exp[-\nu(t_2 - t_1)] = \frac{1 - \nu t_1}{1 - \nu t_2} \quad (4.1)$$

The emission rate, ν , is related to the temperature, T_m , by:

$$\nu = \frac{N_0 \sigma v}{g} \exp\left(-\frac{\Delta E}{kT}\right) \quad (4.2)$$

where N_0 = density of state in the relevant band

σ = capture cross-section

v = thermal velocity

$$= (8kT_m/\pi m^*)^{1/2}$$

g = degeneracy of the level

m^* = effective mass

k = Boltzmann constant

ΔE = activation energy

The activation energy, ΔE , and the capture cross-section, σ , can be evaluated from a graph of $\ln(T_m^2/\nu)$ against $1/T_m$.

Photoluminescence spectroscopy measurements[‡] were made to confirm the presence of copper impurity in the samples. The presence of copper impurity in GaAs can be easily

[‡]Photoluminescence measurements were done with the help of C.K. Teh. Details of the photoluminescence spectroscopy system can be found in her Ph.D. thesis (University of Alberta, 1987).

detected as a 1.36 eV emission line in the photoluminescence spectrum.

Photoluminescence measurements were done with the samples at 4.2 K in a 'Cryotran' continuous flow optical cryostat. A tunable dye-laser (PRA LN102) pumped by a nitrogen laser (PRA LN1000) is used as an excitation source. The excitation wavelength used is 620 nm. The luminescence signal is digitised by a fast 8-bit analogue-to-digital converter. The collection of data and the control of the grating monochromator's setting are carried out automatically by a Timex/Sinclair 1000 microcomputer. Data are then sent serially by RS232 cable to an Osborne 1 microcomputer for analysis, storage and plotting.

4.3 Results

In all the PITS curves shown here, the time t_1 is 5 ms and the time window ($t_2 - t_1$) is 20 ms.

Curve 1 of figure 4.1 shows the PITS curve for an unannealed sample of LEC SI GaAs. Curves 2, 3, 4, 5 and 6 of figure 4.1 shows the PITS curve taken at different depths, for a control sample. The control sample was prepared by annealing at 850°C for 24 hours in a quartz ampoule which had been soaked in aqua regia solution for 24 hours followed by soaking in KCN solution for another 24 hours, then cleaned with dilute HF solution for about 1 hour, and finally rinsed in deionised water.

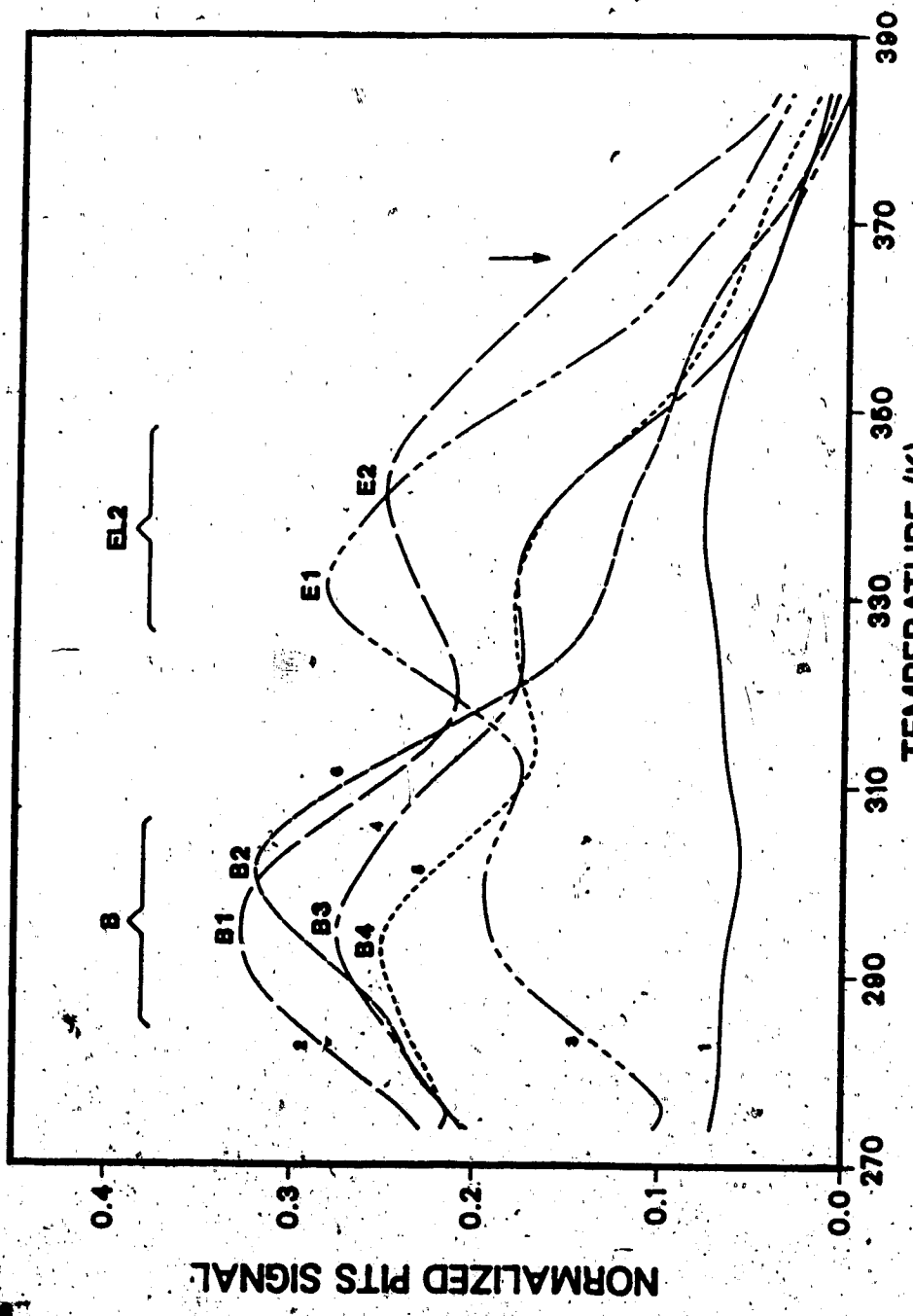


Figure 4.1 PITS curves for both unannealed and control samples.
1) unannealed sample; (2,3,4,5,6) control sample after etching the top surface for the following length of time: 2) 0.5 min.; 3) 3.5 min.; 4) 6.5 min.; 5) 9.5 min.; 6) 18.5 min.

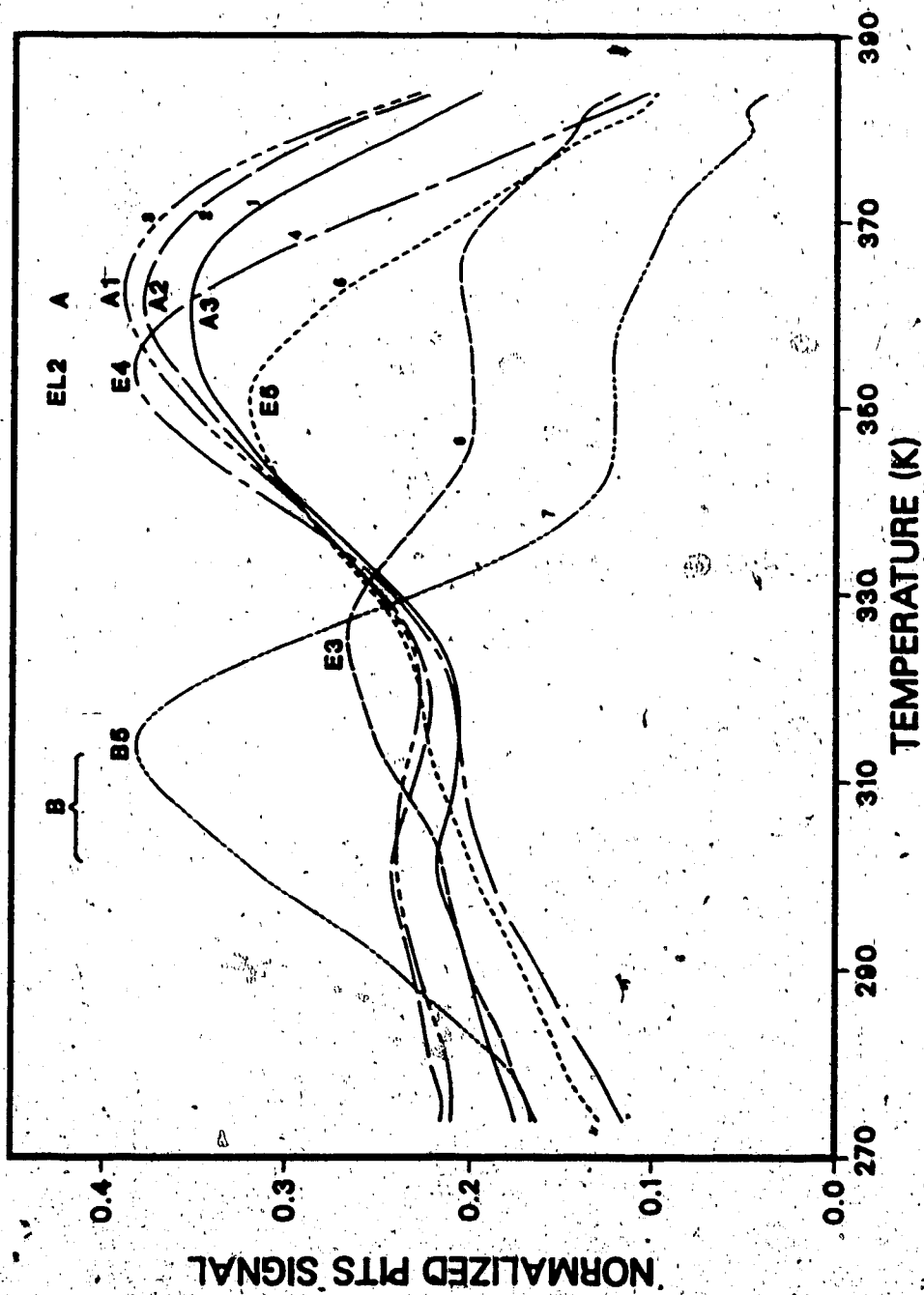


Figure 4.2 PITS curves for copper-contaminated sample.
 Etching time: 1) 0.5 min.; 2) 1.0 min.;
 3) 1.5 min.; 4) 10.5 min.; 5) 16.5 min.;
 6) 22.5 min.; 7) 28.5 min.

Figure 4.2 shows the PITS curves, taken at different depths from the surface, for the deliberately copper-contaminated sample. The temperature range in the depth profiling measurements was, from 273 to 400 K. Only a few representative curves are given in figure 4.2 to avoid cluttering. Depth profiling curves were taken after etching one side of the sample for a specified length of time in $5\text{H}_2\text{SO}_4:1\text{H}_2\text{O}_2:1\text{H}_2\text{O}$ solution.

From the curves in figure 4.1, two groups of peaks can be seen, one of which occurs between 290 and 300 K and the other group occurs between 330 and 350 K. At different depths from the surface, the two groups of peaks are consistently present.

In the case of figure 4.2, three main peaks can be observed at about 310, 355 and 362 K.

For simplicity, the group of peaks at around 300-310 K has been labeled as B and the group of peaks at about 362 K has been labeled as A. The group of peaks between 330 and 355 K is actually the EL2 family of peaks, as mentioned in chapter 3, and will henceforth be referred to as such.

It can be seen from figure 4.2 that near the surface of the sample, peak A dominates. This peak corresponds to an energy level of about $E_v + 0.50$ eV, and a hole capture cross-section of $(4 \pm 1) \times 10^{-17}$ cm². As the sample was etched, this peak initially increased in intensity but then decreased to a level where the emission of the trapped carriers was dominated by the EL2 level. As etching

continued, traces of peak A at about 365 K can still be seen, but the dominant peak gradually shifts towards a position around 300-310 K. As the etching process exposed the center of the sample, peak B, which corresponds to about $E_c - 0.59$ eV and an electron capture cross-section of about $(6 \pm 2) \times 10^{-14}$ cm², reached a maximum. With further etching, the intensity of B decreased again with a corresponding increase in the intensity of A. This is not surprising because diffusions occur from both sides of the center giving a symmetrical diffusion profile. The trapping parameters for all the prominent peaks are tabulated in table 4.1.

Figure 4.3 shows the photoluminescence spectra for both unannealed and control samples. For unannealed samples, there is no peak that can be attributed to copper impurities. However, the photoluminescence spectra for the control sample shows an emission peak at 1.86 eV which is attributed to a copper impurity complex, Cu_{Ga} (Queisser and Fuller, 1966). The appearance of this peak in the control sample, despite the careful cleaning process which the sample and ampoule were subjected to, raises the possibility that the solutions used could be another source of copper contamination. The intensity of this peak increases with depth. Results at different depths are vertically displaced in figure 4.3 for greater clarity.

Results of photoluminescence measurements carried out on a deliberately copper-contaminated sample which is

Table 4.1: Trapping parameters from PITS curves

PEAK	ACTIVATION ENERGY, ΔE (eV)	CROSS-SECTION, σ (cm^2)	PROPOSED ORIGIN
A1	0.52 ± 0.02	$(6 \pm 2) \times 10^{-17}$	$\text{Cu}_{\text{Ga}} \text{V}_{\text{As}}$ (?)
A2	0.50 ± 0.02	$(3 \pm 1) \times 10^{-17}$	"
A3	0.50 ± 0.02	$(4 \pm 1) \times 10^{-17}$	"
B1	0.55 ± 0.02	$(1.3 \pm 0.5) \times 10^{-13}$	$\text{EL3}; \text{V}_{\text{Ga}} \text{V}_{\text{As}}$ (?)
B2	0.57 ± 0.02	$(8 \pm 3) \times 10^{-14}$	"
B3	0.57 ± 0.02	$(1.6 \pm 0.5) \times 10^{-13}$	"
B4	0.56 ± 0.01	$(1.0 \pm 0.5) \times 10^{-13}$	"
B5	0.59 ± 0.01	$(6 \pm 2) \times 10^{-14}$	"
E1	0.75 ± 0.02	$(6 \pm 3) \times 10^{-12}$	EL2
E2	0.78 ± 0.02	$(6 \pm 4) \times 10^{-12}$	"
E3	0.76 ± 0.01	$(7 \pm 3) \times 10^{-12}$	"
E4	0.82 ± 0.02	$(7 \pm 5) \times 10^{-12}$	"
E5	0.80 ± 0.02	$(8 \pm 4) \times 10^{-12}$	"

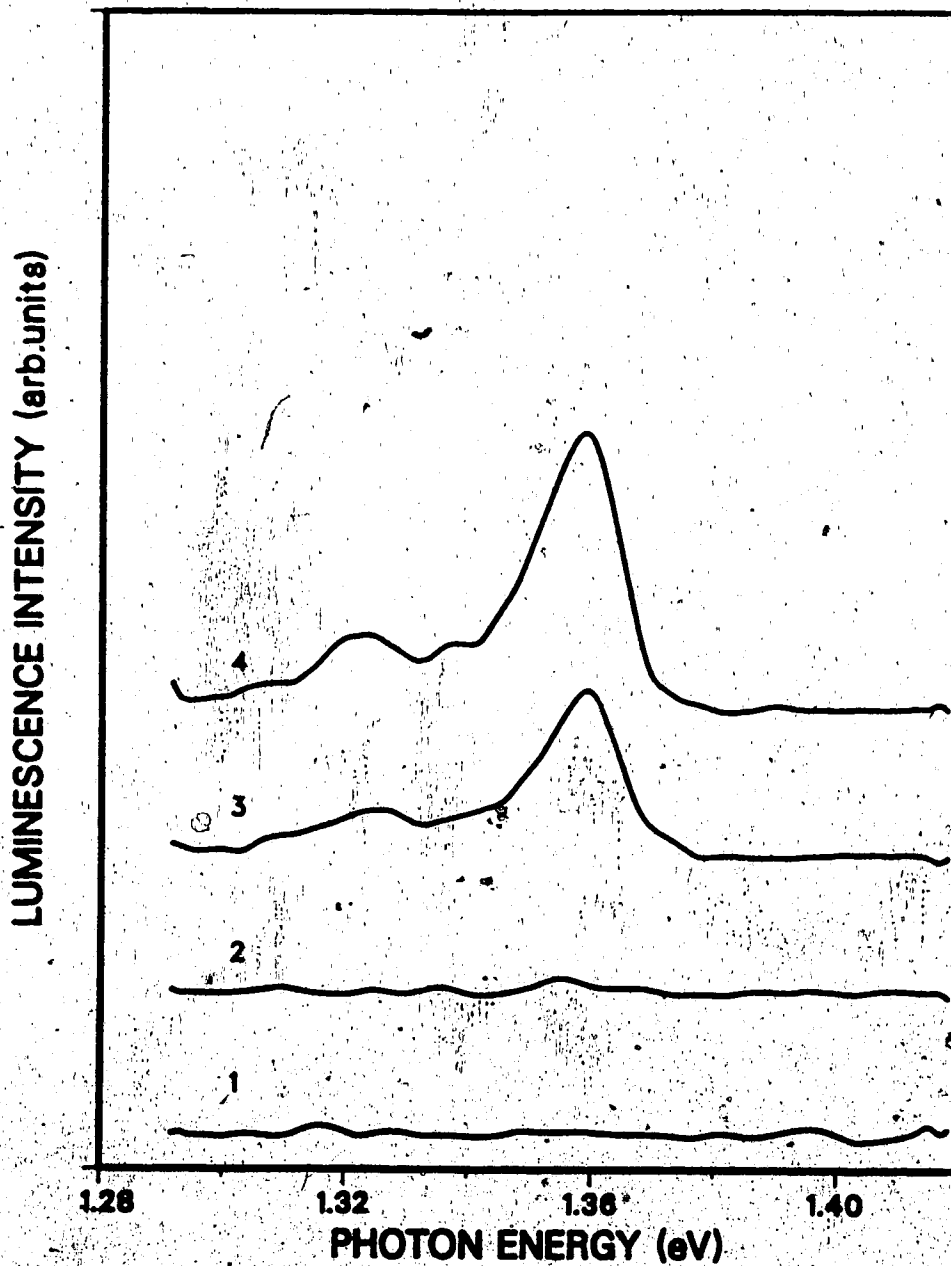


Figure 4.3 Photoluminescence spectra at 4.2 K, for both unannealed and control samples. 1) unannealed sample; 2, 3 and 4 were obtained after etching for 1 min., 10 min. and 30 min. respectively.

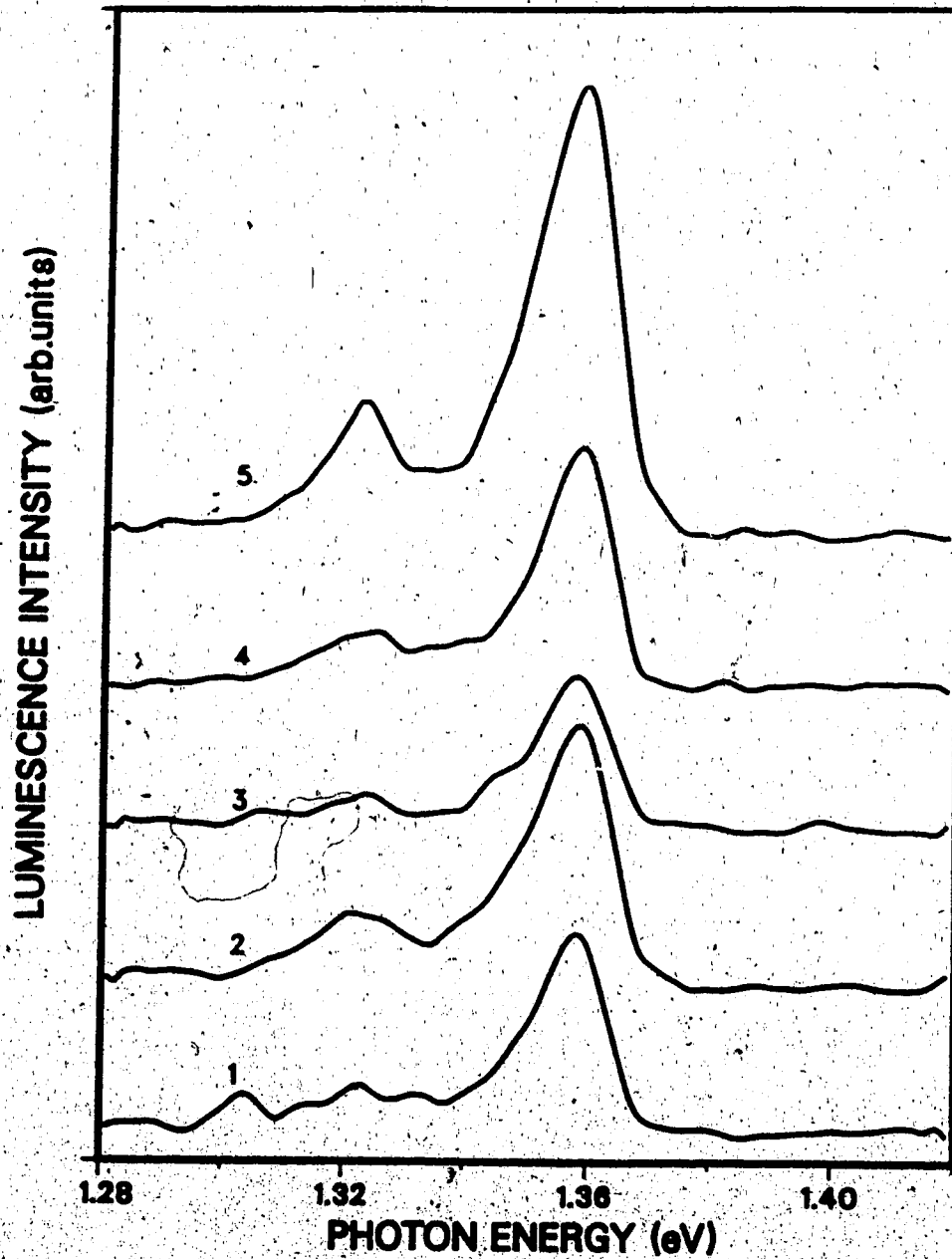


Figure 4.4 Photoluminescence spectra at 4.2 K for copper-contaminated sample. Etching time: 1) 1 min.; 2) 4 min.; 3) 10 min. 4) 20 min.; 5) 30 min.

similar to that used in PITS measurements of figure 4.2, and subjected to identical etching process, are shown in figure 4.4. The spectra have again been displaced vertically for clarity. The presence of copper can be seen at all depths as shown by the emission at 1.36 eV which has been attributed to Cu_{Ga} acceptor level. Only one peak due to Cu_{Ga} can be seen because the S1 response photomultiplier used is limited to photon energies greater than 1.1 eV. From the photoluminescence spectra, it can be seen that the intensity of the peak due to Cu_{Ga} gradually increases with etching time, and hence with depth.

4.4 Discussion

The mechanism responsible for the appearance of the EL2 peak, with an activation energy of $E_c - 0.82$ eV, after annealing, is yet to be determined. The results of Makram-Ebeid et al. (1982) show that the intensity of the EL2 peak at the surface decreases after annealing. They attributed the change to the outdiffusion of EL2 during annealing. In our case, we observed that the EL2 family of peaks usually appears to increase in intensity after annealing.

With reference to the PITS curves in figure 4.1, it can be seen that the intensity of the B peak also increases after annealing which can be due to complex formation involving native defects.

Copper has been known to occupy a level at about 0.4 eV from the valence band (eg. Blanc et al., 1964; Mitonneau et al., 1977; Kullendorff et al., 1983). A search of the literature also reveals values of about $E_v + 0.5$ to $E_v + 0.6$ eV (Sze and Irvin, 1968; Milnes, 1973; Chiao et al., 1975, 1978). From the results published to date no mention was made as to whether these levels are due to the same centers.

From their studies of GaAs grown by horizontal Bridgman and floating zone techniques, which have been annealed with and without copper, Blanc et al. (1964) concluded that there are four lattice defects, two of which are acceptors at 0.17 and 0.48 eV from the valence band, and the other two are donors at 0.2 and 0.56 eV from the conduction band. Owing to the fact that the activation energy is concentration dependent (Harvey, 1961), the above quoted energy levels have an uncertainty of ± 0.03 eV. This means, for instance, that the activation energy of the acceptor level at 0.48 eV can be any value between 0.51 and 0.45 eV. Bube et al. (1962) found a center at $E_v + 0.45$ eV in copper-diffused GaAs. Since this acceptor level is close to the 0.48 eV level, it was suggested by Blanc et al. (1964) that both levels could be due to the same defect involving copper.

Chiao et al. (1978) found from "decayed" thermally stimulated current experiments in LPE GaAs:Cu that there is an acceptor level at $E_v + 0.6$ eV with a capture cross-section of 4.9×10^{-17} cm². From photocapacitance decay experiments, Chiao et al. (1978) also found an acceptor

level at $E_v + 0.42$ eV with a hole capture cross-section around 10^{-16} cm².

The results of Blanc et al. (1964), Bube et al. (1962), Chiao et al. (1978) show that there is a level at about 0.5 eV from the valence band that is related to copper impurity. We proposed, therefore, that the origin of this peak is a copper-related complex, the most likely candidate of which is either $Cu_{Ga}V_{As}$ or $V_{As}-Cu_{Ga}-V_{As}$.

Vorobkalo et al. (1973) found from their photoluminescence studies of n-type GaAs which have been diffused with copper, that there is an increase in the intensity of the 1.0 eV emission peak and a decrease in the intensity of the 0.93 eV emission peak at the surface. However, in the interior of the sample the position of the emission peak gradually shifts from 1.0 eV to 0.93 eV.

Comparing our results with that of Vorobkalo et al. (1973) would indicate that the source of peak A is similar to the one giving rise to the 1.0 eV peak and the source of peak B is similar to that responsible for the 0.93 eV peak.

The presence of a competing process between the two levels responsible for peaks A and B is evident by comparing the intensities of the two relevant peaks in figure 4.2, at different depths from the surface or after each etching process.

Figure 4.5 shows the intensity of the PITS signal for both A and B peaks of the copper-contaminated sample plotted as a function of the etching time. The profile for peak A

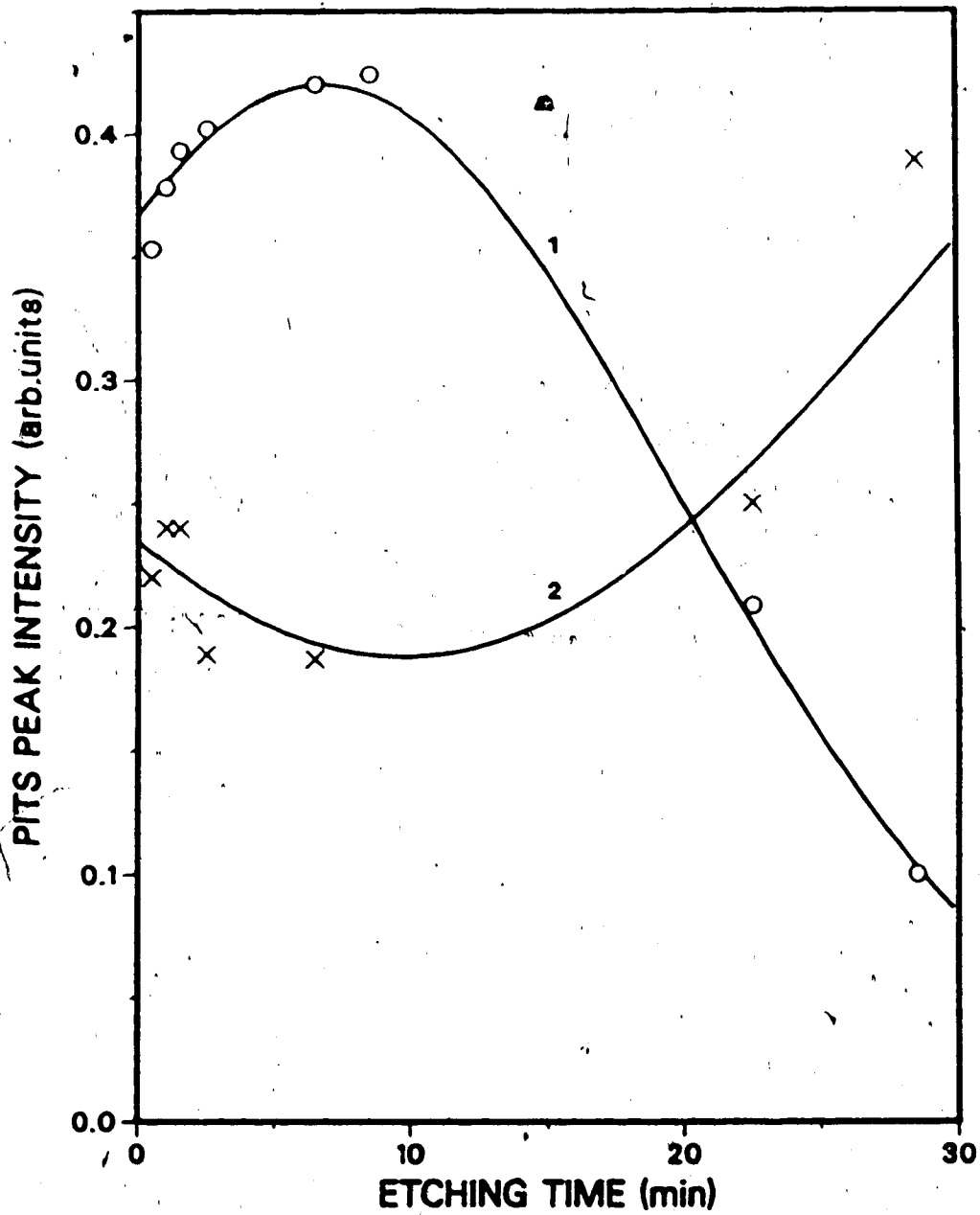


Figure 4.5 Intensities of A and B peaks from PITS curves. Data points were obtained from figure 4.2 and solid curves were obtained using equation 4.3 (curve 1) and equation 4.4 (curve 2). (o) A peak; (x) B peak

can be well represented by a Gaussian distribution curve. The empirical expression for the Gaussian curve as obtained by nonlinear least-squares fitting of the data is:

$$I_A = I_{A0} \exp[-0.5(\frac{t-6.75}{12.98})^2] \quad (4.3)$$

where I_A is the intensity of the normalised PITS signal, I_{A0} is the maximum intensity (=0.4199 for the curve in figure 4.5) and t is the etching time (which can be used as a spatial parameter). The profile of peak B is not a simple Gaussian. An empirical expression for the distribution profile for peak B is:

$$I_B = I_{A0} \{1 - \exp[-0.5(\frac{t-9.7}{20})^2]\} + I_{B0} \quad (4.4)$$

where I_B is the intensity of the normalised PITS signal, I_{B0} (=0.188 for the curve in figure 4.5) is the background intensity of peak B and I_{A0} is the maximum intensity of peak A. Thus, the distribution curve for peak B appears to be related to the maximum intensity of peak A.

The Gaussian profile of the PITS signal for peak A shows that the defect responsible is diffusing inwards. It is most likely to be diffusing inwards with the arsenic vacancies.

Vorobkalo et al. (1973) proposed from their photoluminescence data that the 1.0 eV emission peak is due to $Cu_{Ga}V_{As}$ defect complex and the 0.93 eV peak is associated with $V_{Ga}V_{As}$ double vacancies. The relationship between these two defects is given by:



Evidence that strongly supports the proposal that the source of peak B is a complex involving native defects, V_{Ga} and V_{As} , such as $\text{V}_{\text{Ga}}\text{V}_{\text{As}}$, can be seen from the PITS curves for both unannealed and control samples (which are assumed to be copper-free). These curves are shown in figure 4.1. As mentioned before, these peaks increase in intensity after annealing which show that vacancy association may have occurred during annealing. The PITS curves of figure 4.1 also show a slight "hump" (indicated by an arrow) that could be due to copper-related defects such as those responsible for peak A of figure 4.2, as a result of some copper contamination as shown by photoluminescence spectra of figure 4.3. Even though photoluminescence spectra indicate the presence of copper for the control samples in figure 4.3, it is believed that the amount of copper contamination is minimal and that the density of electrically active copper complexes is small enough that it does not appear clearly in the PITS curves. This is also shown by the fact that a similarly treated control sample was found to be n-type with a resistivity of $9.4 \times 10^7 \Omega \text{ cm}$ and a Hall mobility of $3600 \text{ cm}^2\text{V}^{-1}\text{s}^{-1}$ at 25°C . This Hall-effect result also attests to the thermal stability of the samples used.

* Hall-effect and resistivity measurements were done by Dr. F.L. Weichman.

In routine PITS measurements for various samples of both annealed and unannealed samples of LEC SI GaAs that have been done in this laboratory for the past several years, we have consistently observed that peaks similar to peak B above are frequently obtained. The energy levels of these peaks range from $E_c - 0.5$ to $E_c - 0.6$ eV which strongly indicate that they are due to native defects such as those responsible for EL3 (Martin et al. (1977)). The origin of EL3 is still not known but the results reported here indicate that it is related to $V_{Ga}V_{As}$.

The strong peaks at positions between 290 and 310 K of figure 4.1 strongly suggest that the origin of peak B gives rise to a family of at least 3 different defect levels. It is also possible that peak B of figure 4.2 occurs at a higher temperatures than that of figure 4.1 because of the influence of the EL2 peak at about 330 K.

The photoluminescence results show that the concentration of Cu_{Ga} is increasing inwards with a maximum at the center showing that copper has diffused uniformly throughout the crystal, bearing in mind that the interior of the sample which acts as a sink for copper cannot have a higher concentration of copper than the exterior which is the source. This indicates that the copper at the surface could exist in the form of complexes such as $Cu_{Ga}V_{As}$ or $V_{As}Cu_{Ga}V_{As}$. Furthermore, the decrease of the signal seen at the surface of the annealed sample can be partly due to a degradation in the radiative quantum efficiency of the

luminescent output at the surface. This has also been observed by others (eg. van de Ven et al., 1986). The decrease in photoluminescence signal at the surface could be due to surface damage resulting from the escape of arsenic, creating vacancy-related "killer centers".

There are two mechanisms to explain the results of both PITS and photoluminescence. As has been pointed out earlier, the formation of V_{Ga} and V_{As} is enhanced near the surface of the sample during annealing. It is possible, therefore, that under an arsenic overpressure, more V_{Ga} is created than V_{As} in addition to the native defects such as $V_{Ga}V_{As}$. The higher intensities of EL2 and peak A in the PITS curves of figure 4.3 and the presence of the Cu_{Ga} photoluminescence emission peak (figure 4.4) at the surface could be due to the following processes:

- 1) annihilation of $V_{Ga}V_{As}$ by copper and subsequent reaction with V_{As} to form either $Cu_{Ga}V_{As}$ or $V_{As}Cu_{Ga}V_{As}$ or both,
- 2) creation of EL2 at the surface possibly as a result of a complex reaction involving vacancies and
- 3) creation of Cu_{Ga} by reaction between Cu_1 and the native defects such as V_{Ga} and $V_{Ga}V_{As}$.

Process (1) above requires the annihilation of $V_{Ga}V_{As}$ to form $Cu_{Ga}V_{As}$ which explains the higher PITS intensity of peak A relative to that of peak B near the surface.

At several μm below the surface the concentration of V_{As} is greatly reduced but there is still considerable density of V_{Ga} present as reported by Chiang and Pearson

(1975). With prolonged heating, this region could extend further into the interior of the sample. The likely mechanism to occur is given by:



This mechanism is supported by observation of a higher concentration of the native defect $\text{V}_{\text{Ga}}\text{V}_{\text{As}}$, corresponding to a higher intensity of peak B in the PITS curves of figure 4.2, and an increasing photoluminescence intensity of the Cu_{Ga} emission peak towards the interior of the sample. For a negligibly small concentration of copper contamination, as in the control sample, the concentration of $\text{Cu}_{\text{Ga}}\text{V}_{\text{As}}$ or $\text{V}_{\text{As}}\text{Cu}_{\text{Ga}}\text{V}_{\text{As}}$ and Cu_{Ga} near the surface are probably too low to be detected by PITS (figure 4.1) and photoluminescence (curve 2 of figure 4.3) respectively. However, in the interior of the control sample, $\text{V}_{\text{Ga}}\text{V}_{\text{As}}$ and more Cu_{Ga} are present in accordance with equation (4.6).

4.5 Conclusion

PITS studies of copper-contaminated LEC SI GaAs have shown that there are two other major peaks seen between 273 and 400 K, in addition to the EL2 peak. The energy level of the EL2 peak is at about $E_c - 0.82$ eV whereas the other peaks have activation energies of about $E_v + 0.5$ and $E_c - 0.59$ eV. Depth profiling studies show that these two peaks exist competitively, with the activation energy shifting towards $E_c - 0.59$ eV at increasing depth from the surface.

Photoluminescence studies show the presence of copper throughout the sample indicating that the shift in the peak position is due to the formation of a complex associated with Cu_{Ga} and V_{As} .

Based on the evidence and arguments presented, it is proposed that a single complex, either of the form $\text{Cu}_{\text{Ga}}\text{V}_{\text{As}}$ or $\text{V}_{\text{As}}\text{Cu}_{\text{Ga}}\text{V}_{\text{As}}$, is responsible for the level at about $E_v + 0.5$ eV, whereas a complex such as $\text{V}_{\text{Ga}}\text{V}_{\text{As}}$ is responsible for the level at around $E_c - 0.59$ eV.

Several mechanisms have been proposed to explain the results. The proposed mechanisms, however, are still conjectures and other studies such as the dependence on arsenic partial pressure and length of annealing time should be carried out to determine the validity of the proposed mechanisms and to understand better the behaviour of copper and its complexes in SI GaAs.

Bibliography

- Bahraman, A., and Oldham, W.G., J. Appl. Phys 43, 2383
(1972)
- Bergh, A.A., and Dean, P.J., Proc. IEEE 60, 156 (1972)
- Blanc, J., Bube, R.H., and Weisberg, L.R., J. Phys. Chem.
Solids 25, 225 (1964)
- Bube, R.H., and MacDonald, H.E., Phys. Rev. 128, 2062, 2071
(1962)
- Chiang, S.Y., and Pearson, G.L., J. Appl. Phys. 46, 2986
(1975)
- Chiao, S.S., Mattes, B.L., and Bube, R.H., J. Lumin. 10, 313
(1975)
- Chiao, S.S., Mattes, B.L., and Bube, R.H., J. Appl. Phys.
49, 261 (1978)
- Fabre, E., phys. status solidi A9, 259 (1972)
- Glinchuk, K.D., Lukat, K., and Vovenenko, V.I., phys. status
solidi A69, 521 (1982)
- Guislain, H.J., DeWolf, L., Clauws, P., J. Electron. Mater.
7, 83 (1978)
- Hall, R.N., and Racette, J.H., J. Appl. Phys. 35, 379 (1964)
- Harvey, W.W., Phys. Rev. 123, 1666 (1961)
- Kullendorff, N., Jansson, L., and Ledebø, L.A., J. Appl.
Phys. 54, 3203 (1983)
- Kumar, V., and Ledebø, L.A., J. Appl. Phys. 52, 4866 (1981)
- Lapp, D.V., and Logan, R.A., J. Appl. Phys. 47, 1533 (1976)
- Milnes, A.G., *Deep Impurities In Semiconductors* (Wiley, New
York, 1973)
- Mil'vidskii, M.G., Osvenskii, V.B., Safarov, V.I., and
Yugova, T.G., Sov. Phys. Solid State 13, 1144 (1971)
- Mitonneau, A., Martin, G.M., and Mircea, A., Electron. Lett.
13, 666 (1977)
- Queisser, H.J., and Fuller, C.S., J. Appl. Phys. 37, 4895

(1966)

Rosi, F.D., Meyerhofer, D., and Jensen, R.V., J. Appl. Phys.
31, 1105 (1960)

Stolte, C.A., Semiconductors and semimetals, Vol. 20, p.89
(1984)

Sze, S.M., and Irvin, J.C., Solid State Electron. 11, 599
(1968)

van de Ven, J., Hartmann, W.J.A.M., and Giling, L.J., J.
Appl. Phys. 60, 3735 (1986)

Vorobkalo, F.M., Glinchuk, K.D., Prokhorovich, A.V., and
John, G., phys. status solidi A15, 287 (1973)

Wang, Z.G., Gislason, H.P., and Monemar, B., J. Appl. Phys.
58, 230 (1985)

5. PITS and Photoluminescence Studies of Copper-diffused LEC SI GaAs - Annealing at 550°C

5.1 Introduction

In chapter 4, we proposed, based on the studies of PITS and photoluminescence, that copper creates a complex, believed to be either $\text{Cu}_{\text{Ga}}\text{V}_{\text{As}}$ or $\text{V}_{\text{As}}\text{Cu}_{\text{Ga}}\text{V}_{\text{As}}$, with a defect level at about $E_v + 0.50$ eV and a hole capture cross-section of about 10^{-17} cm². The results were obtained by annealing the samples at about 850°C for 24 hours in a quartz ampoule. The observation that copper can easily contaminate the samples from the quartz tubing, even when there is no direct contact between the two, is significant to the semiconductor manufacturing industry because annealing in quartz containers is part of the manufacturing process. In the wake of the results obtained in chapter 4, the question arises as to whether it is possible to obtain the same results using controlled diffusion so that samples with similar characteristics can be obtained reproducibly. Since annealing at 850°C in the presence of even a small amount of excess copper resulted in samples of high conductivity due to the high diffusion constant of copper in GaAs at elevated temperatures, we decided to carry out the annealing at a lower temperature. This process also allows us to find out whether the defects created at 850°C can also be created at the lower temperature of 550°C.

In the results to be discussed in this chapter, it is confirmed that the level at about $E_v + 0.5$ eV is indeed due to a complex involving copper and arsenic vacancy.

These studies also showed that the defect level at about $E_v + 0.5$ eV found in copper-diffused samples but commonly attributed to iron impurity, is definitely due to a copper complex instead of an iron complex.

5.2 Experimental details

A slice of LEC SI GaAs sample of commercial quality and obtained by courtesy of Cominco Ltd., was first etched in $5H_2SO_4:1H_2O_2:1H_2O$ solution for about 2 minutes and then rinsed in deionised water. A layer of 99.9999% copper was then deposited onto one side of the sample by vacuum evaporation. The sample was then inserted into a quartz ampoule, together with a small lump of 99.9999% arsenic. The quartz ampoule had been previously cleaned with aqua regia, KCN solution and HF solution followed by rinsing in deionised water. The ampoule and contents were then evacuated to about 10^{-6} Torr and sealed. The ampoule containing the sample and excess arsenic was then annealed at $550^\circ C$ for 12 hours.

At the end of the annealing process, the slice of sample was then cleaved into smaller pieces of about 10 mm x 5 mm in dimension. For PITS measurements, ohmic contacts were made by melting 99.9999% indium on the sample followed by annealing at about $300-350^\circ C$ for about 30 seconds in

flowing HCl/N₂ gas.

PITS and photoluminescence measurements were then made as outlined in chapter 4.

5.3 Results

PITS curves for the original and copper-diffused samples are shown in figure 5.1. All the PITS curves shown are for time window $(t_2 - t_1) = 20\text{ms}$ and $t_1 = 5\text{ms}$. Curve 1 of figure 5.1 was obtained on the original, unannealed sample. Curve 2 of figure 5.1 was obtained on the side of the sample on which the copper film was deposited, after removing the film by polishing and etching. Curve 3 of figure 5.1 was obtained on the same side as for curve 2 but after etching off about 150 μm from the surface. Curves 4, 5, 6, and 7 were the results of PITS measurements made on the side which was not covered with copper film. Curve 7 was obtained near the surface and curves 6, 5, and 4 were obtained, in that order, after removing the previous contacts, then polished and etched, and followed by fabrication of new contacts. Each polishing and etching step is equivalent to a removal of about 50 μm off the surface. Figure 5.2 shows the relative positions in the sample from which the specified PITS curves were obtained.

Figure 5.3 shows the photoluminescence spectra taken at different depths from the surface. Curves 1, 2 and 3 were taken at different depths from the surface that was covered with copper film. Curves 4 and 5 were taken at different

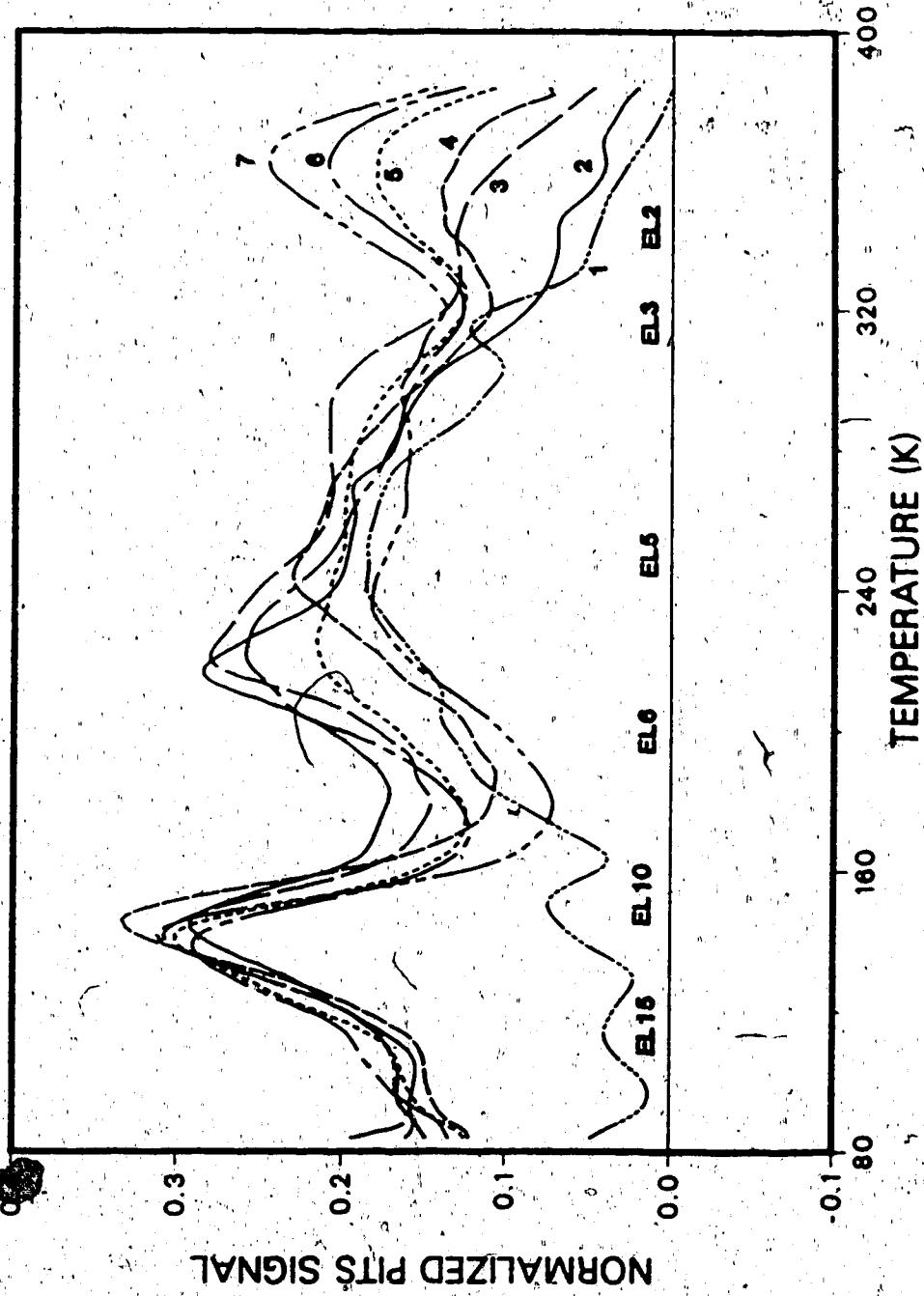


Figure 5.1 PITS curves for both original and copper-diffused samples.
 1: original sample;
 2, 3, 4, 5, 6, and 7: copper-diffused sample

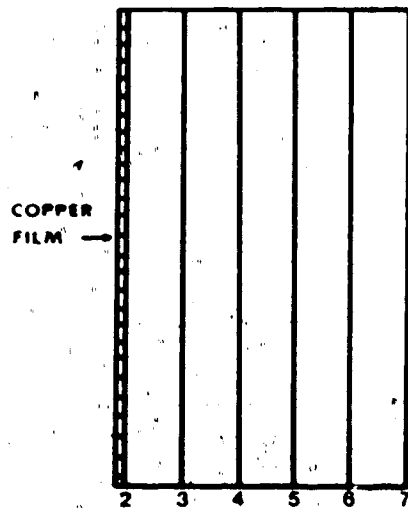


Figure 5.2 Sample for PITS measurements.
The numbers correspond to the PITS curves in
figure 5.1

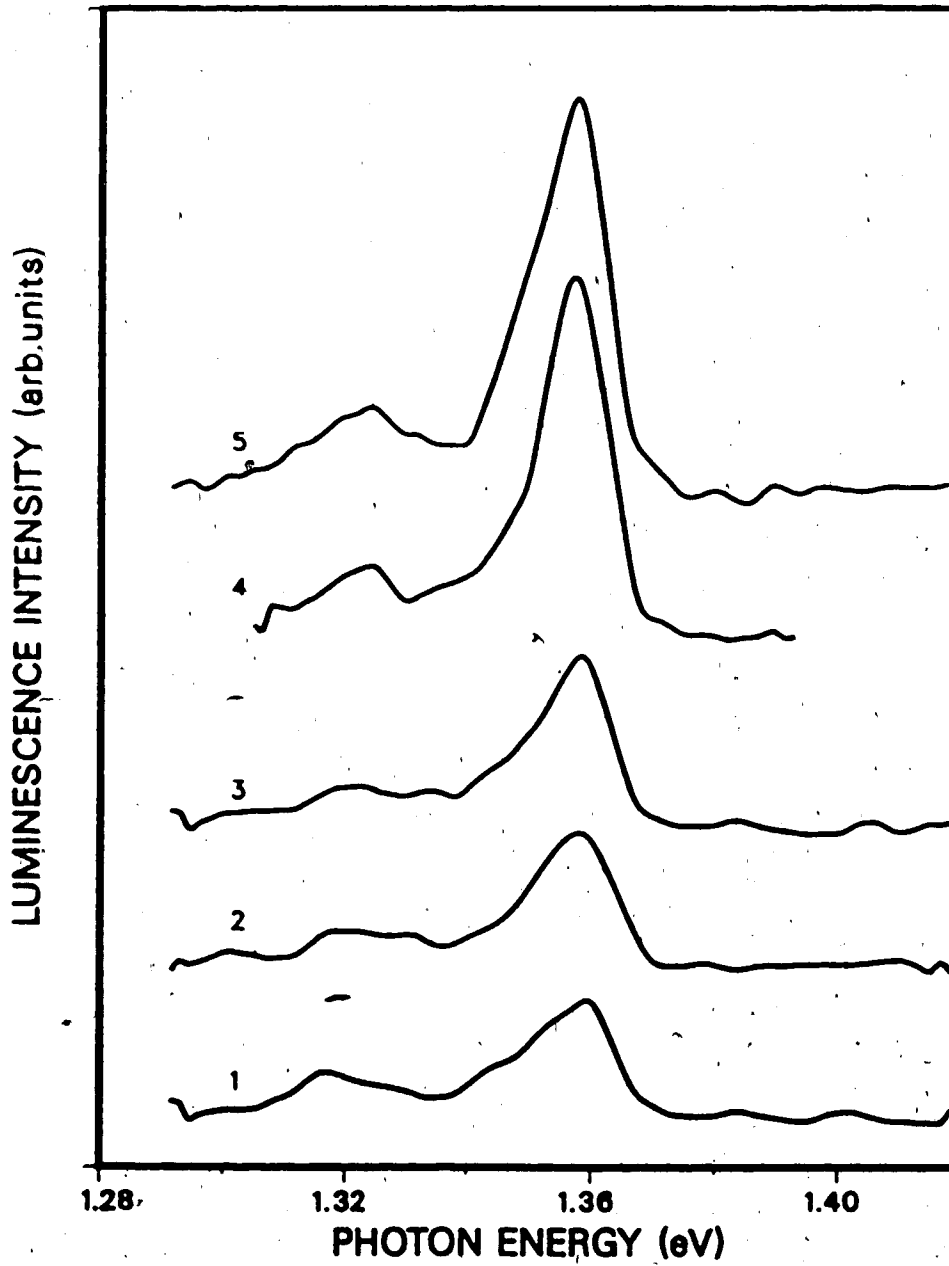


Figure 5.3. Photoluminescence spectra at different depths from the surface.

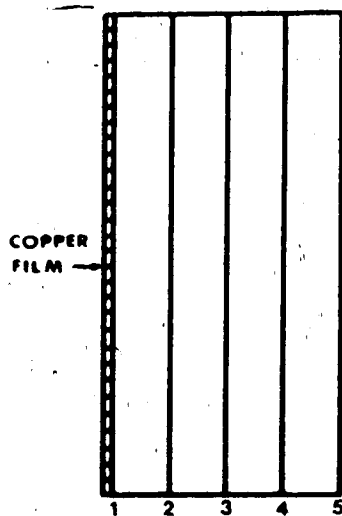


Figure 5.4 Sample for photoluminescence measurements. The numbers correspond to the curves in figure 5.3.

depths from the surface that was not covered with copper. The relative positions at which the spectra were taken are shown in figure 5.4.

5.4 Discussion

With reference to the PITS curve for the original, unannealed sample, the approximate positions of the peaks that have been observed by both deep-level transient spectroscopy (DLTS) and PITS have been labeled according to Martin et al., (1977). Except for the EL2 level which has been identified, the origins of the other peaks are still unknown. Referring to the PITS curves for copper-diffused samples, the peak at about 140 K has an average energy level of $E_v + 0.19$ eV. This peak is commonly observed in electrical measurements of copper-diffused GaAs. Queisser and Fuller (1966) suggest that the complex responsible for this level is likely to be Cu_{Ga} complexed with a vacancy. It can be seen that the intensity of this peak is more or less constant throughout the samples. This can be taken to indicate that copper has diffused uniformly throughout the samples.

Photoluminescence results show that the emission peak at 1.36 eV which is attributed to Cu_{Ga} , is more intense for regions deep inside the samples than for those near the surface. The comparison between the PITS peak at 140 K and the photoluminescence emission peak at 1.36 eV shows that the origin of the copper-related peak at 140 K,

corresponding to an energy level of about $E_v + 0.19$ eV, cannot be due to the same center.

The copper impurity in GaAs also introduces another level at about $E_v + 0.4$ eV with a hole capture cross-section of about 3×10^{-14} cm² (Kullendorff et al., 1983). This would give a peak in the PITS curve in the temperature range of 220-240 K. This same region also corresponds to the region where a broad peak due to EL5 would occur. Since both electron and hole trapping centers give positive peaks in PITS curves, it is difficult to determine the contribution of each center unambiguously. It is tempting to say that the peak at about 220 K in figure 5.1 could correspond to the copper-related defect. If that assumption is true, then it can be seen that such defect centers are more concentrated in the region just below the copper film but is not uniformly distributed throughout the sample.

The peak of interest in the PITS curves of figure 5.1 occurs at about 362 K. The energy level of this peak is at about $E_v + 0.52$ eV and the hole capture cross-section is in the range of 10^{-17} cm². This peak is the same as that referred to as the "A" peak in chapter 4.

We have proposed in chapter 4 that this peak is due to a copper-related complex either of the form $Cu_{Ga}V_{As}$ or $V_{As}Cu_{Ga}V_{As}$. The variation of the intensity of this peak in figure 5.1 as a function of etching time or depth support our proposal that it is related to a copper complex involving Cu_{Ga} and V_{As} .

The presence of a film of copper on one side of the sample has a capping effect, preventing the escape of arsenic from that surface. Hence, the region below the copper film should have a lower concentration of V_{As} than the opposite side. The formation of the defect $Cu_{Ga}V_{As}$ or $V_{As}Cu_{Ga}V_{As}$ is thus inhibited because of the low concentration of V_{As} .

The escape of arsenic through the other side of the sample is unhindered. It is expected, therefore, that a concentration gradient of V_{As} exists in the sample with a maximum at the free surface and a minimum in the region covered by the copper film. The formation of $Cu_{Ga}V_{As}$ or $V_{As}Cu_{Ga}V_{As}$ will follow the concentration profile of V_{As} . The concentrations of such defects should reach a maximum at the uncapped surface and a minimum at the copper-covered surface.

The variation of the intensity of the peak at 362 K in figure 5.1 clearly follows the argument presented above. This peak has a maximum at the surface not covered with copper film and decreases consistently with depth from the free surface, reaching a minimum at the copper-covered surface. It can be seen, however, that there is a trace of the existence of the defects in the region near the copper film. This peak is completely absent in the unannealed original sample. The relationship between the peak at 362 K and the one lying in the range between 290 and 310 K is not as clear in figure 5.1 as it is in figure 4.2. Generally

speaking, it can be seen that a high intensity of the peak at 362 K corresponds with a low intensity of the peak around 290-310 K, and vice versa.

It can also be seen from figure 5.1 that a high intensity of the peak at 362 K corresponds with a low intensity of the peak at 220 K and vice versa. If it is assumed that the peak at 220 K of figure 5.1 is related to a second ionization state of a copper-related defect, $\text{Cu}_{\text{Ga}}^{2-}$ (Queisser and Fuller, 1966), which has a defect level at about $E_v + 0.45$ eV, then we can explain the relationship between the two peaks as being due to the annihilation of $\text{Cu}_{\text{Ga}}^{2-}$ to give $\text{V}_{\text{As}}\text{Cu}_{\text{Ga}}\text{V}_{\text{As}}$ or $\text{Cu}_{\text{Ga}}\text{V}_{\text{As}}$.

5.5 Conclusion

It has been shown that by deliberately diffusing copper from one side of the sample, we have confirmed from PITS results that the peak at 362 K, with a defect level at $E_v + 0.52$ eV, is due to a complex involving Cu_{Ga} and V_{As} , either of the form $\text{Cu}_{\text{Ga}}\text{V}_{\text{As}}$ or $\text{V}_{\text{As}}\text{Cu}_{\text{Ga}}\text{V}_{\text{As}}$.

In addition, several other peaks can also be seen. Correlating the PITS and photoluminescence data, we conclude that the acceptor level at about 0.2 eV, which is commonly seen in Hall effect and thermally stimulated conductivity (TSC) experiments, is not related at all to the 1.36 eV photoluminescence peak. Furthermore, the $E_v + 0.19$ eV peak is also not related to V_{As} .

Bibliography

Kullendorff, N., Jansson, L., and Ledebø, L.A., J. Appl. Phys. 54, 3203 (1983)

Martin, G.M., Mitonneau, A., and Mircea, A., Electron. Lett. 13, 191 (1977)

Queisser, H.J., and Fuller, C.S., J. Appl. Phys. 37, 4895 (1966)

6. General Discussion and Conclusions

6.1 General Discussion

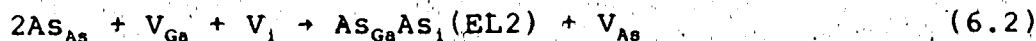
From the PITS measurements of LEC SI GaAs grown with different grades of B_2O_3 encapsulant and different masses of charge, as described in chapter 3, we have shown that there is a family of defect levels with activation energies in the range of 0.75 to 0.82 eV. This is the well-known donor level widely referred to as EL2. The data shows that there are 3 different levels in this family of EL2 trapping centers. The appearance of a similar peak can also be seen in the results of chapters 4 and 5. We then concluded that this family of levels is related to native defects, the most widely quoted of which is the antisite defect As_{Ga} . It has also been proposed (Zou et al., 1983; Lagowski et al., 1983; von Bardeleben et al., 1985) that this family of defects could be due to a complex involving V_{Ga} , V_{As} or As_i . Based on the results of the previous chapters, we will attempt to determine the most likely complex that is responsible for EL2.

The increase in the intensity of the EL2 family of peaks after annealing is in contrast to the observation of Makram-Ebeid et al. (1982). Such an increase can be seen from the results of chapter 4 and 5. An obvious reason is that EL2 defects are being formed at the surface. There are several possible mechanisms to explain the increase in EL2 concentrations.

The formation of EL2 during annealing could be due to the slight overpressure of arsenic and the creation of V_{Ga} (Chiang and Pearson, 1975) giving rise to the antisite defect, As_{Ga} , according to the equation:



von Bardeleben et al. (1985) believe that EL2 is due to a complex of As_i and As_{Ga} giving rise to $As_{Ga}As_i$. If that is so, then the mechanism of formation of EL2 in our case would be:



On the other hand, Zou et al. (1983) proposed that a more likely origin of EL2 defect is $As_{Ga}V_{As}V_{Ga}$. For this type of defect to form at the surface, the mechanism would be:



Lagowski et al. (1983) proposed that a complex such as $As_{Ga}V_{As}$ can account for electronic properties of EL2 better than a simple antisite defect, As_{Ga} . Using this complex as a model for the EL2 defect, the mechanism of formation of EL2 based on our results would be:



The mechanism described by equation 6.3 seems more logical. It is plausible that during annealing, both V_{Ga} and V_{As} are created which then form complexes with either As_i or As_{As} to give $As_{Ga}V_{As}V_{Ga}$.

From the results of chapter 3, it is shown that the broad peak between 220 and 260 K is inversely dependent on the carbon content. We have proposed that this peak is

related to free V_{As} . The breadth of this peak, which encompasses parts of the regions covered by EL6 and EL3, shows that the origins of EL6 and EL3 are related to V_{As} . The position of this peak also coincides with the position of the copper-related peak at $E_v + 0.4$ eV, giving rise to the problem of identifying the peaks. This problem is highlighted in chapter 5 where it can be seen that the peak stretches from 220 to 280 K. The curves in chapter 5 were obtained from copper-diffused samples, hence the $E_v + 0.4$ eV peak must have merged with the peak due to EL5. The merging of the peaks does not signify complex formation of the two types of defects. One method to separate the peaks is to use Schottky barrier contacts and study the dependence of the peak on either the electric field intensity, or the light intensity for both forward and reverse electric fields. However, this would not work in the case of high resistivity material such as SI GaAs due to the fact that the electrical contacts are essentially ohmic.

One of the most significant PITS results of chapters 4 and 5 is the observation of a hole trapping center at about $E_v + 0.5$ eV and the variation of this peak with depth from the surface. We have proposed that this center is due to a complex either of the form $Cu_{Ga}V_{As}$ or $V_{As}Cu_{Ga}V_{As}$. The evidence that supports this proposal is the concentration profile of this defect which follows a Gaussian distribution function typical of an inward diffusion of a species in a medium. Further evidence is also provided in chapter 5, where the

results clearly show that the intensity of this peak correlates with the expected distribution profile of V_{As} .

Safarov et al. (1970) and van de Ven et al. (1986) found from photoluminescence studies that there are two species of copper-related defects, one of which is a fast diffusing complex and the other is a slow diffusing complex found near the surface. Willman (1971, 1973) also made the same observations using absorption measurements and bound-excitons studies. van de Ven et al. (1986) proposed that the slow diffusing complex found near the surface corresponds to $V_{As}Cu_{Ga}V_{As}$.

The results shown in figure 1 of Safarov et al., (1970), clearly show that the bound-exciton lines, C_0 (1.5031 eV) and C_1 (1.4996 eV) increase in intensity inward. If we assume that the measurements were taken near the surface that was originally covered with a copper film during annealing, then the increase in the intensities of C_0 and C_1 with depth corresponds with the increase in the PITS signal at $E_v + 0.5$ eV, with depth from the copper-covered surface (figure 5.1). Safarov et al., (1970) suggested that a complex such as $Cu_{Ga}V_{As}$ will have the same symmetry as the C_0 and C_1 centers. Mil'vidskii et al., (1971), also reported that the C_0 and C_1 centers are related to $Cu_{Ga}V_{As}$.

Lyubchenko et al. (1968) reported, from their photoconductivity experiments, that there are two different types of copper-related centers: the s centers at $E_v + 0.52$ eV and the r centers at $E_v + 0.39$ eV.

If the level at $E_v + 0.5$ eV is indeed related to copper, then a more coherent picture begins to emerge from the vast amount of seemingly conflicting data on the problem of copper impurity in GaAs.

We propose that from both electrical and photoelectronic measurements, it is possible to detect three different copper-related defect levels. The acceptor level at around $E_v + 0.6$ eV seen by Chiao et al. (1978), the level at $E_{sc} + 0.52$ eV seen by Lyubchenko et al. (1968), and the *unknown* level at $E_v + 0.51$ mentioned by Milne's (1973) and Sze and Irvin (1968) are all due to the same center as the one responsible for the PITS peak at around 362 K, which we have proposed to be most likely $Cu_{Ga}V_{As}$. The level at around $E_v + 0.4$ eV reported by Queisser and Fuller (1966), Mitonneau et al. (1977), Kullendorff et al. (1983) and others, is responsible for the PITS peak around 220-240 K. From PITS curves, we have unambiguously separated two different centers owing to the fact that the peaks are far apart. This will preclude any experimental uncertainty that would otherwise have been held accountable if these two results were obtained using other means of measurements.

There is also another level at about $E_v + 0.19$ eV which is clearly seen from our results on copper-diffused samples. This could be the same level reported by Blanc et al. (1964), Queisser and Fuller (1966), Furukawa and Thurmond (1965) and others. According to Allison and Fuller (1965) the level at $E_v + 0.2$ eV found in Te-doped GaAs is due to V_{Ga} .

resulting from a dissociation of Cu_{Ga} . However, they concede that a vacancy-impurity complex could also be responsible for the level at about $E_v + 0.2$ eV. From our PITS results, it is possible to conclude that a copper-related complex is responsible for the observed peak at 140 K with an energy of $E_v + 0.19$ eV.

If the acceptor level at $E_v + 0.5$ eV is related to copper, it is possible that some of the DLTS results, which reveal a level at around $E_v + 0.5$ eV in copper-diffused samples, but which were attributed to iron impurities, could be erroneous. An example of this attribution is the DLTS results reported by Lang and Logan (1976). According to their studies of p-n junctions in LPE GaAs, they found that the copper-related level at $E_v + 0.44$ eV is more or less constant throughout the junction but the defect responsible for the level at $E_v + 0.52$ eV, purportedly due to the iron impurity, has a higher concentration near the junction but rapidly decreases away from the junction. They reported that these two signals are *always* seen in junctions at the epilayer/substrate interface. If these two signals are not related, there is no reason why they should always occur together. According to our results here, the level that was reported to be due to iron is actually a copper complex.

6.2 Conclusions

The high resistivity of LEC SI GaAs requires that a photoelectronic measurement technique be used for the characterisation of defect levels. A microcomputer-controlled photo-induced transient spectroscopy (PITS) system was constructed to provide an effective analytical system to probe the defect levels in LEC SI GaAs in an effort to understand the origins of the defects levels.

In the discussion on the theoretical and experimental aspects of PITS, we have shown that the high resistivity of the material requires certain precautionary measures to be taken in the analysis of the decay time constants because of the non-negligible dielectric relaxation time.

From the PITS measurements of a series of samples with different carbon content, we found that the intensity of the EL2 family of peaks correlate with the moisture content of the B₂O₃ encapsulant. The possible explanations are the increased thermal-induced stresses resulting in higher density of dislocations which, in turn, leads to gettering of the EL2 defect centers, and the preferential exclusion of gallium from the melt. The PITS results also show that the origin of the broad peak EL5 is related to free V_{As}. This indirectly indicates that complexes involving V_{As} are responsible for the EL6 and EL3 levels.

In a series of measurements on copper-contaminated samples, a level at about E_v + 0.5 eV with a hole capture

cross-section of about 10^{-17} cm² was observed in addition to the other commonly seen copper-related levels at $E_v + 0.19$ and $E_v + 0.4$ eV. The relationship between the level at $E_v + 0.5$ eV and V_{As} leads us to believe that the former is due to either $Cu_{Ga}V_{As}$ or $V_{As}Cu_{Ga}V_{As}$. The former is the most likely candidate. We have thus provided evidence that there are three different copper-related centers that can be detected photoelectronically.

The studies of the copper-related levels have provided a better understanding of the roles of copper impurity in GaAs and have also reconciled many of the conflicting results reported in the literature.

From the results that we have obtained, we have shown that there is still much experimental work to be done to determine the exact nature of the commonly seen trapping levels in GaAs such as EL2. In the absence of a complete understanding of the nature of EL2 and the other trapping levels such as EL3, EL5 and EL6, present efforts to produce high quality crystals of LEC SI GaAs are essentially done in the *dark*.

From our results on the diffusion of copper in GaAs, we have shown that there are several avenues for further work, the most important of which is high-resolution photoluminescence spectroscopy over a wider energy range to study the presence of the copper-related defects, and their different rates of diffusion. The results will either confirm or disprove our present conclusions.

Bibliography

- Blanc, J., Bube, R.H., and Weisberg, L.R., J. Phys. Chem. Solids 25, 225 (1964)
- Chiang, S.Y., and Pearson, G.L., J. Appl. Phys. 46, 2986 (1975)
- Chiao, S.S., Mattes, B.L., and Bube, R.H., J. Appl. Phys. 49, 261 (1978)
- Furukawa, Y., and Thurmond, C.D., J. Phys. Chem. Solids 26, 1535 (1965)
- Kullendorff, N., Jansson, L., and Ledebø, L.A., J. Appl. Phys. 54, 3203 (1983)
- Lagowski, J., Kaminska, M., Parsey, J., Gatos, H.C., and Walukiewicz, W., Inst. Phys. Conf. Ser. No. 65, p. 41 (1983)
- Lyubchenko, A.V., Sheinkman, M.K., Brodovoi, V.A., and Krolevets, N.M., Sov. Phys. Semicond. 2, 406 (1968)
- Makram-Ebeid, S., Gautard, D., Devillard, P., and Martin, G.M., Appl. Phys. Lett. 40, 161 (1982)
- Milnes, A.G., *Deep Impurities in Semiconductors* (Wiley, New York, 1973)
- Mil'vidskii, M.G., Osvenski, V.B., Safarov, V.I., and Yugova, T.G., Sov. Phys. Solid State 13, 1144 (1971)
- Mitonneau, A., Martin, G.M., and Mircea, A., Electron. Lett. 13, 667 (1977)
- Queisser, H.J., and Fuller, C.S., J. Appl. Phys. 37, 4895 (1966)
- Safarov, V.I., Sedov, V.E., and Yugova, T.G., Sov. Phys. Semicond. 4, 119 (1970)
- Sze, S.M., and Irvin, J.C., Solid State Electron. 11, 599 (1968)
- von Bardeleben, H.J., Stievenard, D., Bourgoïn, J.C., and Huber, A., Appl. Phys. Lett. 47, 970 (1985)
- van de Ven, J., Hartmann, W.J.A.M., and Giling, L.J., J. Appl. Phys. 60, 3735 (1986)

Willman, F., Blatte, M., Queisser, H.J., and Treusch, J.,
Solid State Commun., 9, 2281 (1971)

Willman, F., Bimberg, D., and Blatte, M., Phys. Rev. B7,
2473 (1973)

Zou, Y.X., Zhou, J.C., Mo, P.G., Lu, F.Z., Li, L.S., Shao,
J., Huang, L., Sun, H.H., Sheng, C., and Sun, Q., Inst.
Phys. Conf. Ser. No. 65, p. 49 (1983)

Appendix A

Derivation of the transient current equation

Symbols:

n : number of electrons in the conduction band

ν : emission rate

v : thermal velocity of the electrons

N : total concentration of trapping centers

n_t : number of trapped electrons

σ : capture cross-section

ΔE : activation energy of the trap

I_0 : excitation intensity

τ : free electron recombination life-time

1. The change of electron concentration, n , in the conduction band is given by:

$$\frac{dn}{dt} = \nu n_t - \sigma v n (N - n_t)$$

$$\text{At equilibrium, } \frac{dn}{dt} = 0$$

$$\text{or } \nu n_t = \sigma v n (N - n_t)$$

$$\therefore n_t = \frac{n \sigma v N}{\nu + n \sigma v}$$

$$= \frac{N}{1 + \nu / n \sigma v}$$

$$= \frac{N}{1 + (\nu / N_0 \sigma v) \exp(-E_f / kT)} \quad (A1)$$

[since $n = N_0 \exp(E_f / kT)$]

At thermal equilibrium, $n_t = fN$
 where f = Fermi function

$$\therefore n_t = \frac{N}{1 + \exp[(-\Delta E - E_f)/kT]} \quad (A2)$$

comparing equations (A1) and (A2) gives:

$$\nu = N_0 \sigma v \exp(-\Delta E/kT) \quad (A3)$$

Equation (A3) disregards degeneracy. If degeneracy is allowed, then :

$$\nu = \frac{N_0 \sigma v}{g} \exp(-\Delta E/kT) \quad (A4)$$

2. The rate of change of the trapped electron is given by:

$$\begin{aligned} \frac{dn_t}{dt} &= -\nu n_t + n(N - n_t) \sigma v \\ &= -\nu n_t + I_0 \alpha \tau (N - n_t) \sigma v \end{aligned}$$

Let $\beta = I_0 \alpha \tau \sigma v$

$$\therefore \frac{dn_t}{dt} = -\nu n_t + \beta(N - n_t)$$

$$\therefore \frac{dn_t}{dt} + n_t(\nu + \beta) = \beta N$$

Particular solution:

$$n_{tp} = \beta N / (\nu + \beta)$$

General solution:

$$n_{tg} = D \exp[-(\nu + \beta)t]$$

$$\therefore n_t = D \exp[-(\nu + \beta)t] + \frac{\beta N}{\nu + \beta}$$

If $n_t = 0$ at $t = 0$

$$\therefore D = \frac{\beta N}{\nu + \beta}$$

$$\therefore n_t(t) = \frac{N}{1 + \nu/\beta} \{1 - \exp[-(\nu + \beta)t]\}$$

When the light pulse is off, then:

$$\frac{dn_t}{dt} = -\nu n_t$$

Solution:

$$n_t(t) = G \exp(-\nu t)$$

Boundary condition: $t = 0$ when light pulse is off

$$\therefore n_t(0) = G$$

$$\therefore n_t(t) = n_t(0) \exp(-\nu t)$$

$$= \frac{N}{1 + (\nu/\beta)} \exp(-\nu t) \quad (\text{A5})$$

If recombination is taken into account, then the change of electron concentration, n , in the conduction band is given by:

$$\frac{dn}{dt} = \nu n_t - \sigma v n(N - n_t) - \frac{n}{\tau}$$

If $\tau^{-1} \gg \sigma v n(N - n_t)$

$$\text{then } \frac{dn}{dt} = \nu n_t - \frac{n}{\tau} \quad (\text{A6})$$

Solving equation (A6) by using $\exp(t/\tau)$ as integrating factor and using equation (A5) gives:

$$\int_0^t \left(\frac{dn}{dt} + \frac{n}{\tau} \right) \exp(t/\tau) dt = \frac{N\nu}{1 + (\nu/\beta)} \int_0^t \exp[(\tau^{-1} - \nu)t] dt$$

$$\therefore n(t) = \frac{N\nu}{1+(\nu/\beta)} \frac{\exp(-\nu t) - \exp(-t/\tau)}{\tau^{-1} - \nu} + n(0) \exp(-t/\tau)$$

$$\text{Current, } I(t) = Cq\mu n(t)$$

$$\begin{aligned} &= \frac{Cq\mu\nu}{\tau^{-1} - \nu} \frac{N}{1+(\nu/\beta)} [\exp(-\nu t) - \exp(-t/\tau)] + \\ & i_0 \exp(-t/\tau) \end{aligned} \quad (A7)$$

Appendix B

Software, circuit diagrams and mechanical part of the PITS system

To select the channel for the A-D converter, use the command *POKE 49345, X* where *X* is the channel number from 0 to 7. The commands to read the data from the A-D converter are *PEEK(49346)* and *PEEK(49348)*. The first *PEEK* command is to read the most significant 8 bits of the 12-bit data and the second *PEEK* command is to read the remaining 4 bits. The 12-bit word can then be reconstructed using the formula:
 $PEEK(49348) + 16 \times PEEK(49346)$.

To activate the electro-mechanical shutter, the command is: *POKE 49326,0*.

The addresses for the various control lines are:

CONTROL LINE	ADDRESS	SLOT
1	49312	2
2	49313	2
3	49314	2
4	49315	3
5	49316	3
6	49317	3
7	49318	4
8	49319	4
9	49320	4
10	49321	1
11	49322	1
12	49323	1

13	49324	1
14	49325	1
15	49326	SD10
16	49327	1

Data Acquisition Program for PITS system:

```

5      Home
50     DIM DX(46,105), TD(256)
60     FOR I=36864 TO 36989: READ D: POKE I,D: NEXT I
111    B$=" ":C$=" ":D$=CHR$(4)
112    PRINT D$;"OPEN CCT"
112    PRINT D$;"DELETE CCT"
115    PRINT D$;"OPEN CCT"
116    PRINT D$;"WRITE CCT"
117    FOR N=1 TO 5:PRINT 0;C$;0;C$;0;C$;0;C$:NEXT N
118    PRINT D$;"CLOSE CCT"
119    HOME
122    PRINT
125    PRINT
127    PRINT TAB(1);:FOR Q=1 TO 38:PRINT "*":NEXT:PRINT
130    PRINT TAB(1);"*";TAB(38);"*"
140    PRINT TAB(1);"*";TAB(13);"PHOTO-INDUCED";TAB(38);"*"
150    PRINT TAB(1);"*";TAB(38);"*"
160    PRINT TAB(1);"*";TAB(8);"TRANSIENT SPECTROSCOPY";
      TAB(38);"*"
170    PRINT TAB(1);"*";TAB(38);"*"
180    PRINT TAB(1);:FOR Q=1 TO 38:PRINT "*":NEXT:PRINT
190    PRINT
200    INVERSE
210    PRINT TAB(38)
220    NORMAL
230    PRINT


```

```
240 PRINT
300 INPUT "TEMPERATURE RANGE? 0=LOW, 1=HIGH ";RA
302 IF RA=0 THEN AR$="LOW"
303 IF RA=1 THEN AR$="HIGH"
310 INPUT "PULSE BIAS ? 0=NO 1=YES ";SV
315 IF SV=0 THEN VS$="CONTINUOUS"
316 IF SV=1 THEN VS$="PULSE"
320 INPUT "FIRST TEMPERATURE ?";ST
330 INPUT "FINAL TEMPERATURE ? ";FT
400 VTAB 13
410 PRINT "TEMPERATURE RANGE IS ";AR$;SPC(14):PRINT
420 PRINT "BIAS IS ";VS$;SPC(15):PRINT
430 PRINT "INITIAL TEMPERATURE IS ";ST;" C"
440 PRINT "FINAL TEMPERATURE IS ";FT;" C"
764 PRINT
765 INVERSE
770 PRINT TAB(38)
775 NORMAL
776 PRINT
777 PRINT
778 PRINT "PRESENT TEMPERATURE IS ":" PRINT
780 GOSUB 4000
800 IT=2:BV=230:A1=0
810 OT=-200
850 IF SV=0 THEN POKE 49312,BV
900 L=1
1000 U1=ST+0.15:L1=ST-0.15
1030 BL=ST-0.2
1050 LB=L1-0.5
1100 GOSUB 5000
1250 IF T0 > FT THEN GOSUB 7190
1300 IF T0 > FT THEN END
1320 IF T0 < OT THEN GOSUB 4000
1360 IF SV = 0 THEN GOTO 1390
```

```
1370 IF T0 > LB THEN POKE 49312,BV
1380 IF T0 < LB THEN POKE 49312,0
1390 IF T0 > BL THEN GOSUB 6200
1400 IF T0 < L1 THEN GOTO 1100
1500 IF T0 > U1 THEN GOTO 1100
1700 POKE 49326,0
1750 FOR N=1 to 116:NEXT N
1800 CALL 36864
1850 IF SV = 0 THEN GOTO 2000
1900 POKE 49312,0
2000 GOSUB 6500
2010 OT = ST
2100 ST = ST + IT
2150 LB = LB +IT
2200 L=L+1
2210 IF L=106 GOTO 2250
2215 GOSUB 4000
2220 GOTO 1000
2250 GOSUB 7000
2260 GOSUB 4000
2300 GOTO 900
4000 SP = ST
4005 IF RA=0 THEN GOTO 4030
4010 MV=-0.1146207E-11*SP^5+0.376307E-9*SP^4-0.776404E-7*
      SP^3+0.4881835E-4*SP^2+0.0384059*SP-0.1399219E-4
4015 DC = 92.1197*MV+513.5354
4020 GOTO 4050
4030 MV=0.813986E-13*SP^5+0.323928E-10*SP^4-0.352121E-7*
      SP^3+0.462812E-4*SP^2+0.0384927*SP+0.962238E-4
4040 DC=93.3161*MV+514.3767
4050 NA=INT(DC/4):NB=DC-NA*4
4060 POKE 49315,NA:POKE 49316,NB
4070 RETURN
5000 POKE 49345,A1
```



```
5010 V1=PEEK(49346):V2=PEEK(49348)
5020 V3=V2*16+V1
5025 IF RA=0 THEN GOTO 5050
5030 V5=V3*0.280785E-2-5.733916
5040 GOTO 6025
5050 V5=V3*0.280585E-2-5.731624
6000 GOTO 6044
6025 T0=-0.001459*(V5^4)+0.046*(V5^3)-0.7715*(V5^2)+
25.9667*V5+0.01207
6030 GOTO 6060
6044 T0=-0.004629*(V5^6)-0.057246*(V5^5)-0.29747*(V5^4)
0.62242*(V5^3)-1.5684*(V5^2)+25.6654*V5-0.023969
6060 VTAB 22
6065 PRINT T0; SPC(10):PRINT
6070 RETURN
6200 V9=0
6201 FOR Z=1 TO 10
6202 POKE 49345,1
6210 V6=PEEK(49346):V7=PEEK(49348)
6220 V8=V7*16+V6
6225 V9=V9+V8
6227 NEXT Z
6230 BL=BL+0.5
6240 RETURN
6500 DX(1,L)=T0+273
6510 K=37118
6520 FOR N=1 TO 256
6530 K=K+2
6540 TD(N)=PEEK(K)+16*PEEK(K+1)
6550 NEXT N
6560 SM=0
6562 FOR R=1 TO 11
6564 SM=SM+TD(R)
6566 NEXT R
```



```
6570 SM=SM/11
6580 V9=V9/10
6600 DX(2,L)=SM-V9
6610 IK=1
6620 FOR P=3 TO 46
6630 F=13+IK
6640 W=5*IK+13
6650 DX(P,L)=INT(TD(F)-TD(W))
6660 IK=IK+1
6670 NEXT P
6680 RETURN
7000 PRINT D$;"APPEND CCT"
7010 PRINT D$;"WRITE CCT"
7070 FOR J=1 TO 105
7080 PRINT B$;DX(1,J);C$
7082 PRINT B$;DX(2,J);C$
7085 FOR I=3 TO 43 STEP 4
7090 PRINT B$;DX(I,J);C$;DX(I+1,J);C$;DX(I+2,J);C$;
    DX(I+3,J);C$
7100 NEXT I
7110 NEXT J
7120 PRINT D$;"CLOSE CCT"
7130 RETURN
7190 KL=L-1
7195 IF KL=0 THEN RETURN
7200 PRINT D$;"APPEND CCT"
7210 PRINT D$;"WRITE CCT"
7220 FOR J=1 TO KL
7230 PRINT B$;DX(1,J);C$
7235 PRINT B$;DX(2,J);C$
7240 FOR I=3 TO 43 STEP 4
7250 PRINT B$;DX(I,J);C$;DX(I+1,J);C$;DX(I+2,J);C$;
    DX(I+3,J);C$
7260 NEXT I
```

7270 NEXT J
7280 PRINT D\$;"CLOSE CCT"
7290 RETURN
8000 DATA 141,253,144,142,254,144,140,255,144,
8,162,0,169,52
8010 DATA 141,250,144,169,255,133,10,169,144,133,11,169,0
8020 DATA 141,251,144,169,147,141,252,144,76,50,144,
173,253,144
8030 DATA 174,254,144,172,255,144,40,96,234,169,1,
141,193,192
8040 DATA 160,0,200,204,250,144,208,250,164,10,200,132,10
8050 DATA 208,15,164,11,200,132,11,173,252,144,
197,11,208,11
8060 DATA 76,38,144,234,234,234,234,234,234,234,234
8070 DATA 173,194,192,129,10,164,10,200,132,10,208,
8,164,11,200
8080 DATA 132,11,76,118,144,234,234,234,234,234,
8090 DATA 173,196,192,129,10,76,50,144

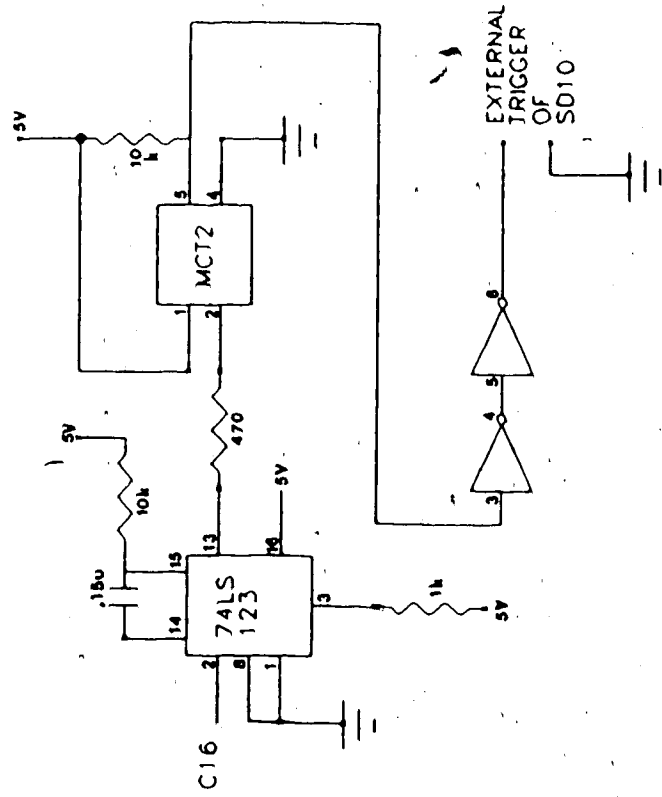
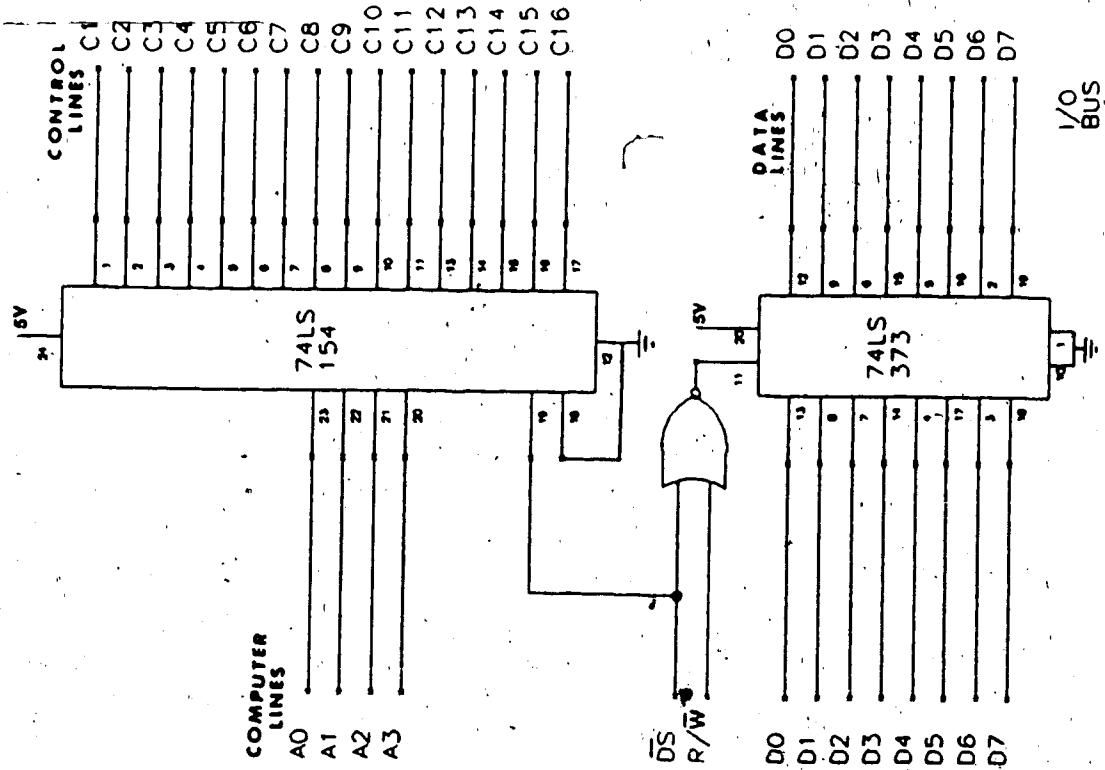
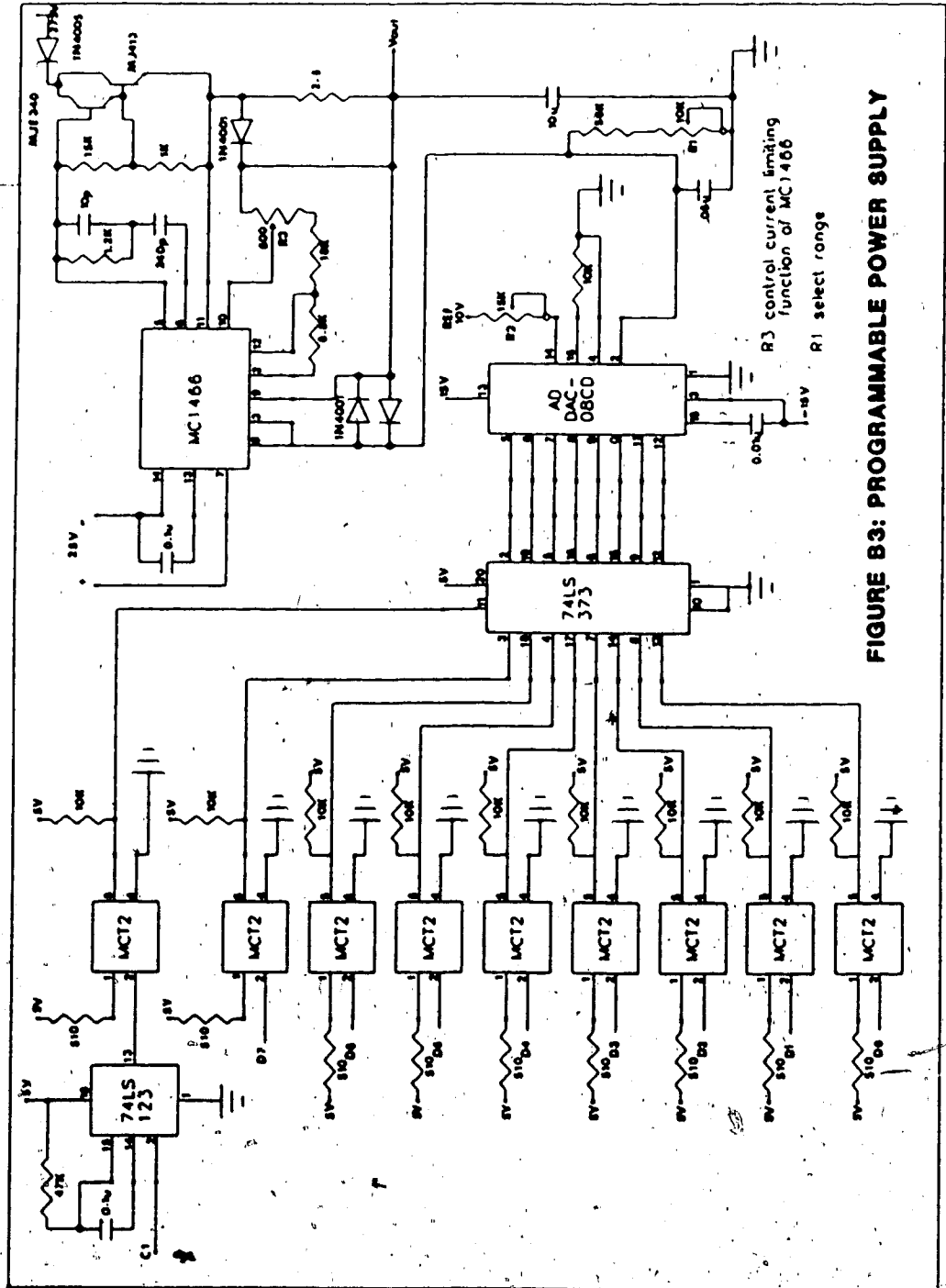


FIGURE B2: SHUTTER DRIVER

FIGURE B1: I/O BOARD



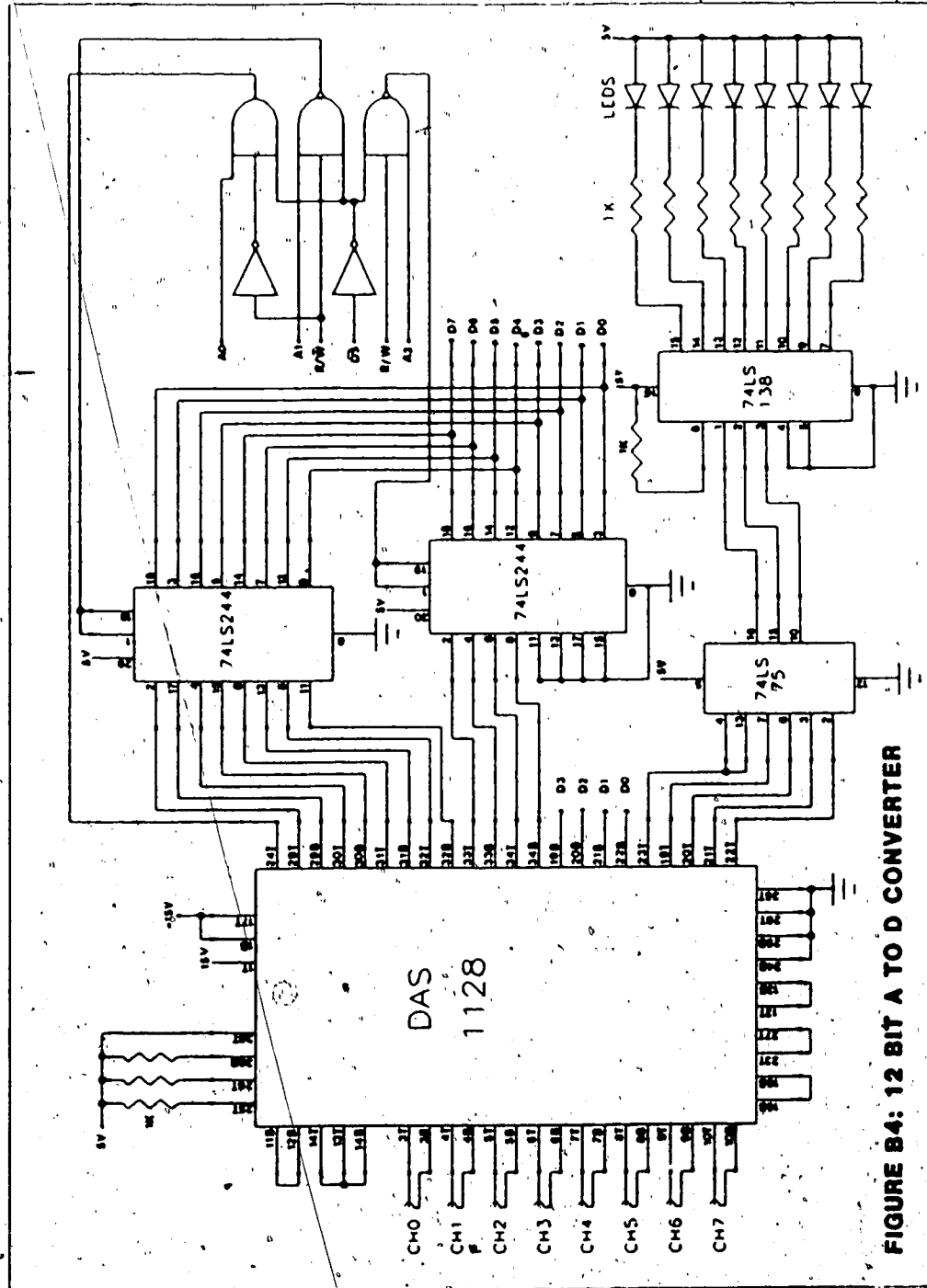


FIGURE B4: 12 BIT A TO D CONVERTER

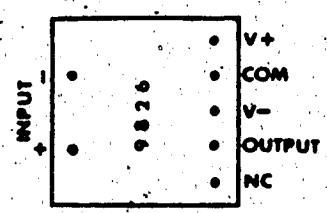
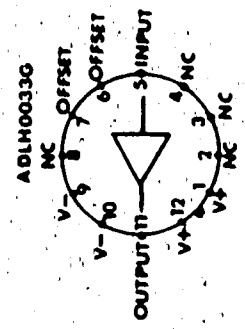
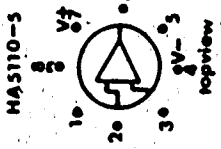
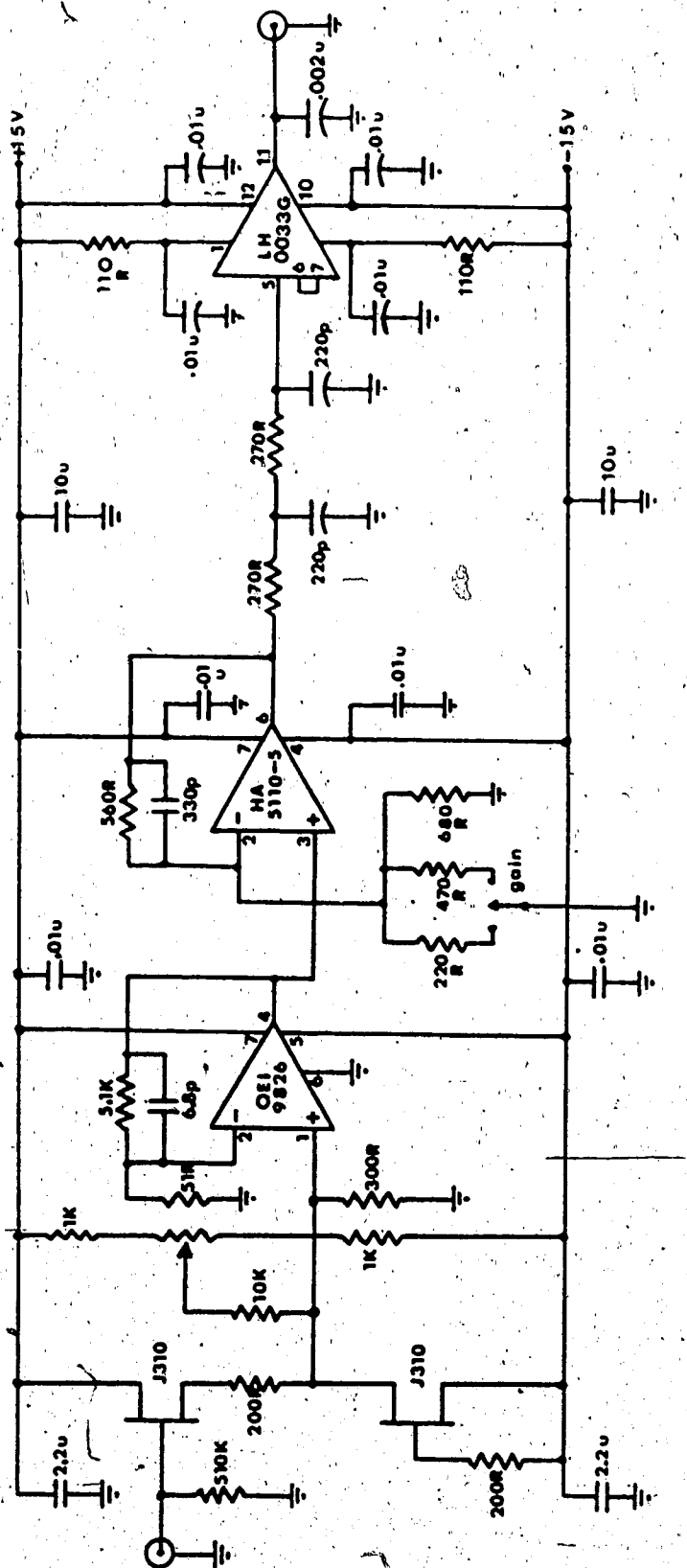


FIGURE B6: AMPLIFIER

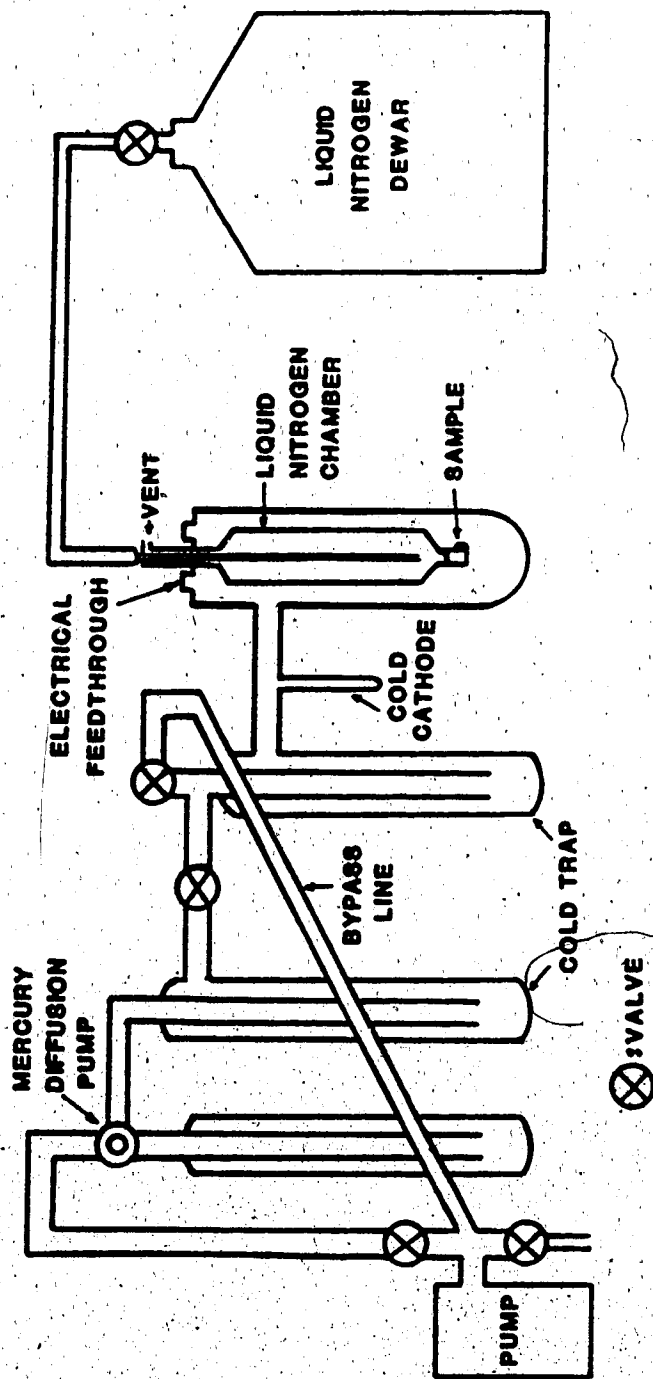


FIGURE B7: MECHANICAL PART OF PITS SYSTEM

VITA

NAME: TIN CHIN CHE

PLACE OF BIRTH: Batu Pahat, Johore, Malaysia

YEAR OF BIRTH: 1955

POST-SECONDARY EDUCATION:

1. B.Sc.(Honours) in Physics and Chemistry
University of London, London, England
2. M.Sc.(Distinction) in Solid State Physics
University of London, London, England

PUBLICATIONS:

1. Effects of internal potential barriers on the photocurrent decay in semiconductors, C.C. Tin and F.L. Weichman, Canadian Journal of Physics, 62, 876 (1984)
2. A microcomputer-controlled temperature controller, C.C. Tin, Analytical Instrumentation, 14, 63 (1985)
3. A new method of analysis of photoluminescence decay curves, C.K. Teh, C.C. Tin and F.L. Weichman, Journal of Luminescence, 35, 17 (1986)
4. Optical and electrical studies of LEC SI GaAs with different carbon concentrations, C.K. Teh, C.C. Tin and F.L. Weichman (Canadian Journal of Physics, May 1987)

PAPER SUBMITTED FOR PUBLICATION:

1. PITS and Photoluminescence studies of copper-contaminated LEC SI GaAs, C.C. Tin, C.K. Teh, and F.L. Weichman (submitted to Journal of Applied Physics)

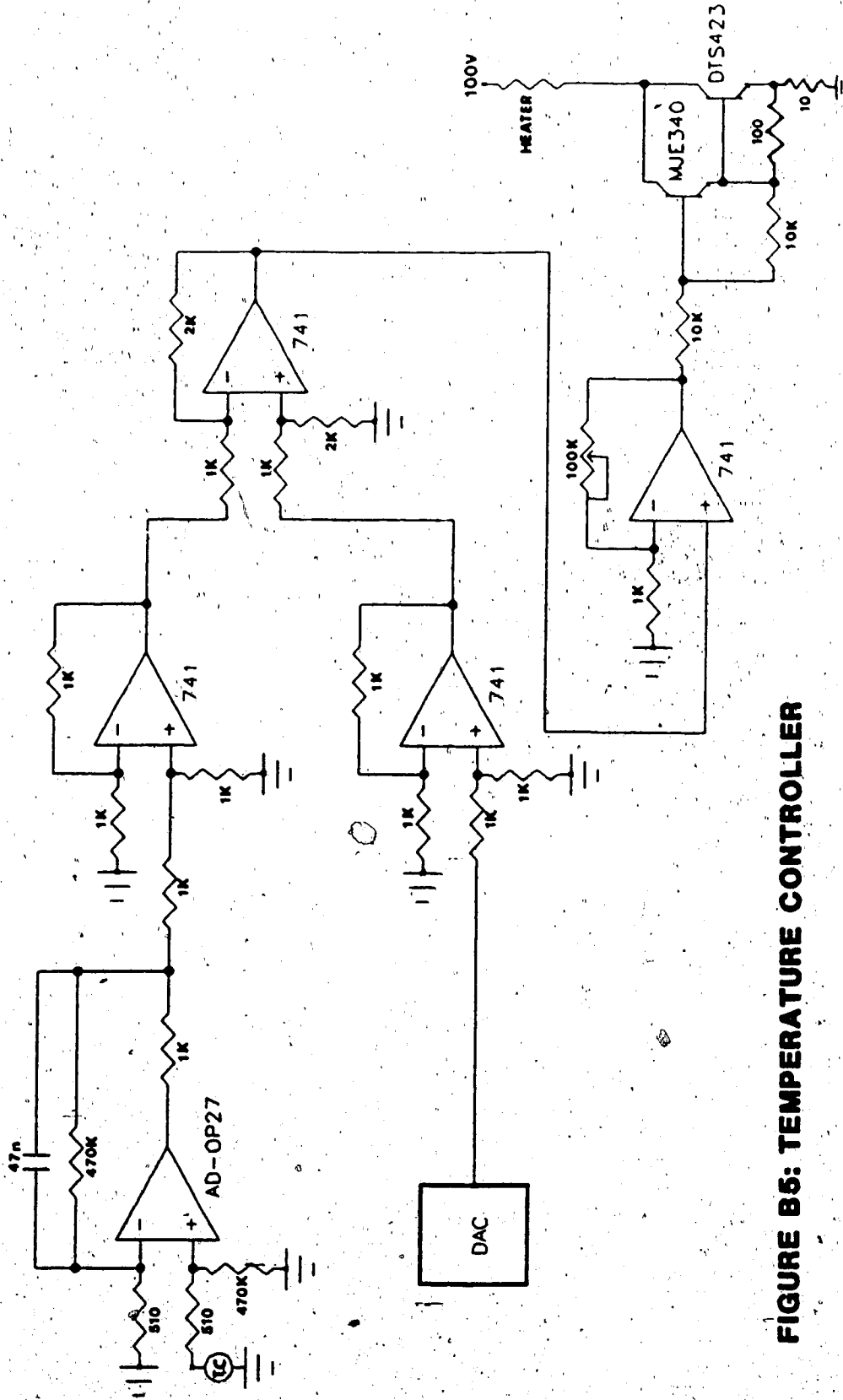


FIGURE B5: TEMPERATURE CONTROLLER